# DYNO-MITE
# Miniature Tire Test Machine

By:
Brandon Miller
Daniel Hoffman
Richard Young

California Polytechnic State University, San Luis Obispo
December 1, 2017

## Statement of Disclaimer

This project is a result of a class assignment; it has been graded and accepted as fulfillment of the course requirements. Acceptance does not imply technical accuracy or reliability. Any use of information in this report is done at the risk of the user. These risks may include catastrophic failure of the device or infringement of patent or copyright laws. California Polytechnic State University at San Luis Obispo and its staff cannot be held liable for any use or misuse of the project.

# Table of Contents

# List of Tables

# List of Figures

# List of Nomenclature

**Dynamometer:** device for measuring force, torque, or power output
**Tire Test Machine:** device for testing axial and torsional output from a tire at different slip angles, speeds, and radial force loads
**Stiction:** force of friction that keeps stationary surfaces from sliding relative to one another
**Closed-Loop:** controller utilizing a feedback loop
**Open-Loop:** controller with a simple gain and no feedback loop
**DC Motor:** motor that operates on DC power
**Motor brushes:** device that conducts current between the rotating shaft of a motor and the stationary DC electromagnet in a DC motor
**T-slot:** aluminum rails with a unique "T" shaped cross section
**Motor response:** a motors physical response to an applied voltage
**QFD:** method to aid in developing customer requirements into engineering specifications
**House of Quality:** graphical QFD technique that somewhat resembles a house

# Abstract

The Cal Poly Mechanical Control Systems Laboratory currently employs an outdated device, known as the Motomatic, to teach students about various motor characteristics and control methods. These include open-loop vs. closed-loop control, speed vs. position control, and DC motor response curves. The current device does not function properly and produces unreliable data due to overwhelming non-linear effects such as stiction and shaft misalignment. Our team was tasked with designing a replacement device that retains many of the same educational goals as the original lab procedure, while also adding new educational goals pertaining to the device system dynamics. The new apparatus, dubbed the Dyno-Mite is a one tenth scale tire testing machine, incorporating two DC brushed motors, adjustable mechanisms, and load cell measuring devices. The design will also pay special attention to modularity so that future adjustments and modifications can be made to the lab apparatus, allowing for instructors to tailor the machine to meet their specific educational goals.

# 1. Introduction

The California Polytechnic State University, San Luis Obispo, Mechanical Control Systems class currently utilizes an outdated apparatus called the Motomatic to teach students about DC motor control and response. The Motomatic devices are over 40 years old. One major issue with the Motomatic devices is the large amount of stiction in the system, which dominates the motor's transient response. Due to this, data collected in the laboratory does not reflect the theory that governs the experiment as accurately as preferred. Bad data prevents students from achieving the learning outcomes and causes students to become skeptical of the theory that governs the experiment, preventing a positive hands-on experience. The Cal Poly Mechanical Engineering faculty arranged a senior project tasked with redesigning a replacement for the Motomatic. The new device is modeled after an industrial tire test machine. The device is portable, outfitted with modern sensors, sourced with low friction components, designed with interchangeable modules and potential research applications in mind, and has a minimum life expectancy of 15 years. The new device is referred to as the Dyno-Mite.

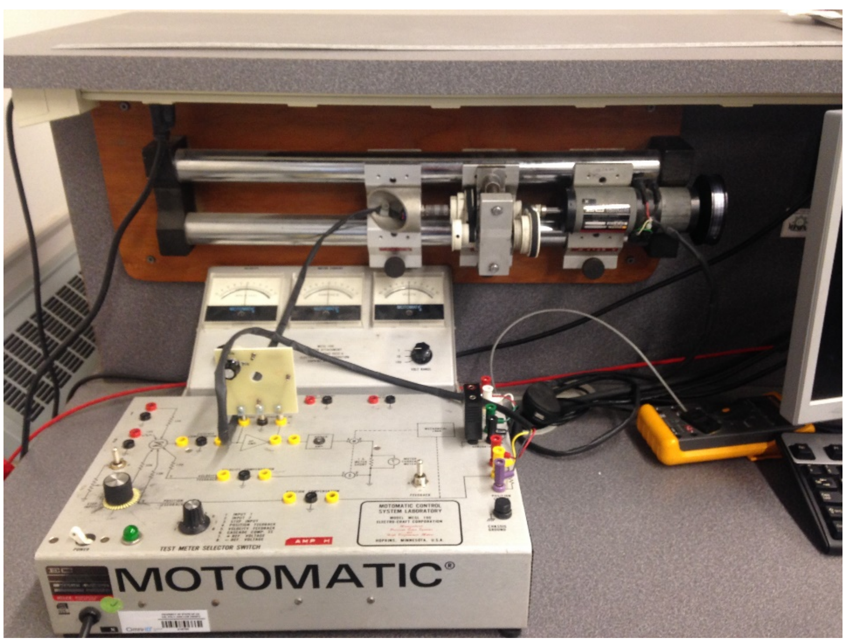


**Figure 1.1** Current Motomatic apparatus

## 1.1 Problem Definition

The main objective of the project was to design, build, and test a machine that provides data that more closely resembles the governing theory of the experiment, so students can prove what is taught in lecture. The controls lab manual and controls textbook were useful references in fully understanding the educational goals of the Motomatic laboratory experiment. These references were influential in developing the technical specifications of the project. The Controls Lab Manual states that a learning objective for the Motomatic lab is to find “the transfer function of the angular positioning system” that allows control of the motor with voltage inputs and promote an understanding of transfer functions in general.

The current Motomatic works using either a position or velocity control feedback loop. The lab procedure focuses on the Motomatic's ability to function as an electromechanical servo. The motor responds to a twist of an input knob on the control panel; the larger the twist, the greater the motor's angular displacement. Ideally, the motor responds linearly to speed and torque control messages, and it responds with an under-damped sinusoidal oscillation about the position it is controlled to stop at. The current device has so much stiction and friction in the system that it does not always respond this way. Rather, the system is dominated by friction and is occasionally overdamped, so it often does not oscillate about the stop position. Additionally, the current device has “dead zones” that make it difficult to measure the voltage change that occurs in the potentiometer during shaft rotation. This makes it harder to calibrate a model for angular displacement, which is crucial for obtaining the angular positioning transfer function.

# 2. Background

Several products currently exist that could be used to replace the Motomatic. However, none of them meet all of the sponsors’ requirements, and all of them include costly features and equipment beyond the scope of the learning objectives specified by the sponsors.

## 2.1 Existing Products

The Lab Volt *Mechanical Training System*, seen in Figure 2.1, is the top competitor, but it has limited motor control capabilities that do not cover all the topics discussed in the lab manual. Additionally, size and weight prevent it from being considered portable or appropriate for the space available in the lab, and it includes unnecessary equipment for laser alignment, vibration analysis, and chain and sprocket drives that increase the cost of the device unjustifiably.


**Figure 2.1** Lab Volt Mechanical Training System Apparatus
<https://www.labvolt.com/solutions/1_mechatronics/98-46101-00_mechanical_training_systems>

The Tech Labs *Electronic Motor Control Learning System*, seen in Figure 2.2, has several similar issues that disqualify it as an acceptable replacement. It is too heavy and bulky to fit the sponsors' requirements, and it has features that the sponsors have not requested. At the same time, it does not have integrated sensors for position, so it would require a retrofit to accomplish everything the sponsors require.


**Figure 2.2** The Electronic Motor Control Learning System apparatus from Tech Labs <http://tech-labs.com/products/electric-motor-control-learning-system>

The National Instruments *ELVIS System*, seen in Figure 2.3, is another competitor the team found. It is challenging to find information on the workings of the system, but it is evident that the sponsors do not want to buy the entire *ELVIS System* to use the DC Motor Control module in order to teach the lab. Furthermore, the DC Motor Control module comes with only one DC motor, and the sponsors have asked the team for a system with two motors; one to provide power and one to provide resistance.

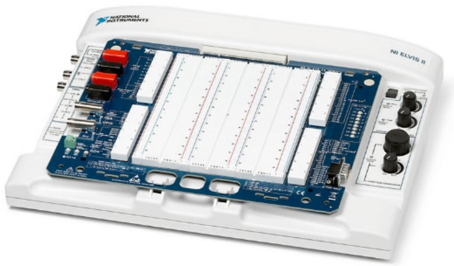

**Figure 2.3** National Instruments ELVIS System <http://www.ni.com/en-us/shop/select/ni-elvis-engineering-lab-workstation>

The Quanser *DC Motor Control Trainer*, seen in figure 2.4, is the top competitor that the team researched. The DCMCT fulfills the most sponsor requirements of any competitor, although it still falls short. The DCMCT uses a DC motor connected to a flywheel to create inertial resistance to motor movements that dominates frictional forces. The device is portable, can be used with analog or digital control inputs, and the website states transfer function representation as part of the possible curriculum. The DCMCT is not an acceptable solution, however, because it cannot function as a scale tire testing device and does not have the ability to add modular loads to the motor.

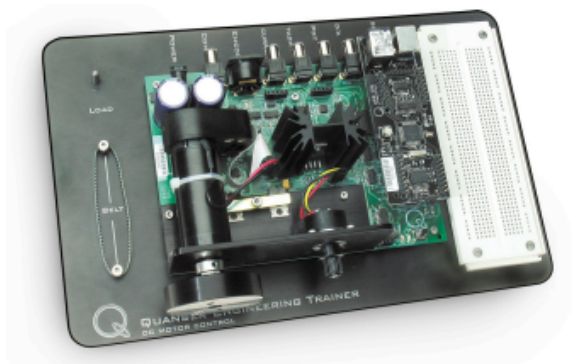

**Figure 2.4** Quanser *DC Motor Control Trainer* <http://quanser.com/Products/Docs/1869/QET_DC_Motor_Trainer_System_Specifications_v1_1.pdf>

Detailed comparisons to existing competition can be seen in the QFD in Appendix A.

# 3. Design Development

The goal of the project was to design, build, and test a scaled down version of an industrial tire test machine to be used in laboratory experiments for the Cal Poly ME-422, Introduction to Mechanical Control Systems Class. In the scope of this project, operability as a tire test machine is defined as the ability of the device to generate tire force curves, plots showing the axial force experienced by the tire at increasing slip angles for a constant speed. The Dyno-Mite will replace the current Motomatic, which has become outdated and costly to maintain. The design focuses on safety, functionality, portability, modularity, and durability. The design created by the team also draws from the previous design to ensure that the original educational objectives are met.

## 3.1 Design Specifications and Requirements

The design includes two electric motors that operate at 24 Volts in compliance with campus policy to avoid needing to follow the campus high voltage safety procedures. The motors are DC brushed motors capable of 3.5 oz-in of torque at 850 rpm. The electric motor powers a shaft that turns a rubber tire. The rubber tire is representative of a full-scale automobile tire. The tire interfaces with a dynamometer drum. The dynamometer assembly is composed of the drum, a variable resistance load device, and an encoder to return velocity and position information. The motor similarly incorporates an encoder to return the same data. Axial and torsional load are determined using bending beam load cells.

The Dyno-Mite has been shaped by a few crucial design considerations set by the sponsors. In order to better identify and organize the project objectives, the team conducted a Quality Function Deployment Analysis. QFD helps to understand the problem, quantify customer requirements, and focus on specific design needs. The QFD can be found in Appendix D of this report. One way to visualize the interrelated factors in QFD is to construct a House of Quality. The House of Quality is divided into eight different sections. The first section is the "who", which identifies the customers and users. The second section is the "what", which represents customer needs and specifications. The third section compares “who vs. what”, ranking the “whats” from the lowest to highest importance with respect to the “who”. The next two sections are the “now” and the “now vs. what”. The “now” are examples of similar designs already in the market. These designs are then compared to the customer wants and needs and ranked from 1 to 4 for each “what”. The next section, the “how”, creates a specific parameter by which to gauge the effectiveness of the design in meeting any specific customer needs. This "how vs. what" section compares the relevance of each parameter to one or more customer needs, and provides either a 1, 3, or 9 depending on the strength of the correlation. The "how much" section quantifies or qualifies the parameters in the "how" section. These are the targets.

See appendices E through I for a full report on the design process utilized by Team Dyno-Mite.

Table 3.1 summarizes all of the design parameters, target values, tolerances, and risk the team considered while designing the Dyno-Mite.

**Table 3.1** List of parameters along with target values to define successful completion of specifications. Including risk assessment and method of complinace determination.

| Spec # | Parameter | Target | Tolerance | Risk<br>*High (H)*<br>*Medium (M)*<br>*Low (L)* | Compliance<br>*Analysis (A)*<br>*Test (T)*<br>*Similarity (S)*<br>*Inspection (I)* |
|---|---|---|---|---|---|
| 1 | Fatigue life to failure | 15 years | min | M | A |
| 2 | Maintenance time per quarter | 1hr per device | max | M | T, S, I |
| 3 | Fasteners torqued to specification | Yes | go / no go | H | T, I |
| 4 | Decibel level | 50 dB | max | L | A, S |
| 5 | Time spent to access a specific part | 5min | max | M | T, I |
| 6 | Labels / Directions for adjustable features | Yes | go / no go | L | I |
| 7 | Physical adjustment limits | Yes | go / no go | L | I |
| 8 | # of accessible pinch points | 0 | go / no go | M | T, I |
| 9 | # of accessible tangle points | 0 | go / no go | M | T, I |
| 10 | % Error btw data and theory | 10% | max | H | A, T |
| 11 | Sensor measurements | force, pos, vel | go / no go | L | I |
| 12 | Interchangeable loads | Yes | go / no go | H | T, I |
| 13 | Cost per device | $1,500 | max | M | I |
| 14 | Area of footprint | 4sq ft | max | M | A, I |
| 15 | % of custom parts sourced | 40% | max | M | I |
| 16 | Emergency shut off | Yes | go / no go | L | T, I |
| 17 | Time spent to make a single adjustment | 5min | max | M | T, I |
| 18 | Clearance for tools | Yes | go / no go | M | T, I |
| 19 | Time to construct apparatus | 3hrs | max | L | T, I |
| 20 | Weight | 50lbs | max | L | T, I |
| 21 | % of parts contained attached to frame | 100% | go / no go | L | I |
| 22 | Max operational voltage | 45V | max | L | A, I |
| 23 | Motor mechanical time constant | 2 seconds | min | L | A, T |
| 24 | Settling Time | 1 second | min | L | A, T |

| | | | | | |
|---|---|---|---|---|---|
| 25 | Scaled torque value | 40mNm | ±10mNm | H | A, T, S, I |
| 26 | Generates tire test curves | Yes | go / no go | H | A, T |

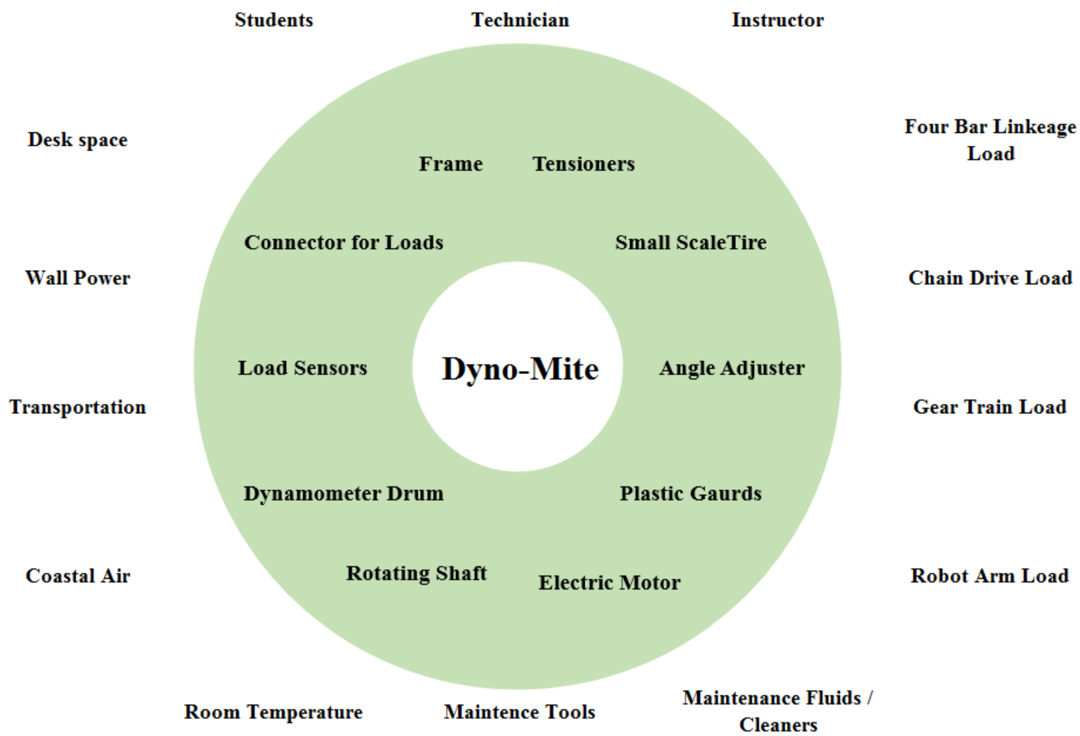


**Figure 3.1** Boundary diagram for the Dyno-Mite. The inner circle represents the encompassing assembly. The blue area represents the subassemblies. The outer area represents environmental factors.

The boundary diagram above, Figure 3.2, is a useful tool in visualizing the hierarchy associated with the design of the Dyno-Mite. The assembly is composed of many subassemblies and parts, which are effected by the environment it is in.

# 3.2 Concept Ideas and Selection

Design specifications and requirements dictated the design of the Dyno-mite and allowed us to identify mechanisms that are crucial to the functioning of this device. For this project, concept ideas are divide into structural components, movement mechanisms, rotating parts, and measuring devices.

All of the structural components were manufactured out of aluminum due to machineability and a good strength to weight ratio. T-slot was utilized frequently due to the ease with which it can be connected to itself. This property makes it useful for building structures that are highly adjustable. Movement mechanisms refer to the angle change mechanism, radial load mechanism, axial load transmitter, and torque transmitter. Rotating parts refer to the rotating tire, flywheel, and dynamometer drum.

For more information on concept ideas and selection, refer to Appendix E.

# 4. Final Design

## 4.1 Functional Description

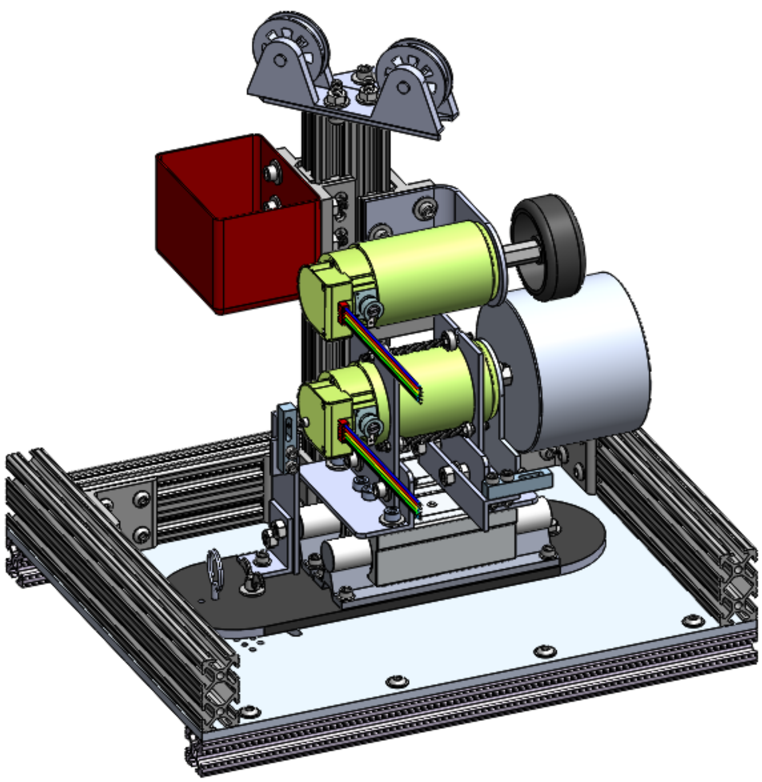

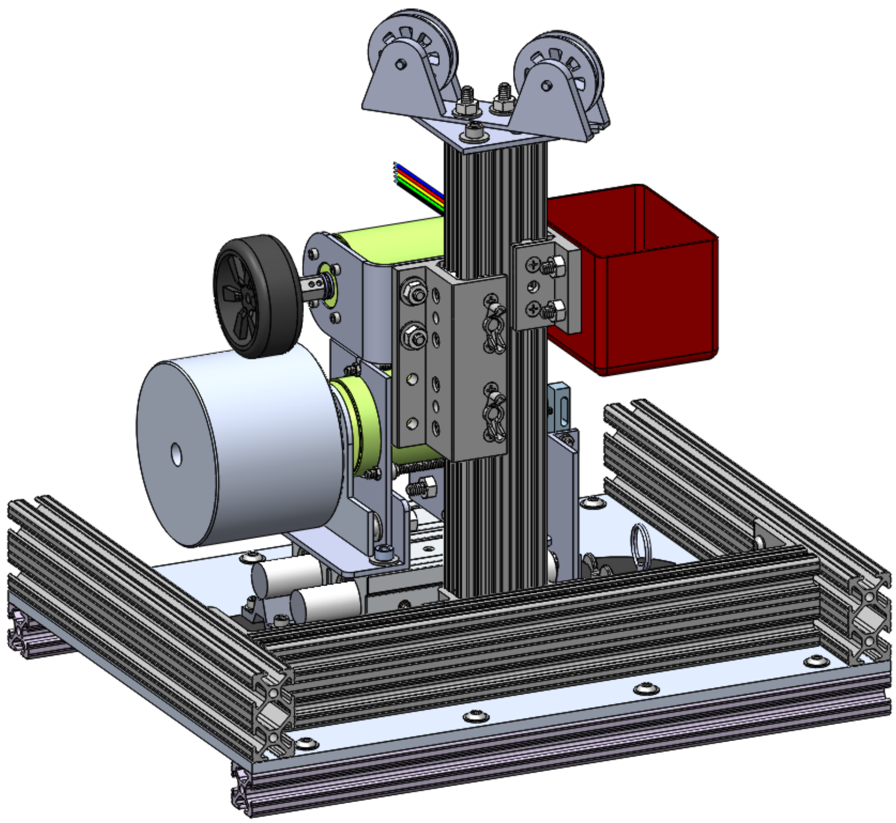

Figure 4.1 Completed assembly for the final Dyno-Mite design

**Radial Force Application Subsystem**: The test tire is secured to a Pittman 14204S006-SP via a screw and shaft collar that has a hex end fitting compatible with the hubs on many RC car tires. The motor is mounted to an aluminum plate which is in turn attached to a 10 series 3 slot mount linear bearing with brake holes manufactured specifically for use with 80/20 products. A 12" long piece of double wide 80/20 is mounted on the base plate normal to the top face, oriented so that the center point of the tire is positioned directly above the center point of the dynamometer drum. The sled and motor assembly is allowed to slide along the 80/20. Because the motor is mounted on a linear bearing that slides in the vertical direction, the vertical force of the motor weight translates to the only support, which is the point of contact between tire and dynamometer drum. Tire force curves rely on calculations of frictional force at the point of contact between the dyno drum and tire, so an accurate measurement of applied radial force is crucial to the success of the tire test procedure. A bucket is mounted to a second linear bearing that slides on the second half of the double wide 80/20 rail. A string connects the motor to the bucket and threads over a pulley assembly mounted on top of the 80/20 rail, allowing the user to remove weight from the point of contact between the tire and dyno drum to simulate a lighter car.

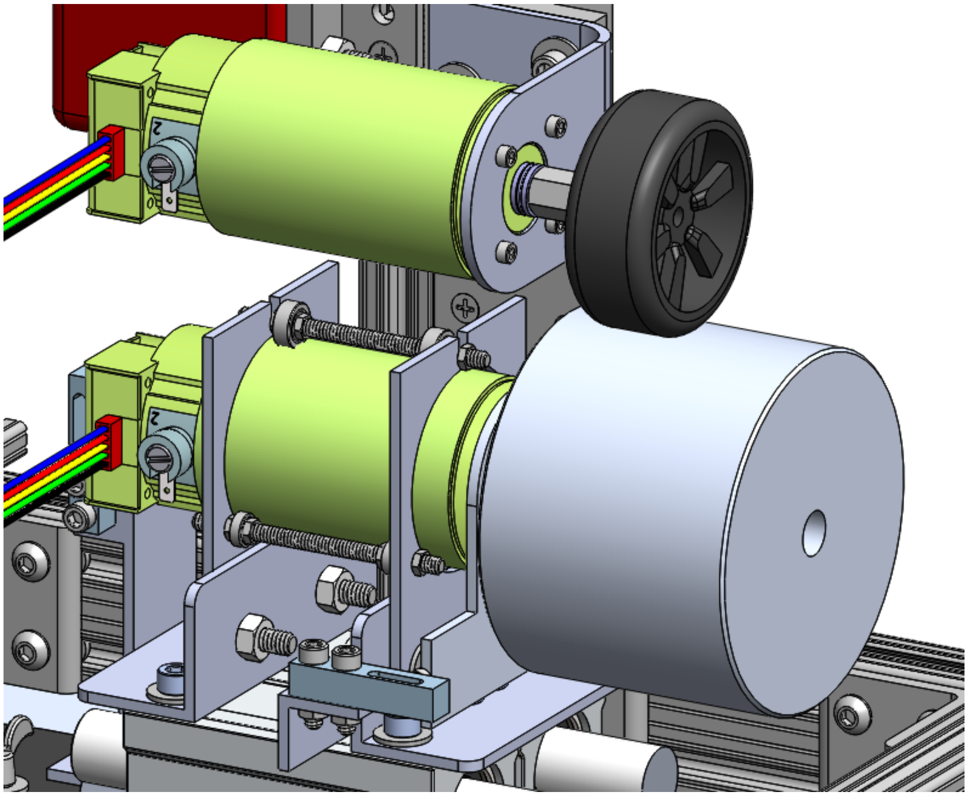

Figure 4.2 Close up of motor-tire assembly

**Motor & Generator Subsystem**: The Dyno-mite employs two Pittman 14204S006-SP brushed DC motors. Angular velocity and position are determined with 500 CPR quadrature encoders mounted on the back of each motor and connected to a Cal Poly proprietary DAQ system. During the tire testing experiment, the motor mounted to the base plate acts as a generator, providing resistance for the upper motor and tire assembly mounted to the 80/20 rail to overcome. This resistance is important in inducing the slip that the tire force curve attempts to reveal. The dyno resistance will be variable via a controller implemented by Professor Birdsong. The dynamometer drum is a 4" diameter, 3" wide rod of Delrin polymer. The Delrin was chosen for its excellent hardness and machinability.

During the DC motor response experiment, the upper motor will have a 6" diameter, 1" thick aluminum fly wheel attached that provides sufficient rotational inertia to give the motor a mechanical time constant of at least 1 second within a wide range of amplifier gain constants. During this experiment the upper motor is moved high enough on its rail and locked in position so that it does not interfere with the lower motor. Students will use the implemented control system to input a step response to observe the motor dynamic response. Although the designed mechanical time constant is 1 second, the actual system dynamic response time will depend on the gain of the controller used, as explained in the lab manual.

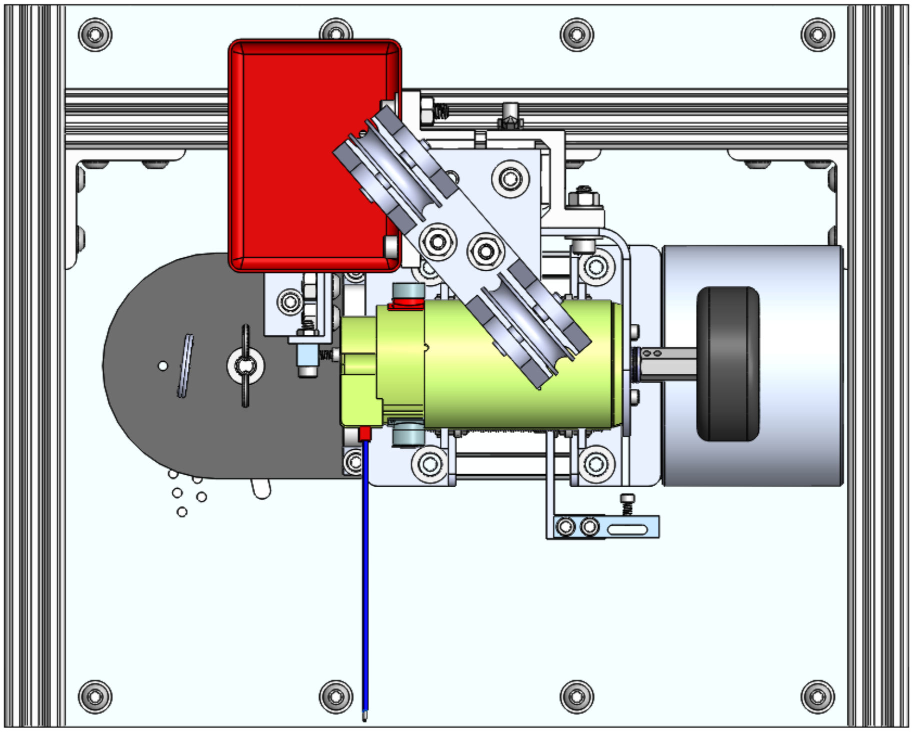

Figure 4.3 Top view of Dyno-Mite complete assembly illustrating tire slip angle setting mechanism

**Angle Setting / Locking / Determining Subsystem**: The lower motor is mounted to a turntable that is constrained in its rotation by a central pin directly below the center point of the dynamometer drum. This allows the user to change the contact angle of the dyno drum and tire while keeping the tire centered directly above the dyno drum. The central pin of the turntable is connected through the device base plate, allowing the turntable to turn freely but constraining it in the vertical direction. Angle selection holes are drilled in the base plate at 1-degree increments, from 0 degrees to 15 degrees. These angles represent the angle between the dyno drum shaft and tire shaft. At 0 degrees the shafts are aligned. A pin slides through the turntable into the base plate hole at the desired angle. This ensures high repeatability at each angle and eliminates the possibility of the turntable slipping from the desired angle during testing. An extra pin connects through the turntable and base plate to ensure the turntable remains flush against the base plate during testing. This pin is constrained to slide in an arc cut into the base plate.

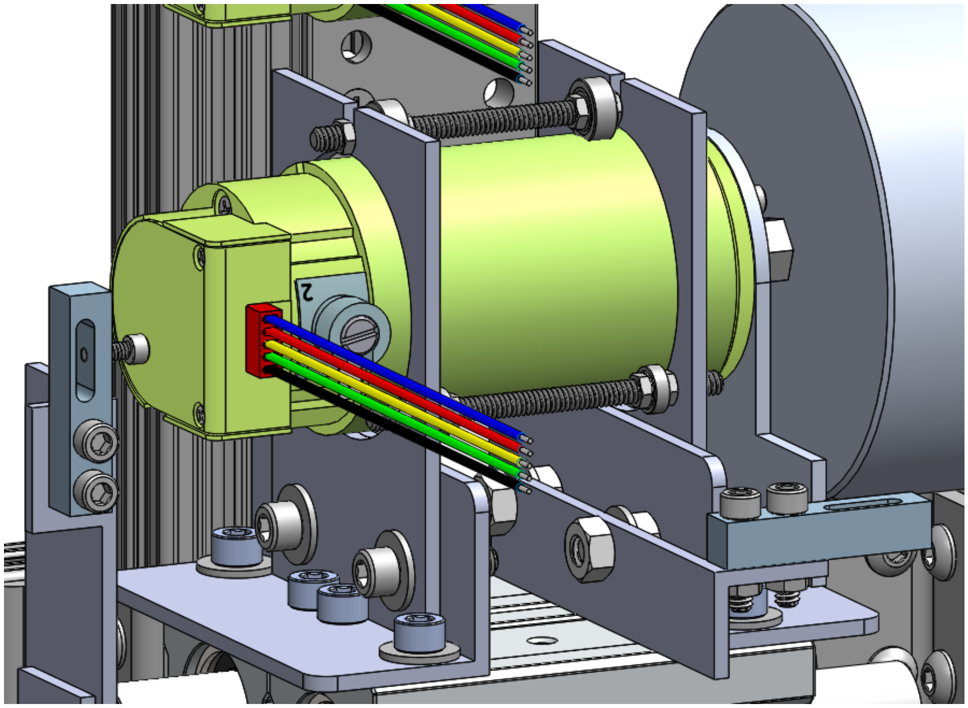

Figure 4.4 Close up of bending beam load cells and journal bearing for load sensing

**Axial and Torsional Force Sensing Subsystem**: All strain is determined using Futek LSM200 bending beam load cells. Torque is determined indirectly through a moment arm mounted onto the face of the lower motor. The arm presses a bending beam load cell rated, for 10lb, oriented on the side of the motor mount to measure the normal force created by the moment arm. The lower motor is mounted in a custom bearing system that allows the motor to rotate freely about the axis to which the torque is applied allowing the full torsional load to be applied to the bending beam load cell. This configuration is designed with robustness in mind. With a moment arm of 2", the max torsional output of the motor is only one-fifth of the load required to damage the load cell, which is rated to accept 150% of its rated load before being damaged. Axial load is determined by positioning a second 10lb bending beam load cell on a mount behind the lower motor. The lower motor is mounted on a linear bearing rail assembly, allowing the motor to slide freely in the axial direction. In this configuration the entire axial load is applied to the bending beam load cell, minus minor frictional losses. A thrust washer bearing is installed between the hex end shaft collar and both motor faces so that all axial force into the motor face is distributed to the motor body, away from the motor shaft bearings. The axial load data will be used directly in the creation tire force curves while the torsional load data can be used to calculate power consumption or power transferred from tire to drum.

**Modularity:** The initial design of the Dyno-Mite comes with modules for a tire test experiment and a step response experiment. The tire, dyno drum, and aluminum flywheel necessary for these experiments are permanently fitted with separate shaft couplers that allow them to be exchanged easily. Likewise, new modules can be fitted with shaft couplers that allow for easy attachment to the motor shafts. The motor shafts are conveniently aligned and pointing in the same direction, facilitating the quick exchange of modules. The distance between the two motors can be increased or decreased as necessary to fit new modules by means of the 80/20 rail and sled that the upper motor is mounted to. Additionally, the upper and lower motors can be repositioned laterally so the motor faces are not coplanar, and the upper motor can be repositioned so the motor shafts are not coplanar.

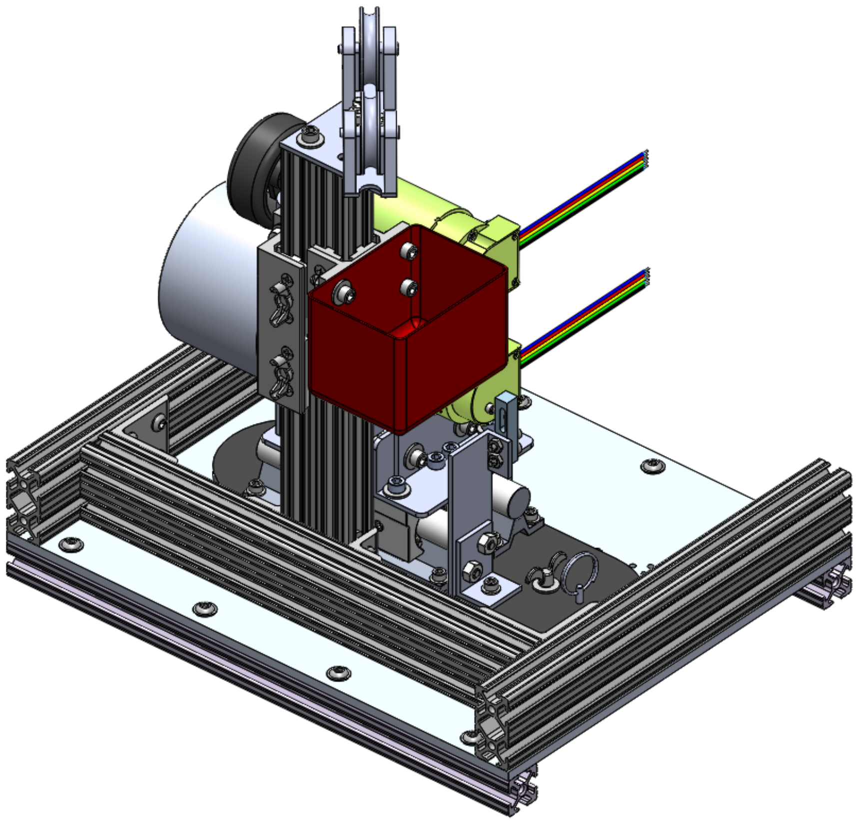

Figure 4.5 View showing the modularity of the Dyno-Mite. The 80/20 rails pictured allow the two motors to move relative to each other in three axes, and the shafts are aligned for easy removal and application of lab modules

## 4.2 Supporting Analysis

Detailed analysis code is included in Appendix J.

**Motor Selection:** The motors were selected based on the requirements for the tire testing experiment with large factors of safety to ensure a robust and durable system. Motor speed and torque specifications were based on a 6000 lbf vehicle operating at 60 mph. The length scale of 1:10 was used to determine the necessary motor speed and torque output combination that would accurately model such a vehicle. The 1/10 scaled vehicle weighs 6 lbf and operates at 6 mph.

Scaling the motor speed was simple, requiring a conversion from miles per hour to revolutions per minute using the unscaled tire circumference. Because this value is free of any length units, it is identical for the scaled model and the unscaled vehicle. It was determined that the motor should operate at 850 rpm.

To determine the required torque, the team relied on Newton's second law. The team calculated the force necessary to accelerate the scaled 6lbf vehicle to 6 mph in 6 seconds, the same 0-60 mph acceleration time as the 250 kW Model S for reference. The torque necessary was calculated by multiplying this force by the tenth scale tire radius. The torque calculated using this method was 3.498 oz-in. The selected Pittman 14204S006-SP is capable of 26 oz-in continuous torque and has a continuous speed of 3630 rpm, leaving the user plenty of headroom if they choose to model heavier vehicles or vehicles operating at speeds in excess of 60 mph.

**80/20 Vibrational and Structural Analysis:** The motor turning the tire is mounted to a 12" rail of 80/20 frame and will be operated at 850 rpm. Because the assembly incorporates rotating elements, the team analyzed the natural frequency of this assembly to determine if the device runs the risk of reaching resonance, causing damage to the rail or other elements of the Dyno-Mite. The natural frequency of the system was determined using the definition of natural frequency equation:

$$\omega^2 = K / m_{eff}$$

The motor and rail assembly bending stiffness, K, was modeled using the transverse stiffness equation for a beam fixed at one end.

$$K = 3EI / L^3$$

These equations together are a function of the 80/20 beam's modulus of elasticity, E, area moment of inertia, I, and length, L, as well as the motor and beam mass combined into an effective mass, $m_{eff}$. The 80/20 modulus of elasticity and area moment of inertia were found on the product specifications sheet, and the effective mass was found by multiplying the beam mass by 33/140 and summing it with the motor mass. The value of 33/140 required to find the effective mass of the beam was derived in ME 318 with the help of Professor Hemanth Porumamilla. The natural frequency of the assembly calculated using this method was 9630 rpm. With the device operating at its maximum possible speed, with no load, the beam still has a factor of safety of 2.5.

To ensure the 80/20 does not sustain any damage due to the axial force applied to the tire, the team analyzed the beam bending deflection and load per unit area. The team used the beam deflection models taught in CE 204 to determine the impact of the axial force on the operation of the Dyno-Mite. The 80/20 beam was modeled as a beam fixed at one end. The corresponding bending equation is:

$$\delta_{max} = PL^3 / 3EI$$

The load, P, was set at 10 lbf, much higher than what is expected during operation, to ensure a robust system. At this load a maximum deflection of 0.0127" was calculated. This value is acceptable to the team because this amount of deflection will not compromise the tire testing ability of the machine. To determine the stress on the 80/20 beam, the team divided the 10 lbf applied load by the 80/20 cross sectional area. The yield strength of the 80/20 aluminum is 35000 lbf/in$^2$, and the calculated maximum stress seen by the beam is a negligible 22.8 lbf/in$^2$.

**Sensor Resolution:** The team was initially unsure if the selected strain sensors would provide the necessary resolution to create detailed and accurate tire test curves. After completing some research, it was discovered that because the selected sensors are analog resistance strain gauges, they produce continuous signals that are limited mainly by the DAQ system resolution and the noise in the system circuitry. Determining the resolution of the whole system including the DAQ requires several steps. First, the rated output of the sensor should be multiplied by the applied excitation voltage to find the expected amplitude of the output signal. Next, divide this signal amplitude by the resolution of the DAQ to determine how many discrete points the DAQ is capable of taking. This value represents how finely the continuous signal will be divided by the DAQ. Finally, divide the applied load by this value to find the fraction of the load that the DAQ can resolve. For example, the rated output of the Futek bending load cells is 1 millivolt/V and the rated excitation is 18V. Our signal amplitude is therefore 18 millivolts. If the DAQ can resolve microvolts, the signal will be divided into 18000 parts. If the expected load is 5 lbf, the system will have a resolution of 0.00028 lbf. This discretization needs to be balanced with the noise in the circuitry and the variance in the load during testing to ensure a clean recording of the signal.

# 4.3 Cost Breakdown

The Dyno-Mite ran over the projected budget of $1500 by $230, but building on the knowledge the team gathered throughout the design and build processes, future iterations of the device can be kept under budget. The current model saw several iterations of crucial subassemblies, requiring purchases of hardware that were not foreseen at the outset of the project. Additionally, most of the hardware is only available in bulk sizing, requiring the purchase of parts that were unnecessary for a building a single prototype but which will be convenient and most cost effective when manufacturing enough for an entire lab of students to use.

The most expensive components of the Dyno-Mite are the Pittman DC motors and Futek load cells. Together these items cost $1238.88, the majority of the allocated budget. The team was in contact with Futek during the build phase of the project, and it seems likely that Futek will be willing to donate load cells for future projects at no or a reduced cost for the university. The next largest cost was the raw materials used in the manufacturing of custom parts for the device. Bulk pricing and recycling scraps between devices will help keep this cost down when manufacturing many devices simultaneously for lab use. The team recommends replacing the 80/20 linear bearing assemblies with VBX linear bearings like the ones in use on the bottom motor assembly. The 80/20 bearings cost $100 whereas the VBX linear bearings only cost $35, significantly reducing the cost for future iterations while also improving performance.

# 4.4 Safety Considerations Discussion

Safety is always a primary concern. The Dyno-Mite will be used in a laboratory setting by students who are unfamiliar with the device. Keeping the users safe and protecting Cal Poly from liability issues is paramount. Being a technical university with many labs and potentially dangerous equipment, Cal Poly already has implemented standards for safety in the laboratories. Keeping within these standards while incorporating additional protective barriers specific to the device will ensure the safety of the students, professors, and equipment. The team has identified potential threats and causes of failure of the Dyno-Mite. A full list of identified and potential risks are contained in the FMEA in Appendix B. The FMEA quantifies the risk of each potential failure, which could include personal injury, damage to equipment, injury to others, or negative affects to data. Some of the highest rated failure risks from the FMEA are summarized in the following paragraphs.

As with the current Motomatic, stiction is a major issue. The Dyno-Mite team aims to keep stiction from overpowering the system over the years of its use. The development of stiction and friction in the DC motor has been identified as a high-risk potential failure mode. Although it is not a big safety hazard it does negatively affect the data and could prevent it from matching the theory, which is the case of the current Motomatic. Stiction can enter the system in numerous ways. Shaft misalignment, inadequate maintenance, old age, excessive loads or vibration, and the collection of dust and other particulates can all lead to increased friction and other nonlinearities. To prevent the chances of these situations occurring the team will develop a recommended maintenance and cleaning schedule along with peak operational load and speed recommendations.

There will be various rotating components on the Dyno-Mite. These have the potential to snag hair or clothing which could induce personal harm or harm the device. These components include the motors, shafts, tire, flywheel, and dynamometer. To mitigate the chances of tangling, the Dyno-Mite implements clear Plexiglas safety barriers, similar to what is currently in use for various other ME lab equipment.

The rotating tire and flywheel of the apparatus present a unique risk. If the shaft supporting these components has too much vibration or is not aligned perfectly then the shaft could wobble. This could throw off the flywheel, causing damage to the device or the user. The tire could do the same or even launch other objects if they fall on the tire while in operation. The pressure applied by the tire to the dynamometer also presents a potential for damage or injury. Operating at somewhat high speed and high forces could cause the tire or flywheel to become misaligned and separate from the device. The chances increase when the steering angle is introduced. The likelihood of these occurrences increase with age and use of the device. Along with the safety barriers previously mentioned, timely maintenance will help to reduce the chances of these failure modes.

Injury caused by the application of the radial load is also possible. It is possible that if the device is bumped or knocked over by accident then the weights could topple off, since they are not rigidly attached. They could then fall on students and cause injury. The Plexiglas barriers limit the risk of the weights falling on the user. This coupled with warnings and following lab rules of wearing closed toed shoes can help to prevent this risk.

To summarize, the main failure modes the Dyno-Mite presents are tangling points attributed to rotating components, parts flying off due to high rotational speeds and the application of load, the development of stiction and nonlinearities in the system due to age and neglected maintenance, weights falling off the device, and vibrational effects that accentuate the above risks. To prevent these issues, we have designed safety barriers that will limit the chances of these occurrences. Further safety precautions include doing vibration analysis of the structure, designing the axial load application device to secure the weights, creating a suitable maintenance schedule to keep parts at peak condition, and adding an emergency shut-off switch on the system controller in the case a dangerous situation arises. The team also plans to incorporate warning labels and instructions that will complement the above precautions, to further reduce the chances of injury and failure.

# 5. Product Realization

All parts were sourced from reliable vendors. Please see attached Bill of Materials as Appendix [I].

The Dyno-Mite prototype was manufactured using the resources found at the Cal Poly's Aero Hangar, Mustang 60', Innovation Sandbox center, and IT Product Fabrication Lab. Both the Aero Hangar and Mustang 60' are fully functioning machine shops with various tools and equipment including cutting tools, mills, lathes, and hand tools. The Innovation Sandbox Center is home to numerous 3D printers, which are often utilized by students for rapid prototyping. The IT Product Fabrication Lab is the only place on campus with a waterjet cutting machine. By utilizing a combination of these resources, the team was able to manufacture a prototype. It is also feasible that future Dyno-Mite devices can be completely manufactured within the breadth of resources at Cal Poly.

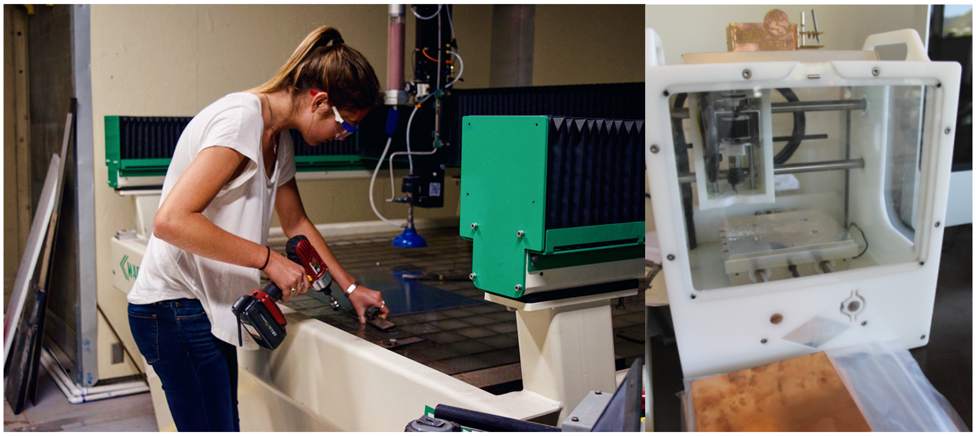

Figure 5.1. Cal Poly IT Product Fabrication Lab (left) and Innovation Sandbox Center (right) <www.cob.calpoly.edu> & <www.polypassions.wordpress.com>

## 5.1 Manufacturing Methods

There are many components that are involved in the Dyno-Mite design. Many are easily sourced from online suppliers or from local hardware stores. Every effort was made to utilize parts and assemblies that would require little to no manufacturing and modification. However, our design does include parts that are unique and must be custom manufactured. These parts can be split up into categories, including structural components, movement mechanisms, rotating parts, and measuring device mounts.

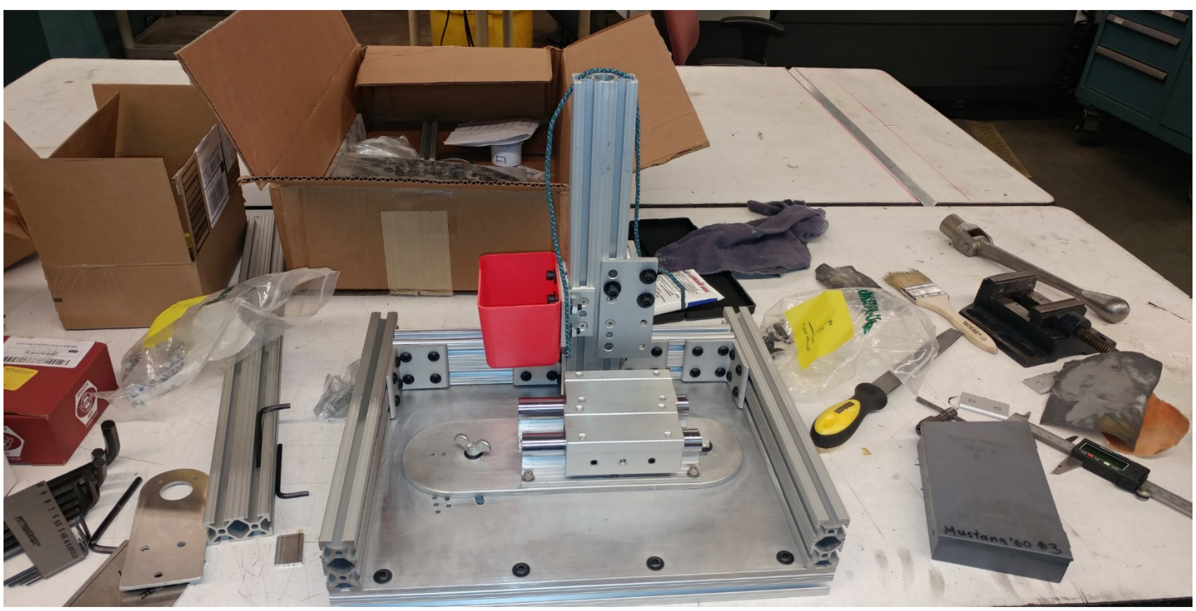

Figure 5.2. Dyno-Mite during early phases of manufacturing and assembly

Structural components include the base, framed with T-slot, and the T-slot tower. The base features were waterjet due to the intricate arrangement and need for accuracy in regards to the curved slot and 1-degree incremented holes. The base plate framing and tower were constructed using 1”x1” and 2”x1” aluminum T-slot. The T-slot was easily measured to length and cut using a fine toothed vertical band saw. T-slot is especially useful for prototypes and modular designs due to the ease with which the stock can be slid and repositioned using common hardware.

The movement mechanisms in the Dyno-Mite include the angle change, radial load, axial load, and torque mechanisms.

The angle change mechanism is made up of two waterjet plates. These plates are mounted on the top and bottom of the base plate. Both plates connect together using a bolt at the point of rotation. The second point of connection between these two plates is a wing nut and captive nut. The captive nut is pressed into the bottom of the bottom angle change plate which allows the wing nut to be tightened so that the two plates clamp onto the base plate. The wing nut travels through the slot in the base plate. There is a third hole which is used with a pin in order to accurately position the plates at each of the angle increments.

The radial load mechanism involves the T-slot tower. Two PTFE linear bearings, specifically sold for use with T-slot run along the sides of the tower. One of the linear bearings is attached to the motor mount, which is a bent piece of waterjet aluminum. The waterjet process was required in order to cut a hole large enough for the face of the motor to fit through. Due to the thickness of the 1/8” aluminum, the metal could not be bent using conventional sheet metal benders. In order to get a good 90-degree bend without cracking the metal, a blow torch was used to soften the metal and the aluminum was then bent carefully on a vice. By using a vice, the metal was bent with the proper radius needed to prevent yielding. The weight of the motor is offset by a pulley system connected to a cup mounted to the second PTFE linear bearing. The cup is used to hold the lab weights. Both PTFE bearings were shimmed using PTFE layers to take up the slack in the bearings, while taking care to not put so much pressure on the wall of the T-slot that they no longer slide easily. The two pulleys, pin, and pulley mount were 3D printed using PLA. The tower extension allows for the positioning of the pulley assembly directly over the center of gravity for both the driving motor and weight offset cup. The tower extension is made out of 1/8” aluminum sheet and was manufactured by hand using a vertical band saw and drill press. The inner hole of the T-slot tower was tapped so that the tower extension could be secured on the end of the tower via a single bolt.

The axial load mechanism uses a set of two linear roller bearings that slide on two parallel round rails, which sit on top of the angle change mechanism. The round rails were ordered as one long piece, cut in half, and new mounting holes were drilled. Since the rails are made out of hardened steel, a carbide tipped chop saw was needed to cut through. The two round rails were then secured into the top plate of the angle change mechanism and fastened into holes drilled and tapped on the surface. The two linear bearings are secured together using 1” angle stock. This angle stock was drilled and cut using a fine tipped vertical band saw. The angle stock also serves as the legs that the torque bearing plates mount to.

The torque mechanism is composed of two torque bearing plates which were waterjet out of 1/8” aluminum. Waterjetting was an easy and efficient way to manufacture the plates precisely. Three threaded rods span the gap between the two plates. Two bearings on each rod were secured using low profile hex nuts. These hex nuts were chosen because they have low clearance and secure the bearings by pressing only on the inner race. The bearings had to be positioned accurately so that the faces of the two plates are perfectly parallel, allowing the motor to rest evenly on the flat outer surface of each bearing.

The hex coupler for both the drive motor and dynamometer motor were modified to fit the .125" motor shaft. The coupler mounting to the drive motor and tire was first drilled out using a drill press. This did not result in a concentric hole, creating in a wheel with a slight whirl mode. The hex coupler for the dynamometer was drilled using a lathe to ensure good concentricity. The hex coupler for the dynamometer motor was further modified. The threaded end was turned down along part of its length to create a perfectly round outer diameter. The Delrin cylinder, or dynamometer drum, was drilled to match this size. The hex coupler was then pressed into the face of the Delrin cylinder, engaging the remaining hex portion on the coupler, to prevent any rotation relative to the coupler. The assembly was then put in a lathe and the walls of the drum were turned down to ensure concentricity.

The measuring device mounts were constructed out of 1/8” aluminum plate and 1” angle stock. These mounts were not developed during our design development phase, and they represent a rough prototype. The plate was cut using a vertical band saw and holes were drilled using a drill press.

All custom parts have the potential to be manufactured using California Polytechnic State University, San Luis Obispo machine shop facilities and resources.

## 5.2 Differences from Original Design

Due to unforeseen issues with manufacturability or unsatisfactory performance, changes were made to many of the subassemblies. The prototype ultimately developed by our group has many differences from the original design.

The radial force application subassembly was altered from the original design to correct for an oversight in our analysis. The project specifics that the device is able provide a radial tire load ranging from 1 to 3 lbf. However, the weight of the driving motor assembly itself was not accounted for. In total, the weight of the motor assembly is just over 3lbs. In order to meet our design specification, we developed a way to offset the weight of the motor assembly, instead of adding weight. The tower was changed from a 1"x1" T-slot to 2"x1" so that two linear bearings could be attached at the same time. A pulley system was decided as a good solution since it minimizes friction. The first iteration included a single 3D printed pulley that sat on top and in line with the axis of the tower, see Figure-14. However, this had mediocre results. The second iteration included two pulleys positioned on a cantilevered plate which located the pulley wheels directly over the center of gravity of the motor assembly and the weight cup, see Figure-14. This created a much smoother action, allowing for easier transference of weight and reduced the jamming of the linear bearings.

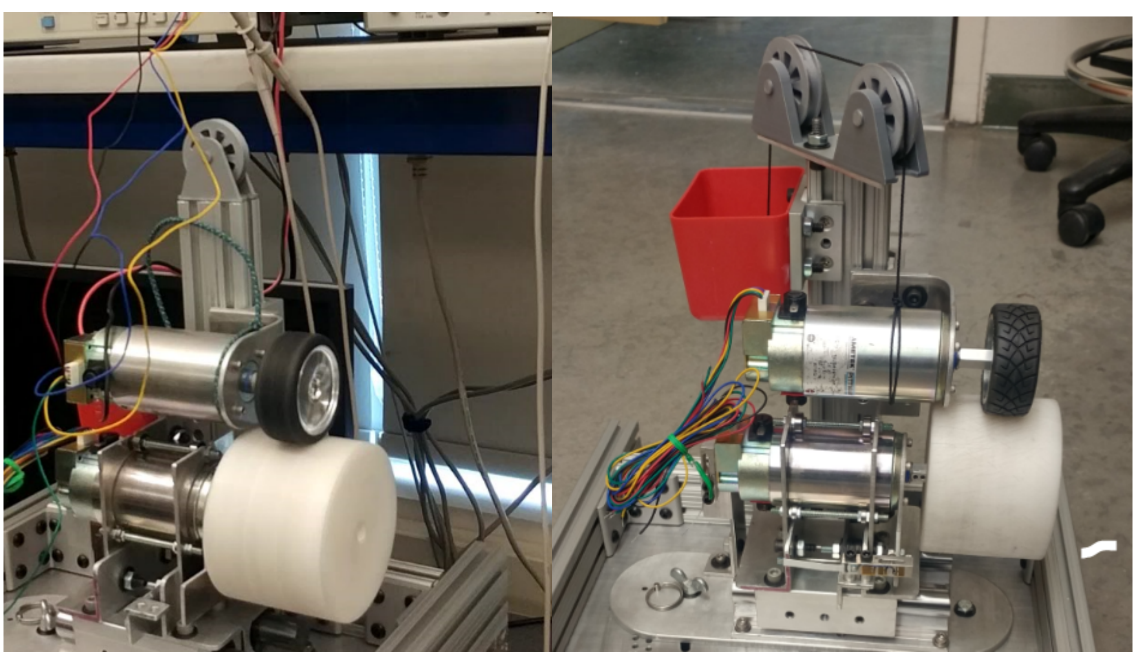

Figure 5.3. The two different pulley design modifications, single pulley (left) and double pulley (right)

The torque bearing mechanism was also changed. The original idea was to press-fit bearings onto an unthreaded aluminum rod and press-fit the rods into the bearing plates. This proved to be challenging to assemble due to the sizing tolerances of the bearings and rod. The team decided to opt for threaded rods with which we could position the bearings and secure the rods in the bearing plates using nuts. After some fit checks, the team realized we needed to replace the nuts with low profile nuts that had a smaller width than the outer diameter of the bearings so that they would not contact the motor. The two bearings located on the top rod of the torque bearings assembly utilize slightly larger bearings which allow for better fit and adjustability of the motor.

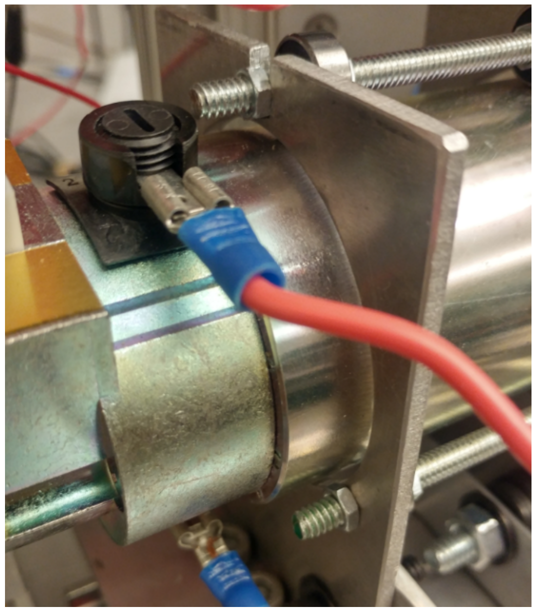

Figure 5.4. View of the Torque Bearing Subassembly incorporating threaded rods

The original design did not incorporate mounts for the load cells. These were manufactured as an afterthought, utilizing extra materials such as the aluminum plate. See Figure 5.5 for reference.

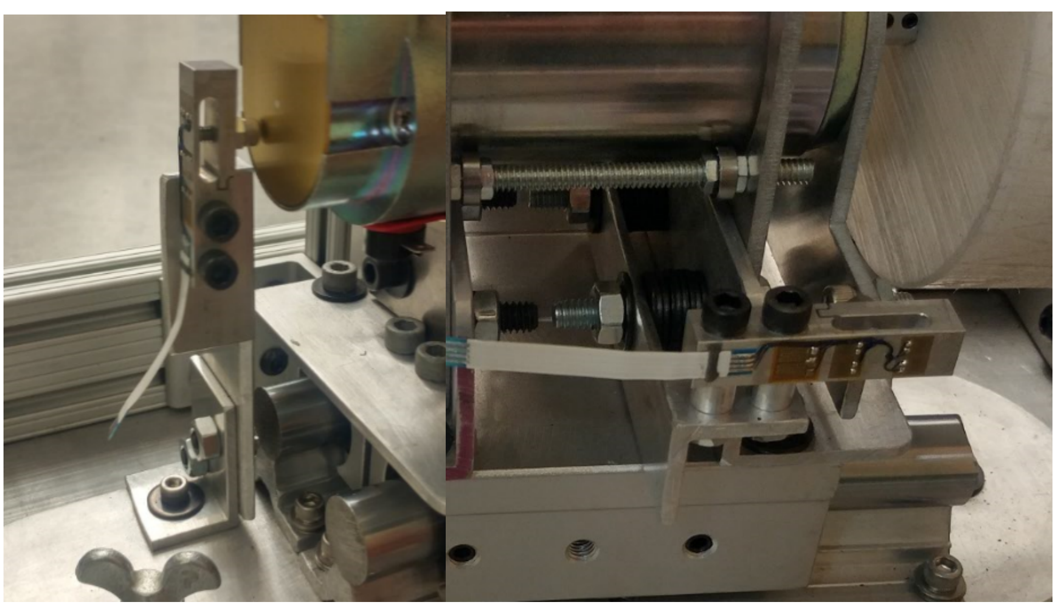

Figure 5.5. Load cell mount prototype, made using aluminum angle stock and plate

The Delrin drum is slightly different than the one originally designed. The Delrin cylinder, ordered with a 4" OD and 3" length, was left with the stock dimensions. This reduces the amount of manufacturing time and also retains the largest contact area for the tire as possible. The dynamometer drum was originally designed with a milled out hex pattern to interface with the hex shape on the coupler. This proved to be too challenging to manufacture with the tools available to us at the Cal Poly machine shops. The drum was also not a candidate for waterjet since cutting through 3" material would yield inaccurate cuts. We decided to instead modify the hex coupler by turning the coupler down to a cylinder for about 80% of its length. This simplified the operation for the dynamometer drum, because only one hole had to drilled. The hex coupler was then pressed into the face of the drum, engaging part of the hex pattern still remaining on the coupler.

The aluminum flywheel was not incorporated in the final design. Although the aluminum flywheel was manufactured, the Delrin dynamometer drum proved to be a sufficient flywheel with a large enough rotational inertia to achieve the desired motor characteristics. This decision had other advantages including reducing the number of components and manufacturing time. This also prevents the need to switch out the tire for the flywheel during the experiment. See Figure-17 for reference.

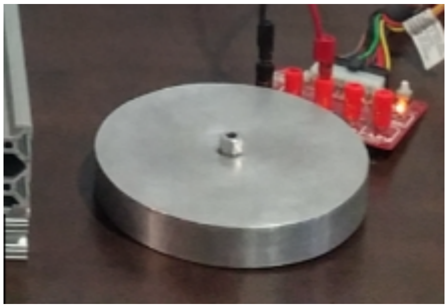

Figure 5.6. Unused aluminum flywheel

The final design does not incorporate any sort of projectile shield. This was determined to be unnecessary after assessing the machine when it was running. There is little change for dangerous projectiles. In the case of tangling, the motors will never be powerful enough to cause extreme bodily harm.

## 5.3 Manufacturing Recommendations

Manufacturing recommendations include making changes to the radial load mechanism, hex couplers, dynamometer drum, and load cell mounts.

The radial load mechanism should utilize the same linear roller bearing and rail pair as the axial load mechanism, shown below in Figure-18. These components have much less stiction and are much more stable and secure than the T-slot linear bearings. The current assembly binds easily, preventing the user from accurately determining the force applied between the dyno drum and tire. The linear bearing system employed in the bottom motor assembly is significantly lower friction and will eliminate this problem.

Figure 5.7. SME20LUU 20mm open block unit motion linear bearings and rail

<http://www.vxb.com>

The hex couplers should in the future be drilled out using a lathe to ensure concentricity. This will greatly reduce vibration in the system. Other options may include sourcing alternative motor shaft couplers that clamp in place of a set screw, especially for the dynamometer drum. See Figure-19 for an example of shaft clamping coupler.

Figure 5.8. Example of a more secure shaft coupler to be used with the dynamometer drum

<http://www.globalindustrial.com>

The dynamometer drum should be secured to the hex coupler using adhesive or keyway. This would result in a more secure attachment and would reduce the chance of misalignment when pressing the coupler into the face of the Delrin drum.

Load cell mounts are the perfect candidates for 3D printed structures. A 3D printed structure would be time effective to manufacture and could be made more stiff than using thin pieces of aluminum plate. Also a 3D printer allows the structure to be made as a single piece instead of a bolted structure, increasing simplicity. Place the torque sensing load cell in a position where torque is sensed by pushing on the load cell. Torque is currently sensed by pulling on the bending beam load cell. Tests conducted after assembly showed that the load cells currently in use work significantly better when pushed. To get more accurate readings of torque in the system, the team recommends that the torque load cell be repositioned so the moment arm on the face of the lower motor presses into the load cell.

Mount the upper and lower motors facing each other, as opposed to the current design where they face the same direction. While the current configuration is useful for increasing the device's modularity, it presents several issues. The current prototype does not account for the equal and opposite axial force that the upper motor experiences. This force, desirable in the lower motor for the purposes of the tire test, pulls the tire off the upper motor shaft, creating a safety issue should the tire come completely off the shaft, and putting undue force on the motor in the axial direction without any system to protect the motor bearings. See Figure-20 for a comparison of the motors on the current prototype versus a conceptual drawing of how they should be arranged.

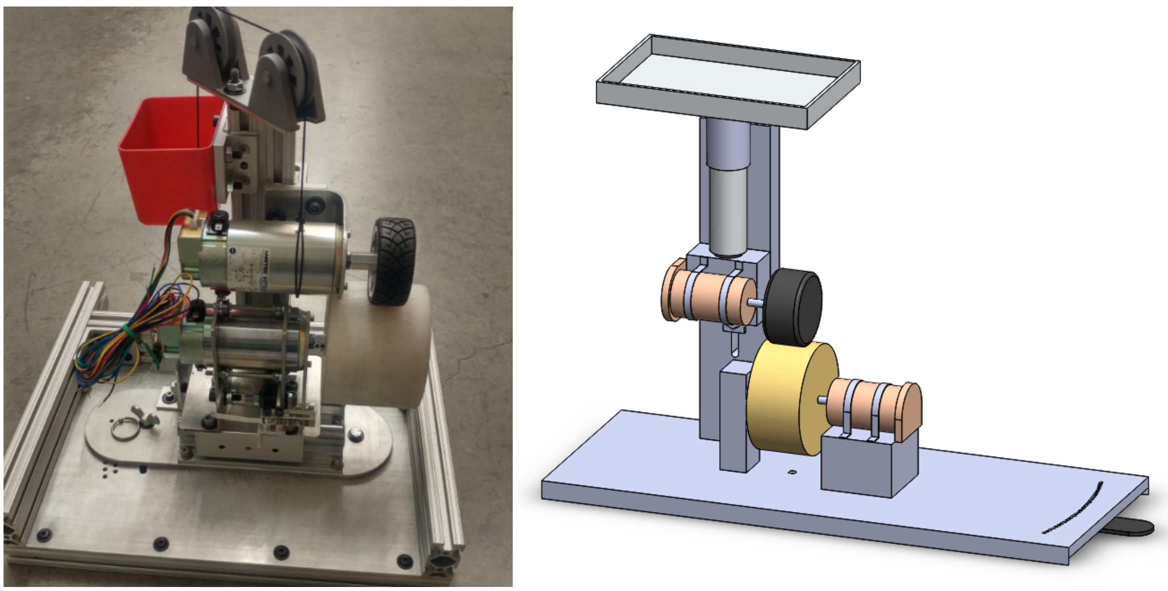

Figure 5.9. Arrangement of the two motors on the current prototype (left) and conceptual drawing (right)

These recommendations should be addressed before a second prototype is constructed. These recommendations will greatly increase the performance of the Dyno-Mite.

# 6. Design Verification

The scope of our involvement in the Dyno-Mite project was limited to the mechanical design. Without a control system on hand to operate the device or a DAQ to collect data from the motor encoders or load cells, the team had difficulty testing certain aspects of our Design Verification Plan. However, the team was able to conduct many individual tests on the motors, encoders, load cells, and functional subassemblies. Below is a list of high level project requirements followed by details about the team's verification efforts. For a full list detailing the points of inspection for our design, please see the full DVPR in Appendix [L].

# 6.1 Test Description and Results

| Force to Overcome Friction | |
|---|---|
| *Direction* | *[lbf]* |
| Axial | 0.2205 |
| Torque | 0.1764 |
| Radial | 0.882 |

Table 6.1 Summarization of frictional forces tested in the three separate bearing assemblies

Table 6.1 shows the results from experimental testing of the force to overcome friction for multiple bearing mechanisms. High friction in the bearing systems is undesirable because it leads to inaccuracies in sensing by creating dead zones. The radial load mechanism needs a force of .882 lbs to overcome friction. Since the mechanism is designed to apply loads between 1-3 lbs, this friction force has a large effect on the efficacy of the device. The friction force will create a dead zone that covers roughly 30% of the total load range. A modified design is needed for future Dyno-Mite iterations. The force to overcome axial and torque friction is much lower in relation to the overall range of forces that they will see, 7% and 19% respectively.

Using a Mini-Instron circuit board, the team was able to verify that both load cells function and deliver the output voltages when the device is in operation. See Figure 6.1 below for pictures of the Mini-Instron and Pittman motor connections.

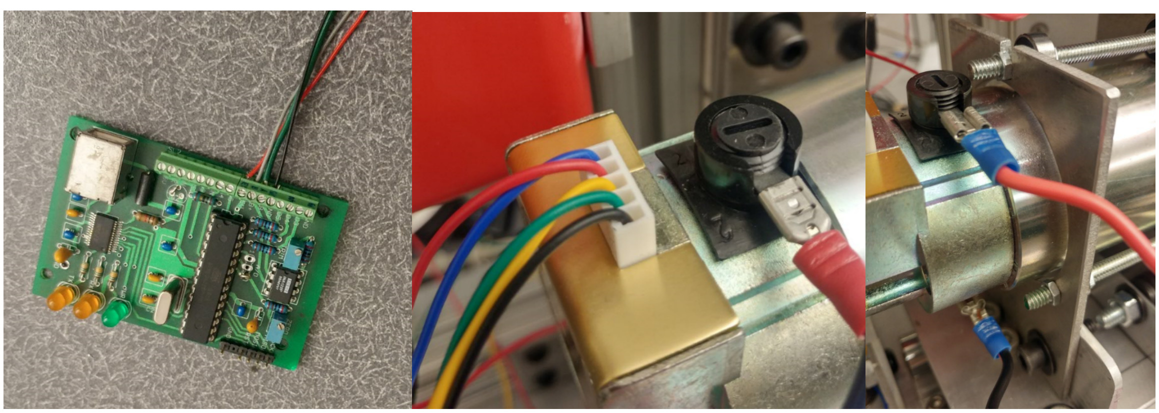

Figure 6.1 Picture of Mini-Instron PCB (left), Pittman encoder leads (middle), and Pittman power leads (right)

It is specified that the Dyno-Mite should achieve experimental results within 10% of theoretical results. Without a controller to maintain a constant motor speed or a DAQ to collect encoder and load cell data, the team was unable to test the device the way it would be operated in an actual tire test experiment. However, using an oscilloscope in the mechatronics lab, the team was able to verify that the encoders on both motors were fully functional. Using the measurement function of the oscilloscope to monitor the frequency of the signal output from the top encoder and a Mini-Instron circuit board to monitor output from the axial load cell, the team was able to approximate a tire test experiment and generate a tire test curve that resembles the trends seen in a full-scale tire test. Without the proper equipment to conduct a more precise experiment the team cannot conclude that this objective was met, but preliminary testing results appear promising. See Figure 6.2 for the plot of axial load cell voltage versus slip angle for a constant speed. In contrast to tire force curves taken from full-scale vehicles, the curve of the experimental data has not started to level off around 8-9 degrees. This may be a result of differences in the tire tread, tire pressure, road surface, speed, and potentially other unforeseen factors. Further testing may dictate the need to revisit theoretical goals. It could be possible that the tires used in the preliminary Dyno-Mite tests have a peak axial load at a greater steering angle.

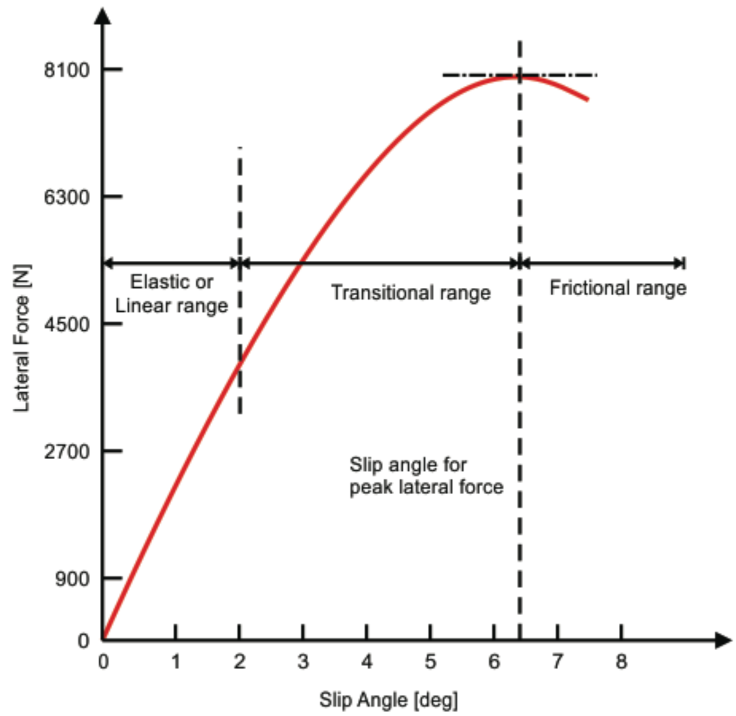


Figure 6.2 Example tire force curve
<https://forums.kartpulse.com/t/the-absolute-guide-to-tires/1292>

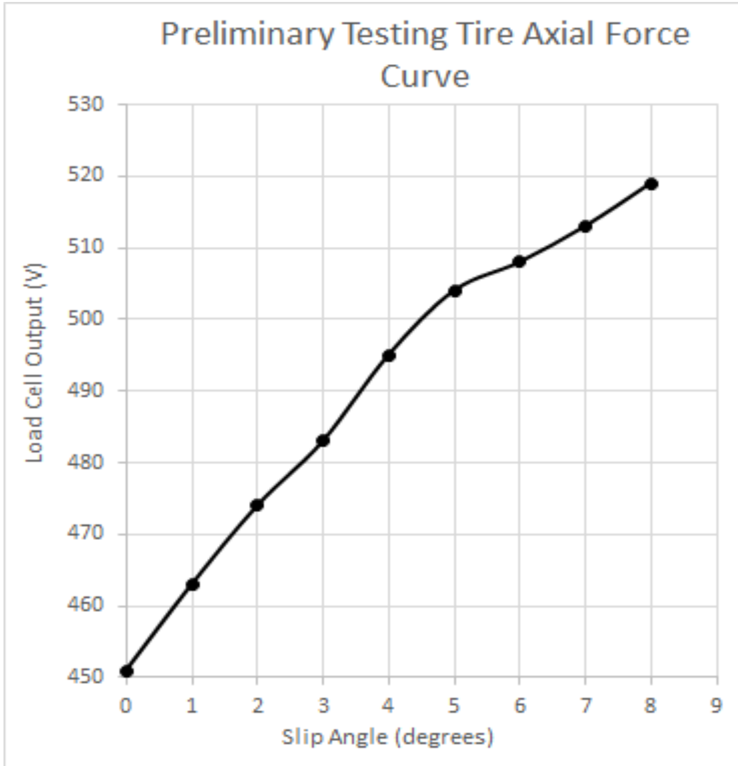


Figure 6.3 Axial load cell voltage output versus slip angle for constant speed

Measurements were taken for the tire force curve and torque curve using a calibrated fish scale in place of the load cells. Since the load cells only produce a voltage, they must first be calibrated experimentally or the data must be converted using a provided conversion constant. See Figure 6.3 for pictures of the scale calibration process and measuring process of the radial load mechanism. The fish scale was used to measure both axial load and the system torque by hooking onto different parts of the motor. Due to vibration and friction, measurements varied by ±50g. Figure 6.4 below illustrates how axial load was measured during testing.


Figure 6.4 Fish scale calibration with 500g weight (left) and radial load measurement (right)

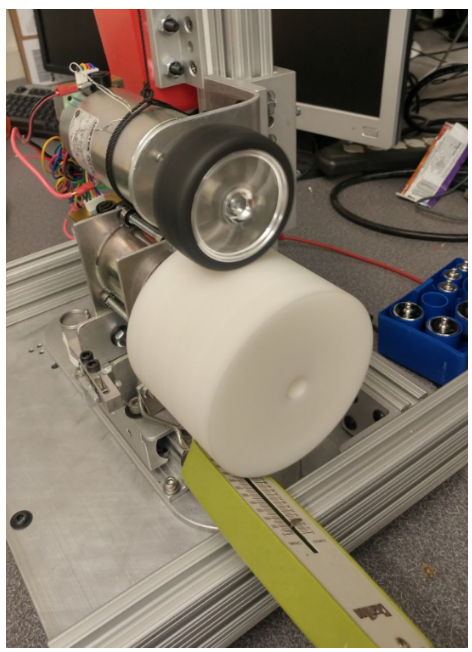

Figure 6.5 Measurement of axial force using fish scale (note that the device is running)

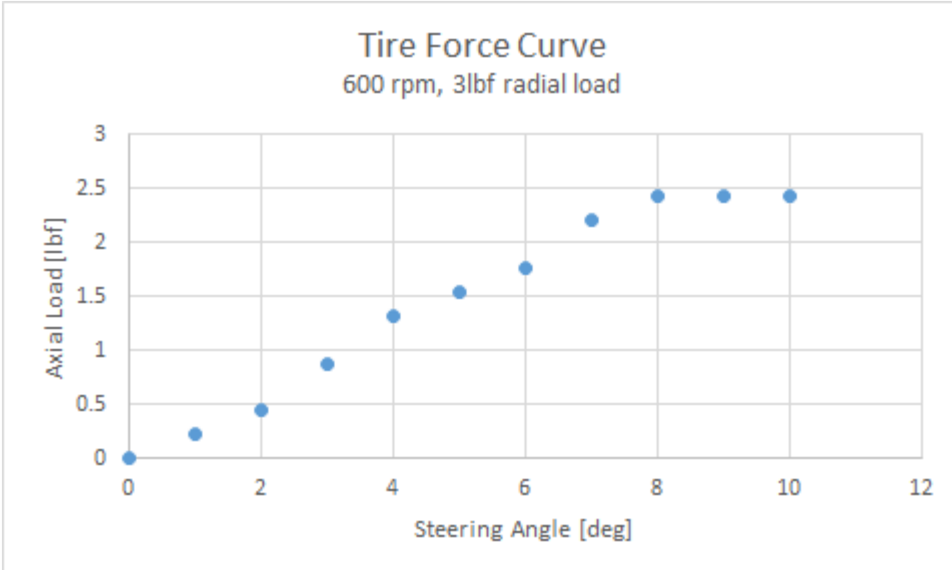


Figure 6.6 Tire force curve generated using calibrated fish scale, taken at constant speed and radial load

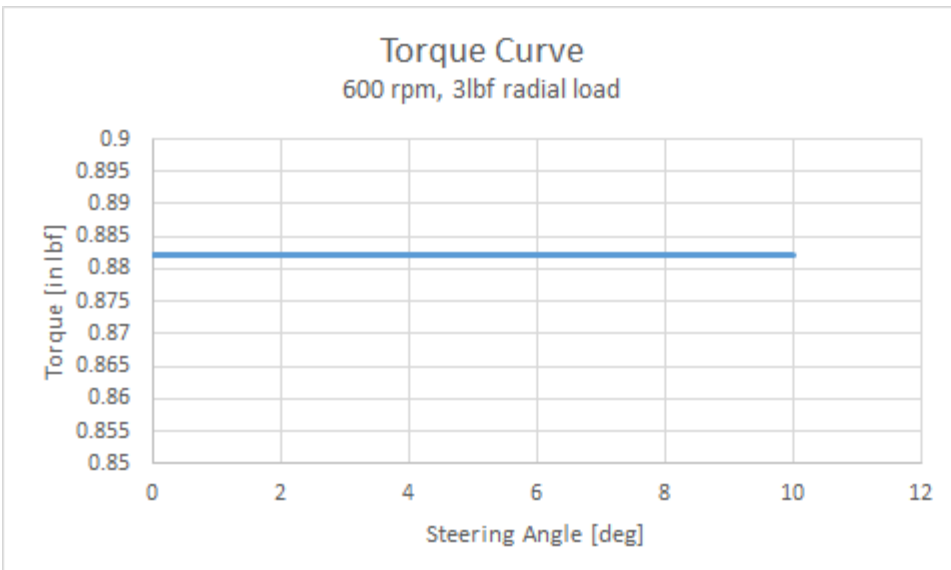


Figure 6.7 System torque curve measured by fish scale at location of torque load cell, taken at constant speed and radial load

Figure 6.6 Shows a tire force curve that follows the general shape of the tire force curve of a full-scale vehicle shown in this report. The axial load begins to peak near 9-10 degrees of steering. The magnitude of the peak force is near 2.5 lbs. Compared to the radial load of 3 lbs applied, the axial load peaks at a value near 100% of the radial load. This is in line with what is predicted from the theory. Figure 6.7 shows the measured torque value versus steering angle for a constant speed and radial load. The torque value remained constant throughout the test, regardless of steering angle. This is justified because the torque is a factor of the resistance between the motor poles for the dynamometer motor being measured. During the experiment, these poles were shorted to provide the maximum resistance. At a speed of 600 rpm and 3 lbs radial load, the maximum torque value is .882 inlbf. The torque arm is approximately 1" in length, and therefore the max load applied to the torque load cell is around .882 lbf.

A more meaningful graph may be a plot of the torque in the system versus speed. As speed increases, the force of air resistance increases, which is the main opposing force working against the forward movement of a car. Air resistance is a factor of velocity squared, and should therefore be increased exponentially in regards to an increase in speed. The air resistance can be modeled by altering the electrical resistance between the driven motor poles; as speed increases, electrical resistance should increase to simulate an increase in air resistance. Measurements of torque during this test should theoretically decrease exponentially as speed increases.

The motor mechanical time constant was specified to be greater than 1 second. The flywheel we designed to meet this time constant was designed to give the motor a 2-3 second time constant. However, these specifications were designed for a motor that had much more power supplied to it. Running the motor around 8V, the flywheel gave the motor a +10 second time constant. This was excessive, so the team looked to the Delrin dynamometer drum to see if it could provide a time constant closer to the specification. When attached to a motor running at 8V, the time constant for the dynamometer drum was near 3 seconds. The motor settling time was not tested due to time limitations. However, we predict based on the time constant that by tailoring the motor controller gains a settling time of over 4 seconds could be met.

With the capability to adjust the relative positions of the two motors in three axes, a simple shaft coupler system for application of new modules, and the ability to change the angle between the motor shaft by up to 15 degrees, the team feels confident that the device meets the modularity requirements as requested by the project sponsors.

## 6.2 Design Verification Plan

The Design Verification Plan is a method used to organize project specifications and develop a quantitative or qualitative method to test whether these specifications are met. Each specification is listed with an acceptance criterion to meet, and either a pass, fail, or partial pass categorization based off prototype testing. See the full DVPR in appendix L for more information.

# 7. Conclusion and Recommendations

The goal of the Dyno-Mite was to design, build, and test a scaled down version of an industrial tire test machine with modularity and versatility in mind to be used in laboratory experiments for the Cal Poly ME-422, Introduction to Mechanical Control Systems Class. The Dyno-Mite will replace the current Motomatic, which has become outdated and costly to repair. The design focused on safety, portability, modularity, and durability. The design created by the team draws from the previous design to ensure that the original educational objectives are met. The team utilized various problem-solving strategies to brainstorm solutions. Detailed analysis and iterative prototyping were used to verify design parameters and test for requirement satisfaction. This document serves as an understanding between the team and the sponsors that the goals, initial design choices, and direction of the project are agreed upon, and thus the objectives of the project were met.

# 8. References

Ridgley, John. "Handbook and Reference for ME 422 Laboratory." (n.d.): n. pag. *Calpoly.edu*. 2004. Web. 6 Feb. 2017.

"LabVolt Series by Festo Didactic - Mechanical Training Systems (46101-00)." *LabVolt Series by Festo Didactic - Mechanical Training Systems (46101-00)*. Lab Volt, n.d. Web. 06 Feb. 2017.

"DC Motor Control Trainer for NI ELVIS." *DC Motor Control Trainer for NI ELVIS - National Instruments*. National Instruments, n.d. Web. 06 Feb. 2017.

"Electric Motor Control Learning System." *Electric Motor Control Learning System | Tech-Labs*. Tech Labs, n.d. Web. 06 Feb. 2017.
<https://www.osha.gov/SLTC/noisehearingconservation/>

Quanser. *QET DC Motor Control Trainer Specifications*. N.p.: Quanser, n.d. *Quanser.com*. Web.

Nise, Norman S. *Control Systems Engineering*. 6th ed. Hoboken, NJ: Wiley, 2015. Print.

C. S. Hearn, D. A. Weeks, R. C. Thompson and D. Chen, "Electric vehicle modeling utilizing DC motor equations," 2010 IEEE/ASME International Conference on Advanced Intelligent Mechatronics, Montréal, ON, 2010, pp. 670-675.

"Using The Deflection Calculator." *80/20® Inc.* 80/20 Inc., n.d. Web. 04 May 2017.

DualM Studio - Http://www.dualm.com - Web Site Design Development, Veliko Turnovo, Bulgaria. "Resolution." *Interface China*. Interface Inc., n.d. Web. 04 May 2017.

Santos, Rodrigo De Oliveira. "The Absolute Guide to Racing Tires - Part 1 - Lateral Force. "*Racing Car Dynamics - Your Uncomplicated Resource to Race Engineering*. N.p., 22 June 2016. Web. 04 May 2017.

# 9. Appendices

[A] Management Plan
[B] Gant Chart
[C] FMEA
[D] House of Quality
[E] Design Development and Specification
[F] Concept Evaluation and Selection
[G] Additional Views of Top Concept Assembly
[H] Pugh Matrices
[I] Weighted Matrices
[J] Bill of Materials
[K] EES Analysis Code
[L] DVPR
[M] Product Specification Sheets
[N] Custom Part Drawings

**Appendix A: Management Plan**

Following the Critical Design Review, the team moved forward with part procurement and manufacturing. The next step was to build a functional prototype the team could use to fully test the specifications. With the prototype in hand, the team was able to modify and iterate the design, moving the Dyno-Mite closer to meeting all the project requirements.

The team aimed to nail down a detailed bill of materials, complete with vendor, vendor part number, corresponding Dyno-Mite part number, cost, material, ordering information, estimated shipping time, links to webpages, links to detailed drawings if necessary, required maintenance descriptions/instructions, and any other specifications such as power supply, tolerances, part accuracy, estimated functional life, etc. Coupled with the BOM is detailed Dyno-Mite assembly instructions, an exploded view, instructions, assembly precautions, and necessary tools.

After ordering parts and assembling the prototype, the team followed testing protocol to determine fulfillment of the design requirements. After seeing how the prototype performed, the team determined which aspects could use improving and attempted to redesign those components with the time remaining in the quarter. The CAD model was updated with each iteration, while maintaining copies of previous iterations for documentation and transparency purposes. The aim of the final quarter of this project was to continue to modify and improve the device for as long as time allowed, or until all involved parties were satisfied.

A large deliverable for the team was the application and operation of the load cells for the Dyno-Mite. This is a key component that will be instrumental in the effectiveness of the Dyno-Mite as a whole. This presented a big challenge for the team as load cell placement can be challenging and ineffective if done incorrectly. The team was aware of this and sought knowledge from our contacts and from literature to establish the best method for load cell placement. Although several different resources were consulted, the torque load cell still has issues for future designers to rectify.

Mathematical analysis preceded many of the final design decisions to verify preliminary design ideas. Theoretical verification results were verified with prototype testing whenever possible. These were done by hand and using the EES computer program. The team wants all engineering logic and reasoning employed to be traceable for any future reviewers of the project.

Members of Team Dyno-Mite were assigned specialty tasks and responsibilities as pertain to each individual's skills and interests. However, all members had equal weight in all matters, and thus tasks were occasionally redefined or reallocated as the team saw fit. Table 3. Displays the finalized responsibility allocations.

**Table A.1** Team Dyno-Mite Member Responsibilities

| Team Member | Responsibilities |
|---|---|
| Daniel Hoffman | Maintains team finances and budget. Collects receipts<br>Creator of testing protocol<br>Will oversee and perform testing of prototype<br>Ensures safety specifications are met<br>Maintains final BOM with all required parameters<br>Determines maintenance and repair considerations |
| Trey Young | Maintains information repositories for team<br>Maintains tasks and facilitates duties<br>Performs mechanical analysis for various systems. Vibrational analysis, structural analysis. Motor spec calculations.<br>Load cell placement research lead<br>Created preliminary BOM |
| Brandon Miller | Main source of communication between sponsor, advisor, and vendors<br>In charge of manufacturing parts, and part procurement<br>Maintains master CAD file, and version history<br>Safety officer. FMEA creator<br>Creator of assembly instructions |

**Table A.2** Task list with approximate completion date

| Task | Completed By |
|---|---|
| Order parts for prototype. Manufacture parts for prototype | 2nd week of May |
| Assembly and testing | 4th week of May |
| Assess risks, failure modes, problematic components. Reiterate design and re-test. | 1st week of June. Continuing until final project expo |

## Appendix B: Gantt Chart

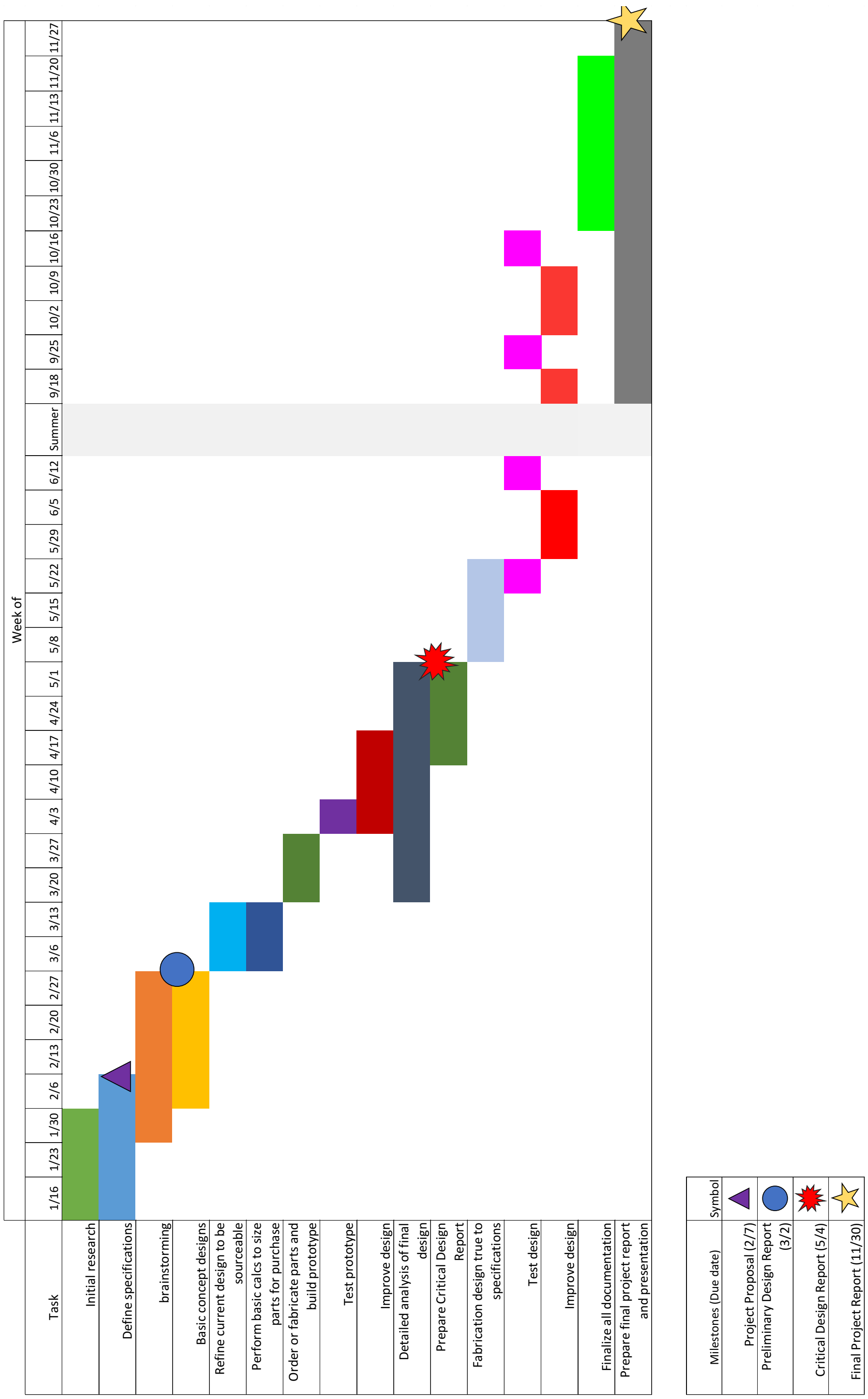

## Appendix C: FMEA

| Function | Function Components | Potential Failure Mode | Potential Cause of Failure | Occurrence | Potential Effects of Failure | Severity | Design Controls | Detection | RPN | Recommended Actions |
|---|---|---|---|---|---|---|---|---|---|---|
| Rotating Components | DC Motor | stall | excessive radial load | 2 | overheat | 9 | sensory observation, feel for excess motor heat | 2 | 36 | Current based emergency off switch |
| | | | | 2 | fatigue of motor components | 7 | maintenance inspection | 5 | 70 | |
| | | brush deterioration | over use | 1 | reduced performance, functionality, and life of motor | 7 | test motor for irregularities compared to datum | 4 | 28 | Routinely scheduled maintenance |
| | | | lack of maintenance | 2 | reduced performance, functionality, and life of motor | 7 | test motor for irregularities compared to datum | 6 | 84 | |
| | | sticking/friction | shaft misalignment | 5 | produces non-linear data | 8 | review response data for non-linearities | 7 | 280 | Eliminate need to align shaft, include aligning design features |
| | | | debris | 2 | produces non-linear data | 8 | review response data for non-linearities | 7 | 112 | Routinely scheduled maintenance |
| | | | lack of maintenance | 10 | reduced performance, functionality, and life of motor | 7 | review response data for non-linearities | 7 | 490 | |
| | | lack of power | improper motor selection | 2 | failure to produce measurable forces | 8 | review force data from prototype testing | 2 | 32 | Select proper motor via preliminary design and analysis |
| | | | | 4 | slow response | 3 | review response data from prototype testing | 2 | 24 | |
| | | spin out of control | no load | 2 | projectiles | 10 | test and inspect prototype for critical areas | 3 | 60 | Implement strong protective covers to protect from projectiles and tangling, design for fail safe secured components |
| | | | | 4 | tangling | 10 | review ergonomics, test consider unaware student scenario, loose clothing, hair, | 3 | 120 | |

| | | | | | | | | | | |
|---|---|---|---|---|---|---|---|---|---|---|
| | | | | | | | jewelry, etc… | | | |
| | | bearing wear | excessive radial load | 4 | increased friction | 6 | review response data for non-linearities | 4 | 96 | limit amount of weights available, design for worst case scenario for max combo of available weights |
| | | | | 4 | damage to motor | 7 | inspect motor bearings | 4 | 112 | |
| | | | | 3 | reduced performance, functionality, and life of motor | 7 | test motor for irregularities compared to datum | 4 | 84 | |
| | Tire | excessive slip | texture of tire and dyno drum | 3 | smoke | 7 | attempt to produce during testing, inspect | 2 | 42 | increase texture of tire and drum contact, increase radial load, shut off machine |
| | | | | 2 | heat | 6 | | 4 | 48 | |
| | | | | 4 | deposits tread material on drum | 4 | inspect contact areas | 4 | 64 | |
| | | | insufficient radial force | 3 | failure to produce measurable forces | 8 | review force data from prototype testing | 3 | 72 | |
| | | | excessive vibration | 4 | damage to apparatus | 8 | test at extreme load cases | 3 | 96 | |
| | | excessive vibration | tire tread characteristics | 3 | excessive vibration | 6 | test and observe prototype while running in different scenarios | 3 | 54 | low profile tire tread, design stiff structure, check for misalignment |
| | | | | 3 | structural damage | 8 | test and inspect structure for damage | 5 | 120 | |
| | | | | 5 | produces inconsistent or inaccurate data | 7 | review data for consistency | 5 | 175 | |
| | | | hub or tire misalignment | 4 | excessive vibration | 5 | test and observe prototype while running in different scenarios | 5 | 100 | |
| | | | | 2 | structural damage | 5 | Implement protective guards | 2 | 20 | |
| | | | | 5 | produces inconsistent or inaccurate data | 8 | review data for consistency | 6 | 240 | |

| | | | | | | | | | | |
|---|---|---|---|---|---|---|---|---|---|---|
| | DC Generator | too little torque | improper motor selection | 3 | unable to provide torque necessary to produce desired loading case | 10 | test, inspect, and review sensor data | 2 | 60 | Select proper generator via preliminary design and analysis |
| | | too much torque | improper motor selection | 3 | damage to apparatus and dangerous to user | 7 | test, inspect, and review sensor data | 6 | 126 | |
| | | sticking/friction | shaft misalignment | 5 | produces non-linear data | 8 | review response data for non-linearities | 7 | 280 | Eliminate need to align shaft, include aligning design features |
| | | | debris | 2 | produces non-linear data | 8 | review response data for non-linearities | 4 | 64 | Routinely scheduled maintenance |
| | | | lack of maintenance | 10 | reduced performance, functionality, and life of motor | 7 | review response data for non-linearities | 7 | 490 | |
| | Shafts | yielding | excessive radial load | 3 | damage to the shaft | 7 | test for worst case scenario | 2 | 42 | Select proper motor shaft size via preliminary design and analysis, implement protective guards around rotating components |
| | | | | 2 | harm to users | 8 | test for worst case scenario | 7 | 112 | |
| | | excessive deflection | excessive radial load | 3 | contact with other components | 8 | test for worst case scenario | 5 | 120 | Select proper motor shaft size via preliminary design and analysis, implement proper clearances |
| | | | | 3 | damage to system | 8 | | 6 | 144 | |
| | | shear | excessive radial load | 2 | damage to system | 8 | test for worst case scenario | 6 | 96 | Select proper motor shaft size via preliminary design and analysis |
| | | | | 2 | harm to users | 9 | | 2 | 36 | |
| | | resonance/vibration | excessive radial load | 3 | damage to system | 8 | test for worst case scenario | 6 | 144 | Conduction vibration analysis |
| | | | | 3 | produces inconsistent or inaccurate data | 8 | review data for consistency | 4 | 96 | |
| | Dyno Drum | vibration/whirl | misalignment | 3 | damage to system | 7 | test for worst case scenario | 6 | 126 | Conduction vibration analysis and shaft whirl case |
| | | | | 6 | produces inconsistent or inaccurate data | 8 | review data for consistency | 4 | 192 | |
| | | | | 2 | harm to users | 9 | test for worst case scenario | 7 | 126 | |

| | | | | | | | | | | |
|---|---|---|---|---|---|---|---|---|---|---|
| Radial Load App. | Weights | movement | vibration | 6 | cause inconsistencies in force readings | 7 | review data for consistency | 2 | 84 | Conduct testing and see take note of how the weights vibration affects the data |
| | | falling out | vibration | 2 | fall on users appendages | 9 | Test at highest vibrational settings | 2 | 36 | test to see if weights could fall out of device |
| | | | | 4 | fall on system components | 8 | | 2 | 64 | |
| | | | | 4 | damage weights | 8 | Inspect weights for damage | 2 | 64 | |
| | Moment arm assembly | excessive deflection | insufficient stiffness | 2 | inaccurate load sensing | 7 | perform analysis and testing | 5 | 70 | Mathematical analysis to justify thickness and length |
| | | | mechanical play | 3 | Components not aligning properly | 7 | testing at all angles for alignment and play | 3 | 63 | |
| | | inaccurate load transfer | sticking/friction | 4 | Not transmitting the forces accurately | 8 | review response data for non-linearities | 4 | 128 | Compare to original data obtained from the new model |
| Steering Angle App. | Pins/Slots | widening | large bearing stresses | 2 | angle device isn't secure from deviations | 7 | select material with adequate strength | 3 | 42 | design with tolerances in mind and inspection after manufacture |
| | | shear | large shear stresses | 2 | broken pins | 8 | select material with adequate strength | 3 | 48 | |
| | | catching | manufacturing error | 5 | pins not fitting in slots or holes | 8 | Perform testing and inspection | 2 | 80 | |
| | Sliding Plates | not able to rotate | friction | 4 | difficult to change angle precisely, wear over time | 8 | Select a material with less friction | 2 | 64 | testing to feel effect of friction and tightness of fasteners |
| | | | over tightened fasteners | 3 | cannot change angle | 8 | adjust tightness of bolts or screws | 1 | 24 | |
| | | | manufacturing error | 5 | cannot change angle | 8 | inspection and testing | 2 | 80 | |
| | | lack of stiffness | manufacturing error | 2 | angle not accurate, can change during use | 6 | analysis of stiffness and deflection | 4 | 48 | Mathematical analysis to justify thickness and length |
| | Angle Reference | inaccurate | manufacturing error | 3 | inaccurate angle callout | 7 | inspection and re-manufacture | 5 | 105 | Inspection of tick marks and double check with a protractor |
| | | | deterioration of tick marks | 9 | hard to read measurement | 5 | design tick marks deep and large enough to maintain visibility | 3 | 135 | |

| | | | | | | | | | | |
|---|---|---|---|---|---|---|---|---|---|---|
| Steering Angle Lock. | Bolts | shear | large shear stresses | 1 | bolts shearing off | 7 | analysis of bolt stresses | 2 | 14 | Mathematical analysis of shear stresses in bolts |
| | | stripping | debris | 4 | loss of functionality | 7 | include spare bolts | 4 | 112 | Cleaning after use to reduce debris |
| | | | not ergonomic to thread | 4 | bolts don't function | 8 | Redesign threads | 3 | 96 | inspection check after manufacturing |
| | Holes | widening | large bearing stresses | 2 | mechanical play | 7 | inspect and perform wobble test by hand | 3 | 42 | Inspection and test to see how loose the angle bar has become |
| | | misalignment with holes | manufacturing error | 5 | Holes loos functionality | 7 | inspection and testing | 2 | 70 | widen the holes or re-manufacture base |
| | | | overly tight tolerances | 4 | bolts don't fit in hole and loos functionality | 7 | perform inspection and testing | 2 | 56 | |
| Determining Load | Weights | inaccurate | manufacturer defects | 2 | weight recorded is not true force on the tire. Data biased | 6 | verify weights for proper mass | 6 | 72 | weigh the weights every once in a while to verify their masses |
| | | | quality of weights | 1 | Not true weight listed | 6 | | 7 | 42 | |
| | | weights falling off device | bumping or vibration | 5 | falling weights, damage to parts or user | 9 | Test at highest vibrational settings | 2 | 90 | Perform vibrational test to see if weights fall out |
| | Frame | deformation | large stresses | 1 | permanent deformation of frame | 9 | test for worst case scenario | 5 | 45 | analysis for frame added safety factor, and testing at highest load |
| | | deflection | lack of stiffness | 4 | misalignment of components, noise in system | 8 | test for worst case scenario | 5 | 160 | |
| | | | large forces | 3 | too much deflection, shaft no longer straight | 8 | | 5 | 120 | |
| | Load Cells | inaccurate | superimposed forces | 3 | not true force desired force output | 8 | testing with known force | 8 | 192 | Perform verification tests with known forces |
| | | | quality of load cells | 3 | noisy or inconsistent force readings | 7 | | 8 | 168 | |
| | | breaking | bumping | 10 | broken load cells | 8 | testing with known force | 7 | 560 | specs for max rated loads compared to expected loads, with factor of safety |
| | | | materials being dropped on them | 10 | broken load cells | 9 | | 6 | 540 | |
| | | | too much radial force | 3 | broken load cells | 8 | | 7 | 168 | |
| | | | pressing on assembly | 10 | broken load cells | 8 | | 7 | 560 | |

44

| | | | | | | | | | | |
|---|---|---|---|---|---|---|---|---|---|---|
| | Encoder | deterioration | extended use | 10 | encoder broken | 9 | review response data from earlier runs | 8 | 720 | Compare recent data to earlier known data to see if the encoder still displays the known values |

## Appendix D: House of Quality

| Legend | |
|---|---|
| Category | Scale |
| Whats vs. Whos | 1-17 (1 most important) |
| Nows vs. Whats | 1-4 (4 best) |
| Hows vs. Whats | 1 (low correlation), 3 (med), 9 (high) |

| Whats | Item No. | Whos: Lab Students | Lab Instructors | Technician | Builders | Hows: Fatigue life to failure | Maintence time per quarter | Fasteners torqued to specification | Decibel level | Time spent to access a specific part | Labels / Directions for adjustable features | Physical adjustment limits | # of accesible pinch points | # of accesible tangle points | % Error btw data and theor. | Sensor measurements | Interchangeable loads | Cost per device | Area of footprint | % of custom parts sourced | Emergency shut off | Time spent to make a single adjustment | Clearence for tools | Time to construct apparatus | Weight | % of parts contained attached to frame | Max opertaional voltage | motor time constant | settling time | overshoot | scaled torque value | Nows: Current Motomatic | Volt mechanical training system | Quanser DC motor control trainer | NI Elvis | Tech Labs Electric Motor Control Learning System |
|---|---|---|---|---|---|---|---|---|---|---|---|---|---|---|---|---|---|---|---|---|---|---|---|---|---|---|---|---|---|---|---|---|---|---|---|---|
| | | 1 | 2 | 3 | 4 | A | B | C | D | E | F | G | H | I | J | K | L | M | N | O | P | Q | R | S | T | U | V | W | X | Y | Z | 1 | 2 | 3 | 4 | 5 |
| Rugged | 1 | 6 | 6 | 2 | 4 | 9 | 9 | 9 | | | | | | | | | | | | | | | | | 1 | | | | | | | 3 | 4 | 4 | 4 | 3 |
| Quiet | 2 | 4 | 11 | 13 | 16 | | | | 9 | | | | | | | | | | | | | | | | | | | | | | | 4 | 3 | 5 | 3 | 4 |
| Easy to Repair | 3 | 14 | 5 | 1 | 6 | 3 | 3 | | | 9 | | | | | | | | | | 9 | | | 9 | 1 | | | | | | | | 2 | 2 | 5 | 2 | 2 |
| Fool Proof | 4 | 1 | 7 | 4 | 14 | | | | | | 9 | 9 | 9 | 9 | | | | | | | | 3 | | | | | | | | | | 1 | 2 | 4 | 2 | 2 |
| Meets Educational Goals | 5 | 5 | 1 | 14 | 15 | | | | | | 1 | | | | 9 | 9 | 3 | | | | | | | | | | | 9 | 9 | 3 | 9 | 2 | 4 | 2 | 4 | 4 |
| Inexpensive | 6 | 17 | 16 | 8 | 3 | | | | | | | | | | | 3 | | 9 | | 3 | | | | | | | | | | | | 4 | 1 | 3 | 1 | 1 |
| Tabletop Size | 7 | 10 | 13 | 7 | 7 | | | | | | | | | | | | | | 9 | | | | | | 1 | 3 | | | | | | 4 | 1 | 5 | 1 | 3 |
| Safe | 8 | 3 | 9 | 11 | 10 | 3 | | 3 | 3 | | 9 | 9 | 9 | 9 | | | | | | | 9 | | | | | | | | | 1 | | 2 | 4 | 4 | 4 | 4 |
| Modular | 9 | 9 | 8 | 15 | 8 | | | | | 3 | 1 | 1 | | | | | 9 | | | | | | | | | | | | | | | 1 | 4 | 2 | 4 | 3 |
| Portable | 10 | 11 | 10 | 5 | 9 | | | 1 | | | | | | | | | | | 9 | | | | | | 9 | 3 | | | | | | 2 | 1 | 5 | 1 | 3 |
| Apparatus Self Contained | 11 | 12 | 14 | 10 | 5 | | | | | 3 | | | | | | | | | 3 | | | | 3 | | 3 | 9 | | | | | | 4 | 3 | 5 | 3 | 4 |
| Industrial Appearance | 12 | 7 | 12 | 16 | 13 | | | | | | | | | | | | | 1 | | 1 | | | 1 | | 1 | | | | | | | 2 | 4 | 2 | 4 | 4 |
| Readily Available Parts | 13 | 15 | 15 | 3 | 2 | 3 | | | | | | | | | | | 1 | 3 | | 9 | | | | | | | | | | | | 1 | 2 | 4 | 2 | 2 |
| Easy to Adjust | 14 | 2 | 2 | 9 | 12 | | | | | 3 | | | | | | | 3 | | 3 | 1 | | 9 | 3 | 1 | 1 | | | | | | | 2 | 3 | 3 | 3 | 3 |
| Easy to Construct | 15 | 16 | 17 | 12 | 1 | | | 1 | | 3 | | | | | | | 3 | 3 | | 1 | | | 9 | 9 | | | | | | | | 3 | 1 | 5 | 1 | 2 |
| Research Application | 16 | 13 | 4 | 17 | 17 | | | | | | | | | | 3 | 1 | 3 | | | | | | | | | | | 3 | 3 | | | 1 | 4 | 2 | 4 | 3 |
| Compatible with Lab Space | 17 | 8 | 3 | 6 | 11 | | | | 1 | | | | 3 | 3 | | | | | 3 | | | | | | | | 9 | | | | | 4 | 3 | 5 | 3 | 4 |
| Targets / How Much | | | | | | 15 years | < 1hr per device | Yes | < 50 dB | < 5min | Yes | Yes | 0 | 0 | < 10% | force, pos, vel | Yes | < $1500 | < 2'x2' | < 40% | Yes | < 5min | Yes | < 3hrs | < 50lbs | 100% | < 45V | > 2 seconds | > 1 second | < 80% | 40mNm, +- 10mNm | Sum | | | | |
| Weighted Importance | | | | | | 18 | 12 | 14 | 13 | 21 | 20 | 19 | 21 | 21 | 12 | 13 | 22 | 16 | 27 | 24 | 9 | 12 | 25 | 11 | 16 | 15 | 9 | 12 | 12 | 4 | 9 | 407 | | | | |
| % Importance | | | | | | 4.4% | 2.9% | 3.4% | 3.2% | 5.2% | 4.9% | 4.7% | 5.2% | 5.2% | 2.9% | 3.2% | 5.4% | 3.9% | 6.6% | 5.9% | 2.2% | 2.9% | 6.1% | 2.7% | 3.9% | 3.7% | 2.2% | 2.9% | 2.9% | 1.0% | 2.2% | 100.0% | | | | |

**Appendix E: Design Development and Specification**

Preliminary Design Specifications

The design will incorporate two adjustable features vital to the function of the machine. The first adjustment is the ability to change the force that the tire applies to the dynamometer. This represents the weight of a vehicle distributed through a single tire. The second adjustment is the ability to change the steering angle between the tire and the dynamometer. This simulates slip when turning, and allows users to analyze the force applied to the road when turning. These adjustable features will incorporate labels, directions, and physical limits so that they cannot be adjusted in a way that would damage the apparatus or injure the user. The major components of the Dyno-Mite assembly will be contained within a frame, while maintaining the possibility of interchangeable loads, so that the device is portable. In addition to increased portability, this ensures the accuracy and consistency of crucially positioned components.

One goal is to ensure the device has a functional life of 15 years. This value was specified by the team sponsor. This ensures a long-term, reliable apparatus that would provide a good return on their investment. It is important to provide the most value possible to the students of Cal Poly. This has been labeled a medium risk target because it can be achieved with thorough analysis and high quality components.

The team believes a well-designed device should not require constant maintenance as some of the current devices do. One of the design targets is to limit the time required to keep the device in working order to one hour per quarter. This has been labeled a medium risk target because it can be more challenging and costly to design a more rugged system, but this can be achieved through rigorous testing and comparison to the current device.

The sponsors' plan is to use eight or more of these devices simultaneously in the controls lab when instructing students, and it is important to be able to communicate with students while the devices are running. The team has decided to aim for a total of less than 50 dB output in the classroom among the devices. This value was chosen after researching average decibel levels for classroom conversation This has been labeled a medium risk target because noise can be limited easily with the use of good bearings and proper lubrication.

To ensure maintenance is as simple and painless as possible, the team is committed to designing a device that is quick to assemble and disassemble. The team defines "quick" as requiring no more than five minutes to access any part on the device for repair or replacement. This is a medium risk target.

The team is committed to an informative, streamlined user experience, and believe an important part of this is to ensure students can intuitively use any adjustment mechanisms on the body of the device. The team plans to include informational labels on all adjustment mechanisms to hit this target. This parameter is considered low risk and will be accomplished through inspection and testing.

To make the device safer and foolproof, the team will included physical limitations on all adjustment mechanisms that will prevent dangerous or incorrect adjustments. These additions are simple to integrate into the adjustment assemblies, therefore, this is a low risk parameter that is accomplished through inspection.

The device will have several moving parts and will be rotating at high velocity while in use. This introduces the possibility of pinching if used incorrectly or carelessly. The team has decided to make it a priority to eliminate or cover all accessible pinch points. This is a medium risk target because it is extremely crucial to student safety, and it will be accomplished through inspection and testing of suspected pinch points.

It is easy to be careless, especially for students who are trying to move quickly to complete the lab. Therefore, the team wants to design with the safety of the user in mind. Since the Dyno-Mite will include rotating parts, there is the danger of tangle points. The design will have limited exposed tangle points. This could be executed a number of ways, for example through the use of plastic guards. This parameter will have a medium risk of completion and can be verified via testing and inspection.

In order to make the machine safer, the inclusion of an emergency shut off switch is necessary. With a medium power electric motor, rotating machinery, and pinch points, an emergency shut off switch will greatly reduce the chance or severity of an accident. This is a low risk parameter. This can be verified through testing the switch and inspection.

One critical aspect to the effectiveness of the Dyno-Mite is that it must provide consistent and accurate data. The Motomatic gives data that does not substantiate theory taught in the class. This is due to high friction and stiction in the system and outdated sensors. Bad data directly conflicts with the most important reason to do a laboratory experiment, which is to conduct a hands-on activity that confirms theory presented in the classroom. The team has set a goal for the Dyno-Mite to achieve less than 10% error between the experimental data recorded and the theoretical data. This is a mission critical parameter that is dependent not only on the quality of the parts sourced, but design for manufacturability, and expected tolerances among parts. This parameter is high risk, and will be overcome by sourcing quality parts, and creating a good design that is rigid and aligned. This will be confirmed via analysis and testing.

The Dyno-Mite is to be monitored with sensors that are able to record data that could ultimately be used to find the torque applied by the motor, the torque applied by the load, the position and velocity of the tire, and the position and velocity of the load. This could be achieved in many ways, using different types of sensors. As long as the sensors implemented on the machine can provide these measurements or provide data that could be used to calculate these measurements, then the parameter is met. This is vital to meeting the educational goals set by the customer. This parameter has a low risk, due to the plethora of precise sensor types available, for various applications. This will be verified through inspection.

A substantial design consideration set by the customer was to design with modularity in mind, specifically for interchanging different loads into the system. The risk of achieving this is high. It might be simple to meet the goal of developing a certain type of connection that allows for interchangeability, however, modularity is a large concern when creating the layout of the machine. Some of the loads proposed by the sponsors were a four-bar linkage, chain drive, gear train, and robotic arm. Special attention and consideration will be payed to creating a layout that is compatible with many different attachments. This will be done by being generous with space, and considering all types of motion and collision points. This parameter will ultimately be verified through testing and inspection.

The customer specified that in order to make at least 10 units of the Dyno-Mite, no more than $1,500 should be spent per unit. This has been assessed as a medium risk parameter. However, there are always unforeseen expenses. This parameter will be verified via inspection.

In order for the Dyno-Mite to be portable and fit on the laboratory bench tabletops, the team set the target for the footprint of the base of the frame to be no more than 2 sq-ft. This is a medium risk parameter. It is crucial that a good layout be created in order to minimize space, while still considering constructability, reparability, and sturdiness. Once parts have been sourced and the sizes determined, an understanding of the risk may change. This parameter will be verified via analysis and inspection.

The Dyno-Mite should be inexpensive and have easily sourced parts. One parameter that the team came up with, that affects these two needs, is the percent of custom parts sourced. This should be no more than 40%. The parts being considered are specific to structural components. It is beneficial to have as many parts sourced from manufacturers as possible. This has been determined as a medium risk parameter due to the large support of the engineering community at Cal Poly, sponsors, and the vast number of things that can be ordered off the internet. The compliance will be verified through inspection.

To make the Dyno-Mite easy to use, the team decided upon a parameter that quantified the time spent for a user to make a single adjustment to the assembly. It was agreed that it should take no more than 5 minutes. The adjustments referred to in this parameter are the tire force and steering angle adjustments that will be used multiple times during execution of the laboratory experiment. This parameter is medium risk and can be verified through testing and inspection.

In order for the Dyno-Mite to be easy to repair and quick to remove parts, the design must allow for clearance of tools to access screws, bolts, and fasteners. The team wants a technician to be able to access any part for replacement or repair as quickly and easily as possible. If a technician must remove multiple parts just to access the screws for the part he wants to fix then the team considers that a failure of the design. This is a medium risk parameter as it has a large effect on other related parameters such as maintenance time per device per quarter and time spent to access a specific part. This parameter can be verified through inspection.

In an attempt to keep overall complexity and part count down, the team set the parameter that the overall time to construct the final assembly should be less than 3 hours. This does not include the manufacturing time. This is a low risk parameter as this full-scale assembly should only have to be performed once per device for the life of the device. This parameter can be verified through testing and inspection.

Weight is an important variable to consider, as it has an effect on the design's portability. This is a low risk parameter because it should be easy to keep the design below 50 lbs given the proposed size of the design and the relatively low power of the devices and motors. The combined weight should be comfortably within human carrying capacity even if the team only pays slight attention to the weight of the parts. This parameter will be verified by testing and inspection.

Containing all of the parts on one solid frame is a critical parameter that directly impacts the portability and basic layout of the team's design. This is low risk and will be easy to determine if the specification has been achieved simply by inspection. As long as all the parts, aside from the controls unit, are securely attached to the frame so that it can all be picked up as one unit, then the team has successfully fulfilled this parameter.

Something simple but important to consider is compatibility with the lab space currently in use. This includes making sure that the device operates below the range of 45 V to ensure the safety of users and avoid violating campus safety policy regarding voltages over 45V. This is a low risk parameter as it will be considered in the selection of a motor. This parameter will be verified by analysis and inspection.

A crucial value in choosing the motor for the Dyno-mite, is to select a motor with a motor time constant that will be long enough for the system to speed up with a $1^{st}$ order response. In order for the speed up time to remain a $1^{st}$ order response, the motor mechanical time constant must be substantially greater than the motor inductance time constant, in the realm of around 1000 times longer. This is dependent on the motor characteristics and the inertia in the system. Another reason a long mechanical time constant is desirable is that it allows the student to observe the transition to steady state. If the time constant is too short, the transition will appear "instantaneous", and students won't get the benefit of observing the phenomenon they are testing. The settling time constant is typically four times the mechanical time constant. We estimate that the optimal motor time constant must be no less than 1 second in order to meet these requirements because the motor inductance constant is usually on the order of a few milliseconds, and a settling time of four seconds is ample time to observe the DC motor response characteristics. This parameter will be verified via analysis and testing.

Settling time refers to the time it takes for a motor to reach and remain within 98% of the desired control parameter, whether that be position or speed. This parameter is related to friction in the system, inertia, and controller characteristics. By selecting a mechanical time constant of at least 1 second, we are specifying a settling time of approximately four seconds, or four times the time constant. This will be confirmed through analysis and testing.

Choosing a motor with an appropriate torque range is crucial to accurately modeling a full scale vehicle. The Dyno-Mite will model a vehicle traveling between 40 and 70 mph. Figure 3.1 below, shows the Torque-Speed curve of different Tesla Model S versions. We used the average torque value of the Tesla Model S within this speed range as a reference. We analyzed the dimensions of torque and determined that if we are scaling the vehicle length dimensions, the torque should be scaled by a power of 5. We also assumed that, because most modern cars utilize a rear differential, all of the torque output would be through one tire at a time. This means we scaled the entire torque output from the vehicle and didn't divide the torque by the number of powered tires on the car. This allowed us to arrive at the value of 2.5 mNm ± 0.5 mNm for the Dyno-mite. We used this value to select a motor that is able to provide sufficient torque at the test speed. This parameter will be confirmed through analysis, testing, similarity, and inspection.

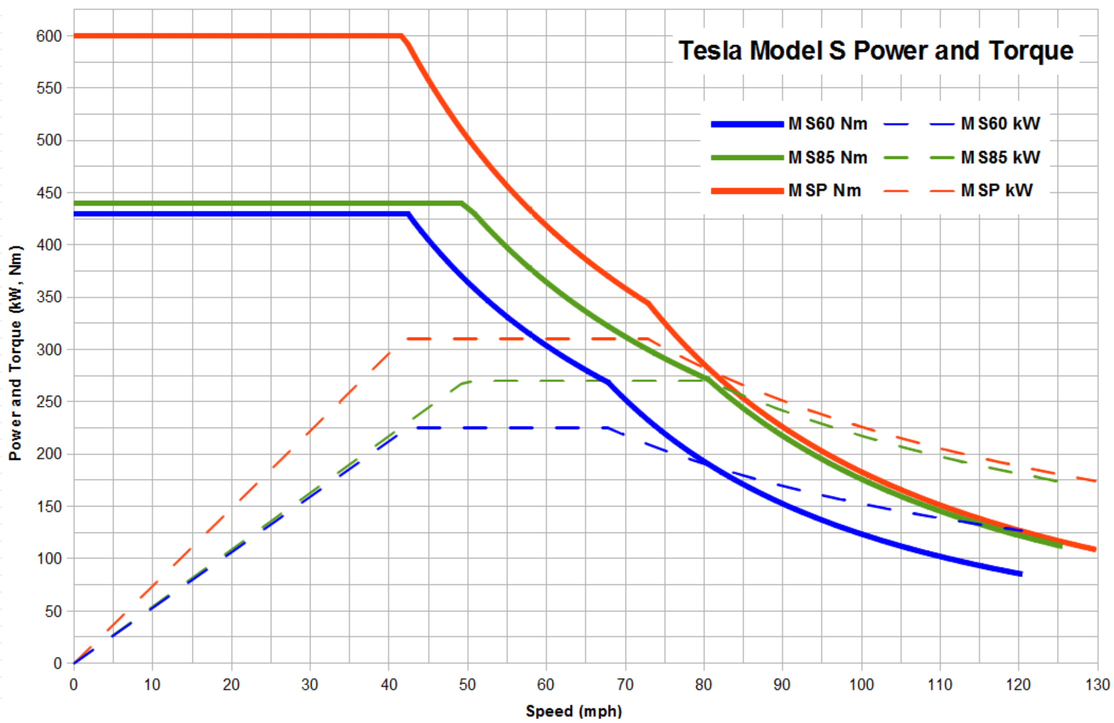


**Figure E.1** Vehicle performance curves of different Tesla Model S versions

**Appendix F: Concept Evaluation and Selection**
.
The top concept for the Dyno-Mite uses a brushed DC motor, weights to set the radial load, a three-pin rotating platform to change the steering angle, bolts and holes to lock the steering angle, a load cell positioned on the motor to determine axial load, strain gauges to determine shaft torque, and a shaft encoder to determine shaft position and velocity.

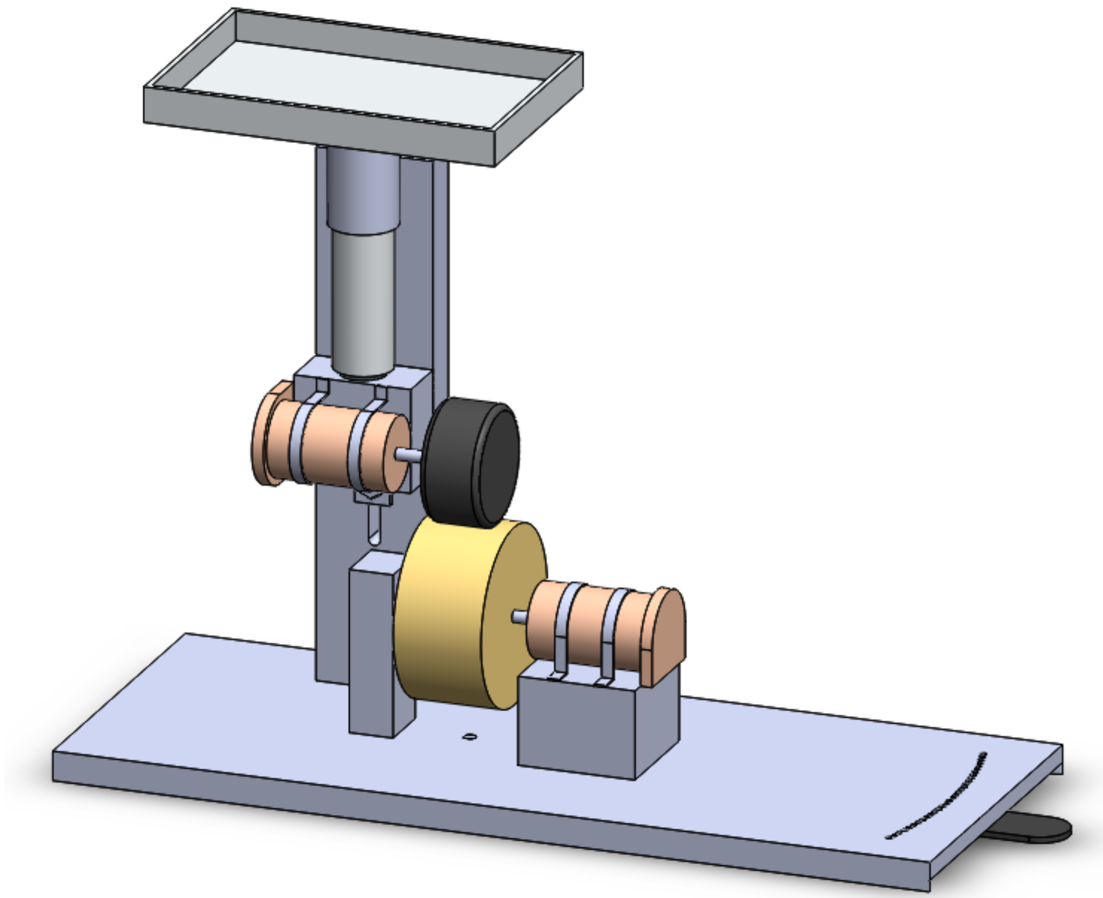

**Figure F.1** Isometric view of the assembly containing examples of each top-rated concept. Portrays one possible design iteration of the concepts. Does not show load cell locations or strain gages. Additional views can be found in Appendix C.

The top concept was determined through preliminary analysis using comparison matrices. This concept was synthesized from several functions identified as critical to the design that have various potential solutions. The functions identified were shaft rotation or DC motor choice, setting and determining radial load, changing and locking steering angle, determining axial load, determining shaft torque, determining shaft position, and determining shaft velocity. After analyzing the outcomes from the Go/No-Go process, Pugh Matrices, and Weighted Matrices, a top concept was selected by combining the highest ranking solutions from each function.

The Go/No-Go process assessed all potential ideas with respect to each function, and eliminated any that clearly violated specifications. Those that did not pass this test were considered No-Go and discarded before further levels of analysis.

The next step of our analysis process was to develop a Pugh Matrix for each function. Pugh Matrices rank concepts based on each of the criteria for that specific function with reference to one concept which acts a datum. The concepts are then given either a '+' for exceeding the datum, a '-' for underperforming compared to the datum, or an 'S' if they perform similarly. These scores were used to gain greater insight into achievability of requirements, deeper understanding of problems and potential solutions, and modification of solutions to better fit the criteria.

For each function, a Weighted Matrix was used to give numerical values to each concept to provide greater insight into the merit of each option. This allows for more detailed comparisons with the criteria due to increased fidelity. Weighted Matrices provide a better perspective on the strengths and weaknesses of solutions, especially with reference to the most important criteria. Weighted Matrices help in the final selection of top concepts.

**Table F.1** Table organizing the top concepts from the weighted matrices for each function. The concepts listed are explored further in the following sections.

| **Function** | *Radial Load App./ Det.* | *Steering Angle App.* | *Steering Angle Locking* | *Axial Load Det.* | *DC Motor* | *Torque Det.* | *Position/Velocity Det.* |
|---|---|---|---|---|---|---|---|
| **Top Concepts** | Weight<br><br>Spring/Lead Screw | 3 Pins<br><br>Slot Guide | Bolt in Hole<br><br>Clamp Plates | Load Cell<br><br>Strain Gauge | Brushed<br><br>Brushless | Calculate<br><br>Load Cell | Encoder |

**<u>Radial Load Application and Determination</u>**

Function Description: The radial load is the force applied to the tire and dynamometer drum. Force application and determination were two separate categories during our design selection phase, but the two top concepts fulfill each task simultaneously, so the team combined them into in one category to eliminate redundancy.

Criteria: When completing the weighted matrices for the radial load application and determination categories, the team decided that the most important criteria were accuracy and ease of implementation. The team weighted these criteria heaviest because our top priority is ensuring a high quality educational experience and the longevity of the device through simplicity of design and ease of repair.

**Weights**

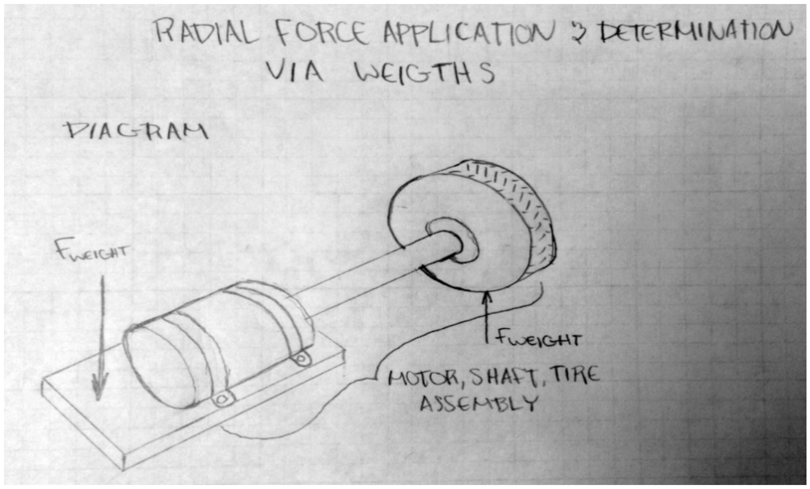


**Figure F.2** Hand sketch diagram illustrating the weights concept for setting and determining radial force. Shaft length exaggerated for clarity.

Weights are used to place a downward force on the motor, shaft, tire assembly that is translated down the shaft to the point of tire/dyno contact. This may either be achieved by stacking weights, hanging them, or using a moment arm in combination with a weight. Using weights eliminates the need to measure the force because the force is already known.

| Pros | Cons |
|---|---|
| • Durable<br>• Few moving parts<br>• Force is a predetermined value labeled on the weight | • High part count<br>• Potential balance issues |

**Spring/Lead Screw**

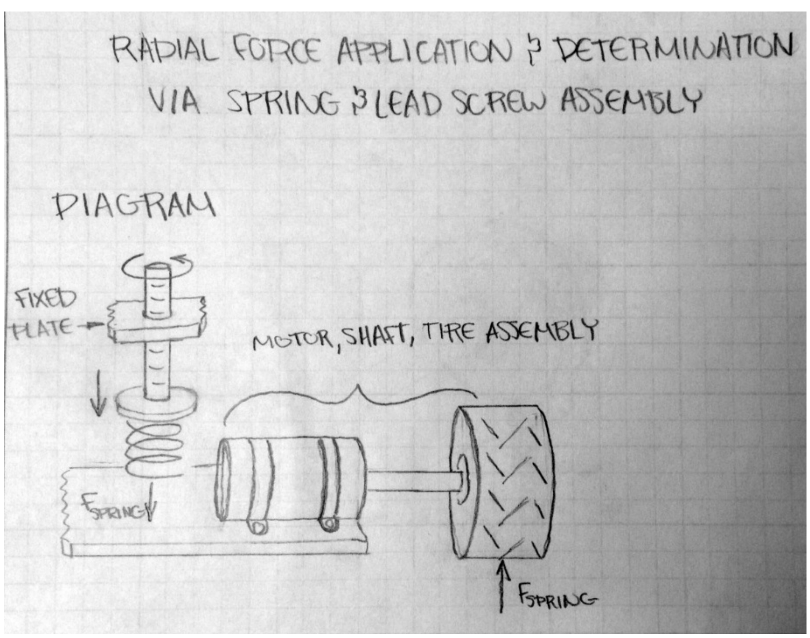

**Figure F.3** Hand sketch diagram illustrating the spring and lead screw concept for setting and determining radial force. Shaft length exaggerated for clarity.

A lead screw is used to compress a spring to exact displacements that will place a corresponding downward force on the motor, shaft, tire assembly that is translated down the shaft to the point of tire/dyno contact. The displacement would be measured using a ruler. This concept may not be as accurate due to measurement error and changes in spring elasticity.

| Pros | Cons |
|---|---|
| • Infinite variability in forces, up to the max spring displacement before permanent deformation | • More moving parts<br>• Accuracy<br>• Ease of implementation |

**Top Choice**

The top concept for the radial force application and determination function was weights. This is based on the teams weighted design matrix. Weights are ideal because they are highly durable and greatly simplify the design of the apparatus by eliminating extra moving parts and reducing the number of required sensors.

**Steering Angle Adjustment Mechanism**

Function Description: Steering angle is the contact angle between the tire and the dynamometer drum. This is used to create an axial force reacting on the tire.

Criteria: When completing the weighted matrices for the steering angle application category, the team decided the most important criteria were ease of adjustment and ruggedness. The team weighted these criteria heaviest because we expect this function to see a lot of repeated use. The team wants to ensure the function does not detract from the user experience, and the team has made device longevity a high priority.

**Three-Pin**

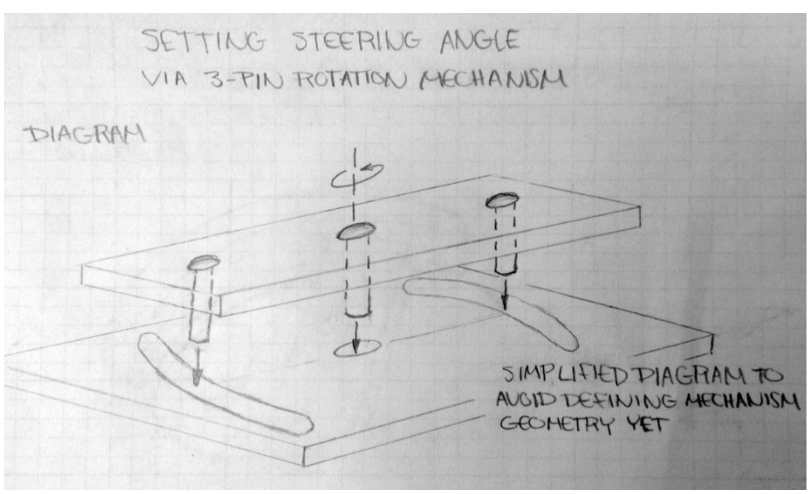

**Figure F.4** Hand sketch diagram illustrating the three-pin concept for applying the steering angle.

The rotating plate is constrained to turn around a center pin. Two pins on the outer edge of the plate are constrained to slide in curved slots of appropriate radii to create a smooth, continuous rotation.

| Pros | Cons |
|---|---|
| • Good stability<br>• Lends itself to both angle locking methods | • Low friction |

**Slot Guide**

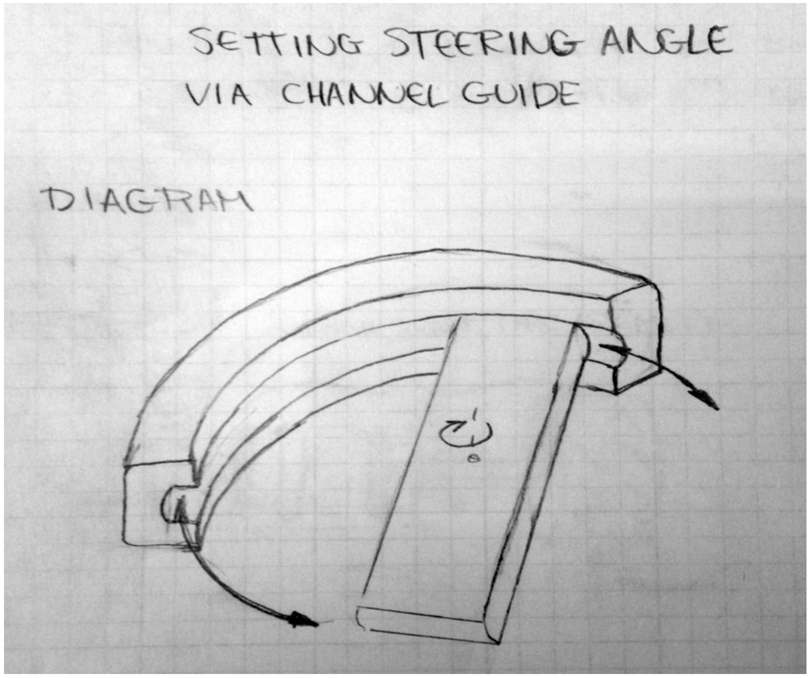


**Figure F.5** Hand sketch diagram illustrating the slot guide concept for applying the steering angle

The outer edge of the rotating plate is constrained to turn in a circular channel cut into the stationary plate.

| Pros | Cons |
|---|---|
| • Very high stability<br>• High friction | • More difficult to implement either angle locking methods<br>• Challenging to cut channel into stationary plate |

**Top Choice**

The top concept for steering angle application is the three pin mechanism. The three pin mechanism works well for the device because it provides high stability, and it is more simple to integrate slots into the base of the device than a circular channel.

**Steering Angle Locking Mechanism**

Function Description: The object of this function is to maintain the desired steering angle for the duration of the test.

Criteria: When completing the weighted matrices for the steering angle locking category, the team decided the most important criteria were accuracy and efficacy. The team weighted these criteria heaviest because our top priority is ensuring a high quality educational experience that accurately reflects the dynamics of a turning tire.

**Bolt & Hole**

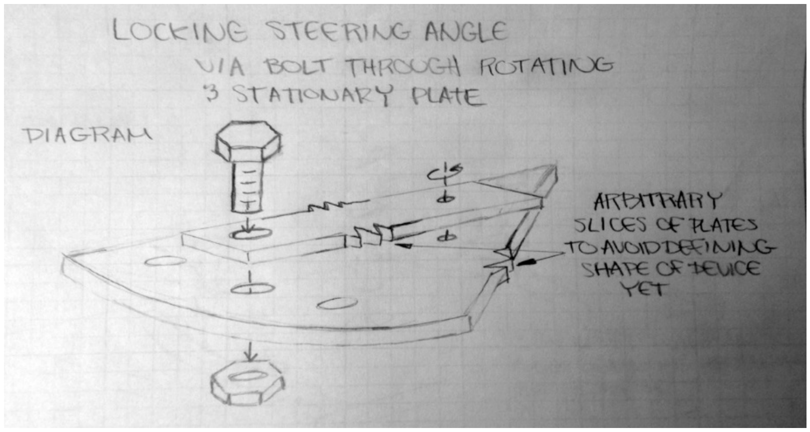


**Figure F.6** Hand sketch diagram illustrating the bolt & hole concept for locking the steering angle

Holes are placed in the stationary plate at the desired steering angles. A hole of a corresponding size is placed on the outer edge of the rotating plate. A bolt slides through the hole on the rotating plate and into the hole at the desired steering angle. A nut threads onto the end of the bolt to secure it in the hole and provide some clamping force on the two plates.

| Pros | Cons |
|---|---|
| • High precision and accuracy<br>• Clamping force reduces play around bolt | • Limited angle choices<br>• Higher part count |

**Plate Clamp**

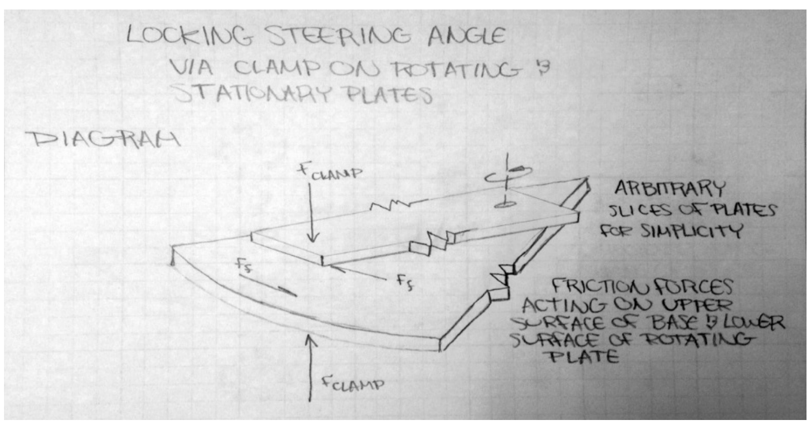


**Figure F.7** Hand sketch diagram illustrating the plate clamp concept for locking the steering angle

A clamp is used to press the rotating and stationary plates together. Friction from the induced normal force is used to prevent the plates from slipping relative to each other.

| Pros | Cons |
|---|---|
| • Infinite angle choices between minimum and maximum angle allowed by angle setting mechanism | • Potential for failure if induced friction is not high enough |

| | |
|---|---|
| • Low part count | |

**Top Choice**

The top concept for steering angle locking is a bolt through the moving and stationary plates. This concept fits the design well because it combines the accuracy and precision of a pin lock with the limited play of a clamping mechanism.

**Axial Load Determination**

Function Description: Axial load is the force in the direction of the shaft, that will result from changes in the steering angle of the tire. Using this data, in combination with slip angle and different radial loads, a tire force curve can be constructed. Figure 4.7, below is an example of a tire force curve with different trendlines for different radial loads.

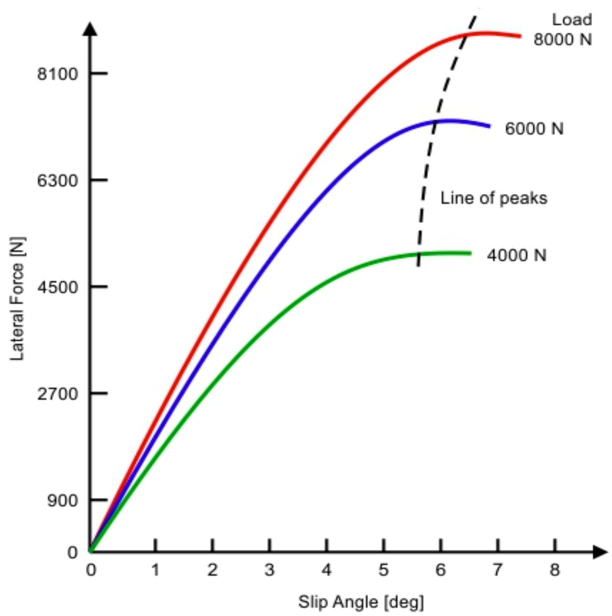


**Figure F.8** Example of a tire force curve. The graph plots the lateral force felt by the motor with respect to slip angle. Each curve represents a different radial load.
<http://racingcardynamics.com/racing-tires-lateral-force/>

Criteria: Accuracy and ease of implementation were the criteria identified as most important. Due to the relatively small forces that must be recorded in the system, accuracy is very important when choosing a load measuring device.

**Load Cell**

The load cell being considered in this analysis is a strain gauge load cell. A strain gauge load cell consists of a strain gauge attached and arranged on specific geometry designed to amplify and measure forces in specific directions. Load cells save application time associated with adhering strain gauges directly to structures.

| Pros | Cons |
|---|---|
| • Installation time<br>• Does not require specifically designed structures | • Cost |

**Strain Gauge**

Strain gauges are appealing due to their low cost and ability to sense small changes within structures. However, strain gauges must be applied precisely by skilled technicians, which comprises a majority of the cost associated with this measuring method. The layout of strain gauges must also be thoroughly thought out, this requires geometries that cater specifically to strain gauges so that accurate measurements can be taken of small forces and the directions of forces can be determined.

| Pros | Cons |
|---|---|
| • Cost | • Requires specific structural geometries<br>• Installation time<br>• Fragile |

**Top Choice**

The top choice for measuring axial load is the use of a load cell. This is optimal due to the ease of installation and compatibility with simpler structural geometry. One drawback of load cells is that those designed to measure small forces are often more expensive because they require an internal geometry that is both sensitive enough to detect small changes and strong enough to provide necessary structural strength. This drastically increases the price of the load cells. It is expected that the cost of a precise load cell to measure small forces will be too large to fit within the project budget. If this proves to be the case, the second choice would be to utilize strain gauges.

**DC Motor**

Function Description: This function compares the two types of DC motors, brushed and brushless.

Criteria: The most relevant criteria when selecting a DC motor were cost, amount of internal friction, maintenance time, life span, and ease of implementation. Low friction is crucial to the design. Friction in the system directly effects performance characteristics which can translate to experimental data that does not reflective theory and may affect the educational goals of the lab experiment. What is also important to view from a design perspective is the simplicity of implementation in comparison to the benefits of a more complicated system.

**Brushed motor**

Brushed motors contain small metal brushes made of conductive material that physically contact and translate current between the rotor and stators. Brushed motors can have varied speed by changing input voltage and, based on speed and torque characteristics, can be held at constant speed. Brushed motors are chosen over brushless motors for basic applications, however, they have lower efficiency and require more maintenance than brushless motors.

| Pros | Cons |
|---|---|
| • Cost<br>• Ease of implementation | • Maintenance<br>• Lower efficiency |

| | |
|---|---|
| • Less dependent on external controllers | • Higher friction |

**Brushless motor**

Brushless motors contain a permanent magnet as the rotor which rapidly switch phases in the windings causing the motor to rotate. Brushless motors have a greater torque to weight capacity than brushed motors. Since brushless motors have no brushes, there is no mechanical contact with the rotor and therefore less friction inside the motor. This translates to less wear, greater efficiency, and better cooling characteristics. Brushless motors often are capable of operating at higher speeds than brushed motors.

| Pros | Cons |
|---|---|
| • Less Friction<br>• Requires little maintenance<br>• Highest efficiency | • Cost<br>• Dependent on external controllers, which may be more fragile |

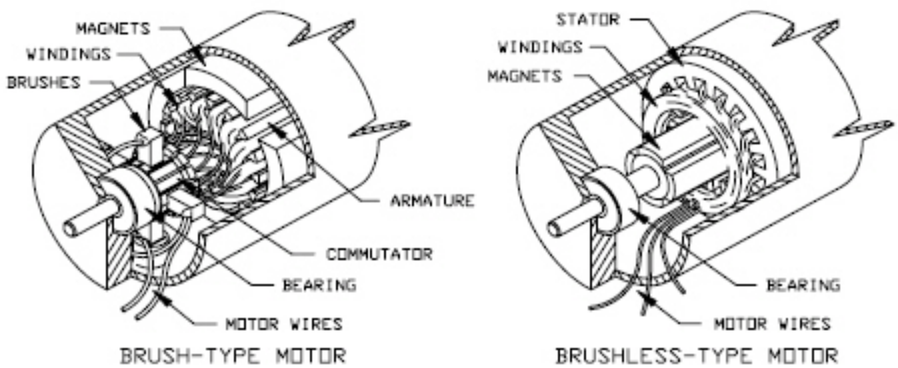


**Figure F.9** Schematic diagram of brushed and brushless motor.
<http://www.fadalvmcparts.com/images/brush_brushless_motors.jpg>

**Top Choice**

The top choice from this analysis is the brushed motor due to the benefits of its cost, simplicity, and ease of implementation. It is expected that the benefits of a brushless motor, most importantly reduced friction and less maintenance, do not outweigh the benefits of selecting a brushed motor. A large factor in specifying a motor for this project will depend on axial and radial load ratings. Motors of this size often have relatively low force ratings.

**Determine Torque**

Function Description: An important aspect of a DC motor is the mechanical output torque. In order for the dynamometer to provide the user with useful information it must be able to determine the output torque of the motor as it is loaded and unloaded.

Criteria: Accuracy and ease of implementation were identified as the most important criteria in selecting a method to determine torque on the shaft.

**Calculate**

Mechanical output torque is calculated using the voltage-current-power relationship, as well as the power-torque-speed relationship. voltage and current information to determine power applied by both the motor attached to the tire and the motor attached to the load assembly. Including motor efficiency into these calculations is a large contributor to accuracy. However, motor efficiencies are unpredictable and vary randomly with changes in load. Motor efficiency is very low at low speeds, and this magnifies the unpredictability of efficiency.

| Pros | Cons |
|---|---|
| • Cost<br>• Does not require specific structure<br>• No associated lifespan or durability | • Accuracy |

**Strain Gauge**

Strain gauges will be used to measure torsional forces, which can be used to calculate torque on the shaft. A concern with strain gauges is whether it is possible to achieve large enough strain in the structure to measure with the strain gauges.

One idea for developing the structure to attach the strain gauges is to mount a thin shaft or tube to the motor. The shaft will be centered with the centerline of the motor. With this structure, strain gauges could be used to measure both axial load and torsion independently of other forces. One uncertainty with this method is if the strain in the structure will be large enough for the strain gauges to measure. In doing preliminary calculations, even the thinnest shafts and tubes will not create enough strain for this system. Strain was in the magnitude of 10’s of μ-strain based off preliminary calculations. It is often necessary to receive strains upwards of 200 μ-strain in order for the strain gauges to work. This is not feasible.

Other potential structural geometries will be developed and analyzed in an attempt to create large enough strains in the system to measure. However, if this is unsuccessful, load cells will be the next measurement device to be looked at. Load cells for this particular application would put the project over budget, so further brainstorming must be conducted to achieve a feasible solution. Common arrangements of strain gauges can be seen below, Figure 4.10.

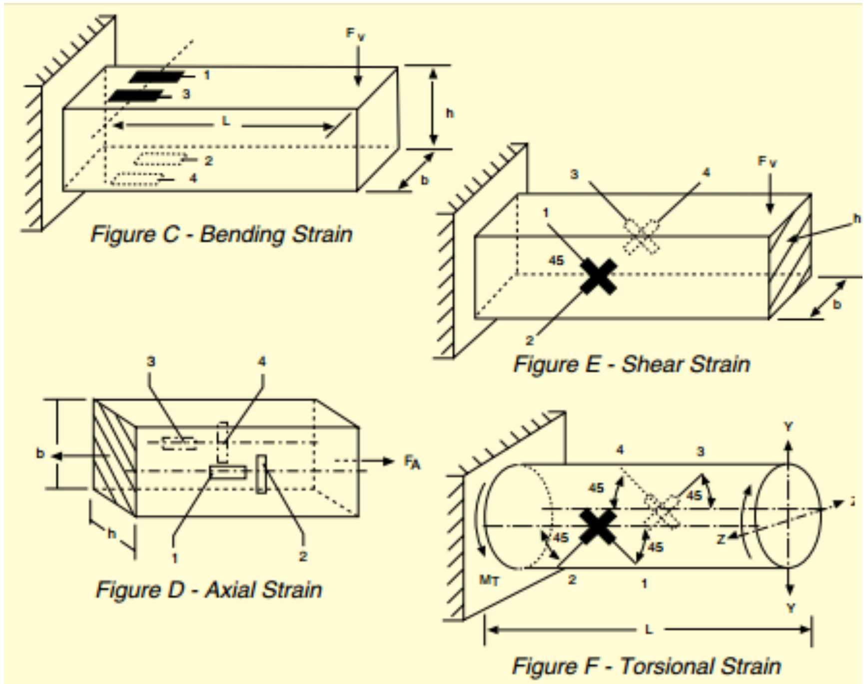


**Figure F.10** Diagram examples of strain gauge positioning to measure different forces.
<https://www.omega.com/faq/pressure/pdf/positioning.pdf>

| Pros | Cons |
|---|---|
| • High accuracy<br>• Measure torque directly | • Ease of implementation<br>• Force sensitivity |

**Top Choice**

The concept selected as the best choice for determining torque in the shaft is to use strain gauges. Strain gauges, if implemented well, can provide very accurate data. The calculation based method was disqualified due to the large unpredictability of motor efficiencies, which would translate to very inaccurate and unreliable data.

**<u>Determine Angular Position and Velocity</u>**

Function Description: To learn how to control a DC motor, it is critical to be able to measure the motor speed and position. Without knowing these parameters, it is impossible to determine if the implemented controls are working as desired.

Criteria: Accuracy and ease of implementation were identified as the most vital criteria determining angular position and velocity of the shaft.

**Encoder**

An encoder mounted onto the shaft of the motor sends voltage signals that can be converted to position information and integrated to determine angular velocity. An encoder determines both speed and position simultaneously. It provides steady, accurate feedback pulses. An encoder is also very compact and durable.

| Pros | Cons |
|---|---|
| • Resolution<br>• Accuracy<br>• Determines speed and position simultaneously<br>• Durability<br>• Size | • Cost |

**Top Choice**

The top concept for angular position and velocity determination is a shaft encoder. Although it is the most expensive option, the shaft encoder is a good fit for our design because it is rugged, durable, highly accurate, and capable of determining both parameters simultaneously, unlike any other method we examined. This reduces the part count for the device and simplifies the device design, construction, and repair.

**Appendix G: Additional Views of Top Concept Assembly**

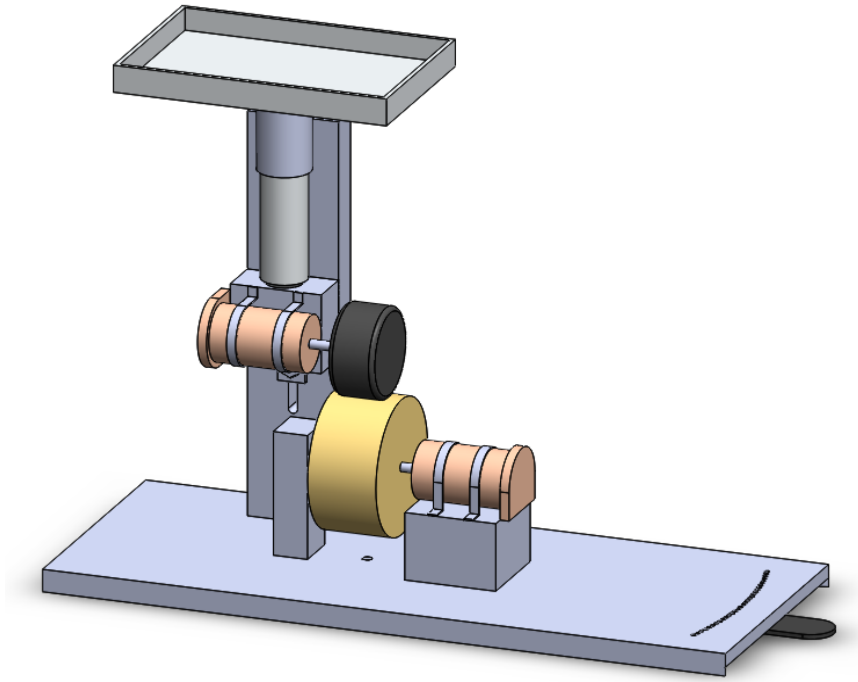

**Figure G.1** Isometric view, un-rotated, tire contacting dyno

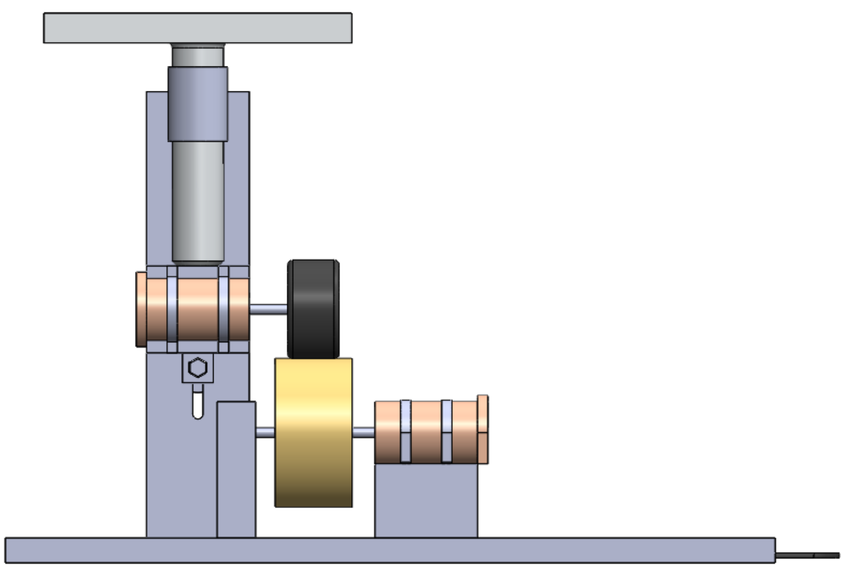

**Figure G.2** Front view, un-rotated, contacting

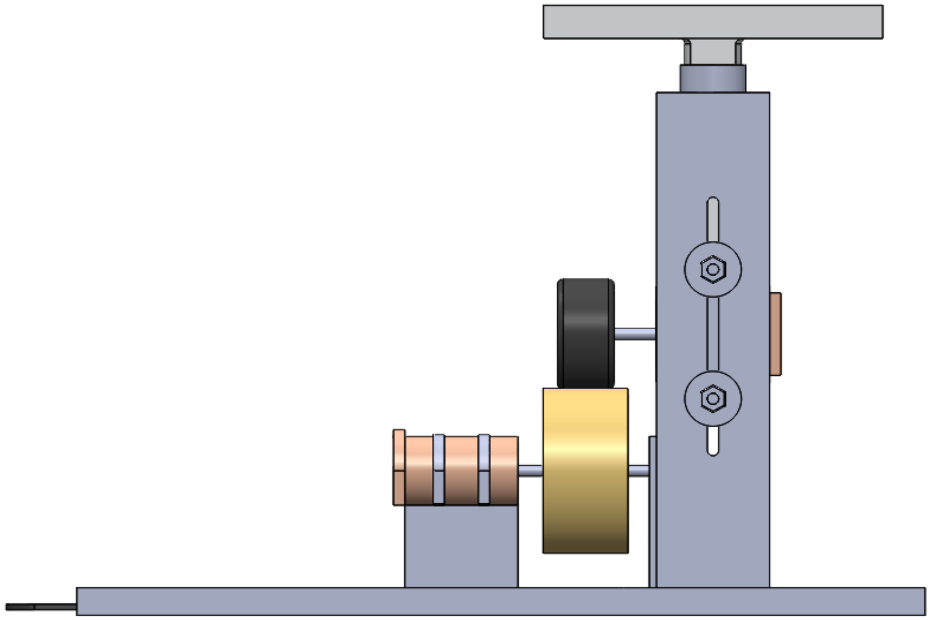

**Figure G.3** Back view, un-rotated, contacting

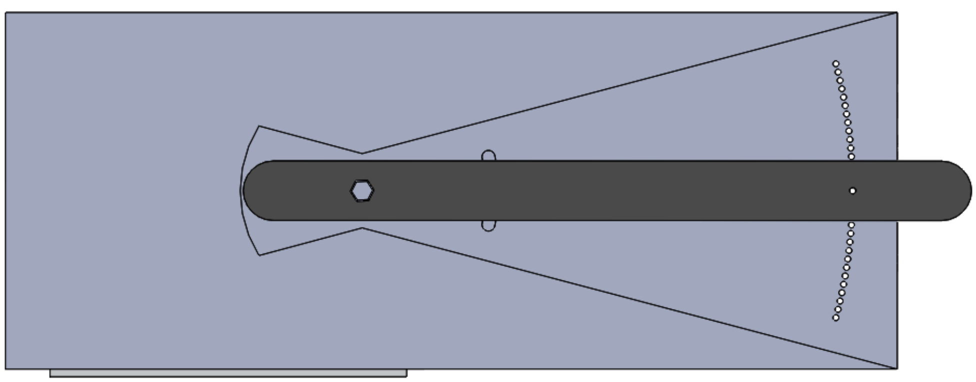

**Figure G.4** Bottom view, un-rotated

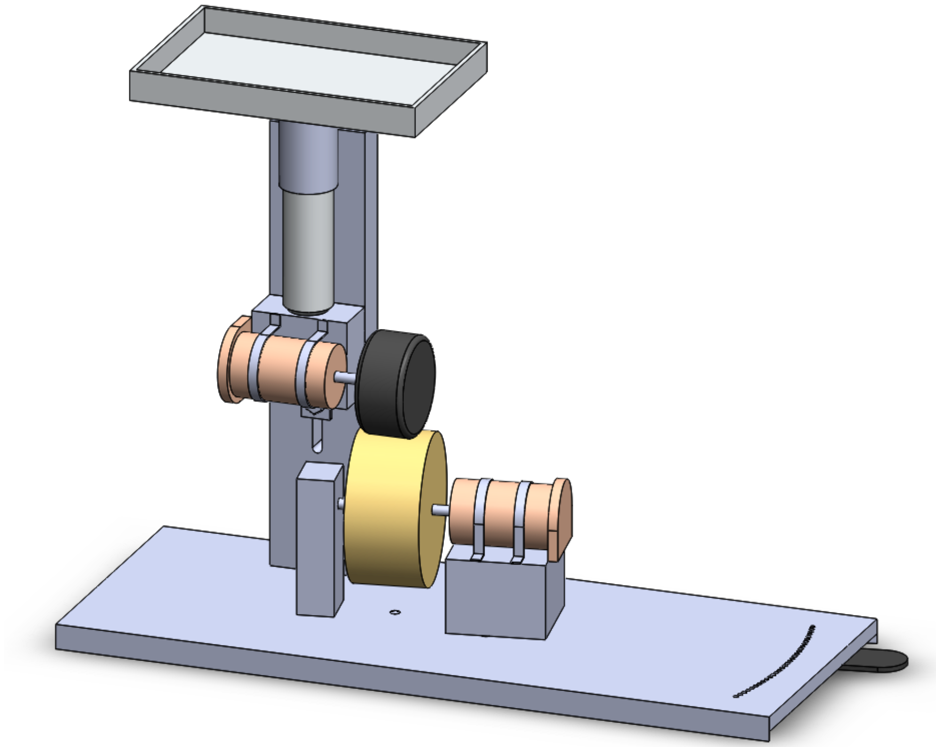

**Figure G.5** Isometric view, dyno rotated at 10°, contacting

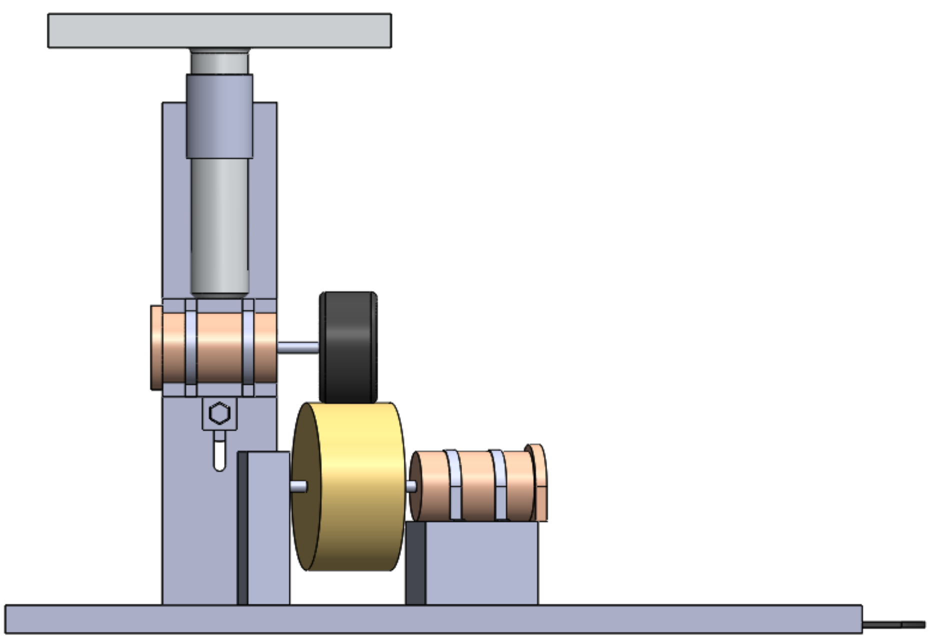

**Figure G.6** Front view, rotated at 10°, contacting

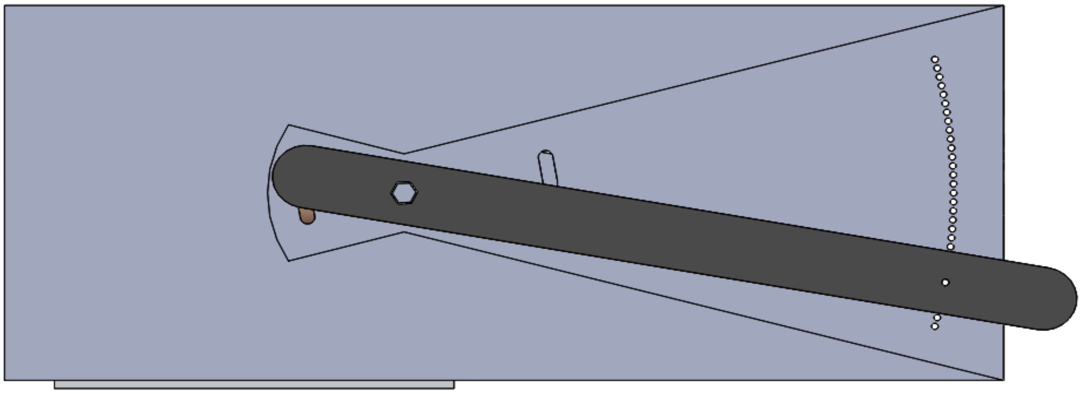

**Figure G.7** Bottom view, rotated at 10°

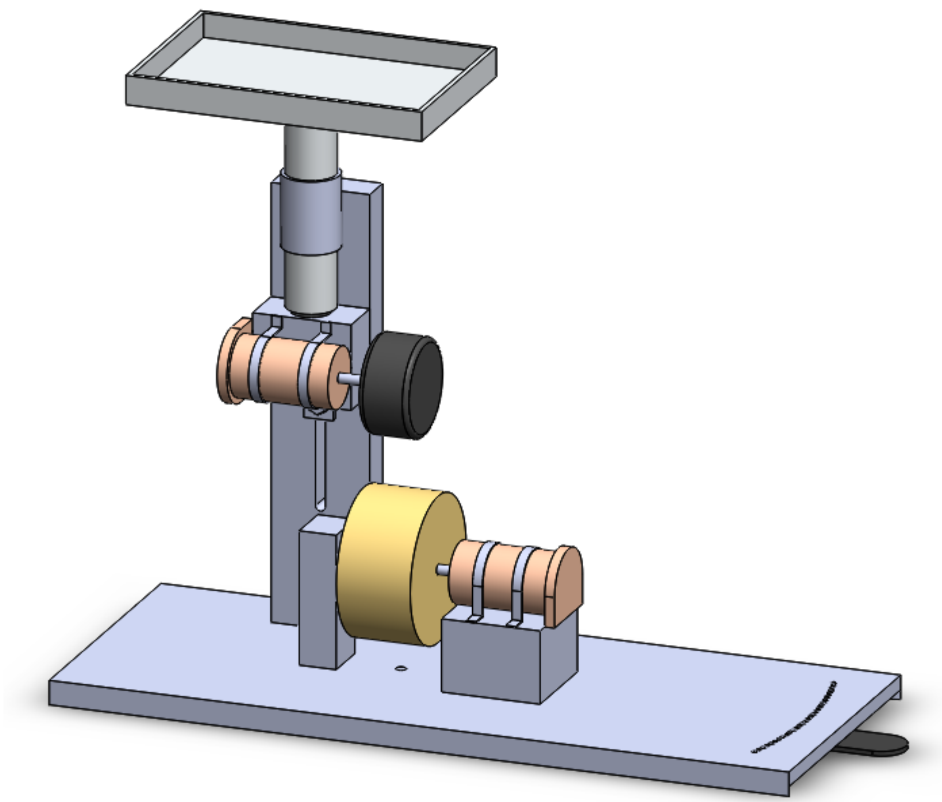

**Figure G.8** Isometric view, un-rotated, tire lifted from dyno

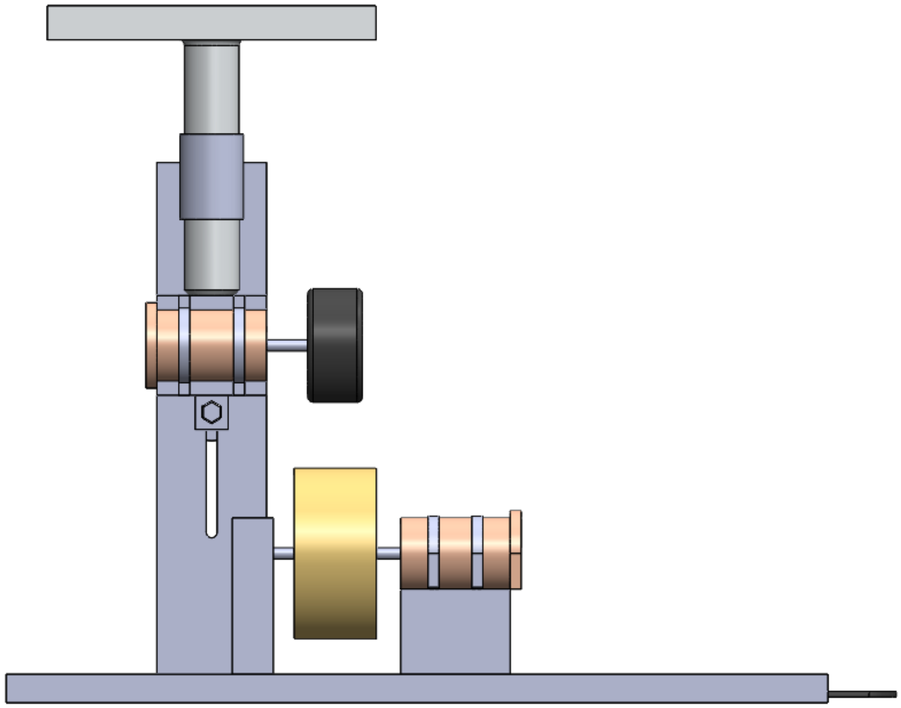

**Figure G.9** Front view, un-rotated, lifted

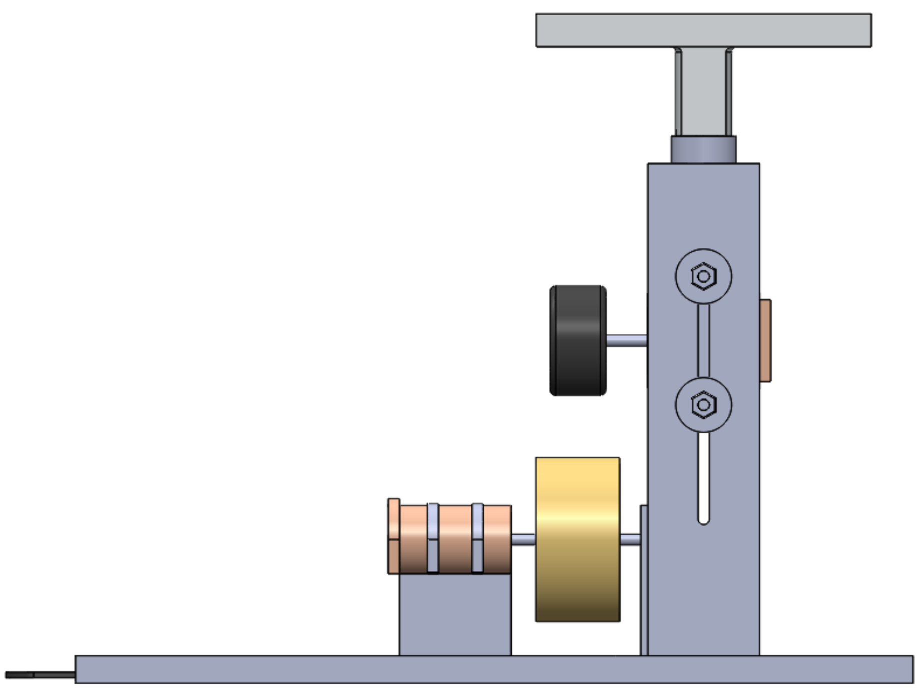

**Figure G.10** Back view, un-rotated, lifted

**Appendix H: Pugh Matrices**

| **Setting Force** / **Criteria** \ **Concept** | Manual + Spring | Elastic | Weights + Piston | Weight + Spring | Weight + Pulley/Tension | Manual + Piston | Hydraulic | Manual + Pulley/Tension | Manual + Rack/Pinion | Manual + Lead Screw | Spring + Piston | Spring + Lead Screw |
|---|---|---|---|---|---|---|---|---|---|---|---|---|
| Cost | Datum | S | - | - | - | - | - | S | - | - | - | - |
| Accuracy | | + | + | + | + | S | + | S | S | S | + | + |
| Resolution | | - | - | - | - | S | + | S | S | S | S | + |
| Stability | | S | + | S | S | + | + | S | + | + | S | + |
| Ease of Adjustment | | - | - | - | - | S | S | S | S | S | S | S |
| Bulk | | + | - | - | - | S | - | - | - | - | - | - |
| Design Simplicity | | S | - | - | - | - | - | S | - | - | - | - |
| Ease of Force Determining | | S | + | S | + | - | - | - | - | - | S | S |
| 2-5 lb Range | | S | + | S | + | S | - | S | S | - | S | S |
| Fun/Satisfaction | | S | + | + | - | S | + | - | + | + | + | + |
| Ruggedness | | - | + | S | + | + | - | + | - | - | S | - |
| Life Span | | - | + | S | + | + | + | + | - | + | S | S |

**Figure H.1** Pugh Matrix for setting force

| **Determining Force** / **Criteria** \ **Concept** | Spring Constant | Weight | Hydraulic/Pnuematic | Strain Gauge on Shaft | Force Sensor Under Motor |
|---|---|---|---|---|---|
| Ruggedness | Datum | + | - | - | - |
| Cost | | + | - | - | - |
| Resolution | | - | S | + | + |
| Bulk | | S | S | + | + |
| Life Span | | + | + | + | + |
| Ease of Physical Implementation | | + | + | - | S |
| Ease of Control Implementation | | S | - | - | - |
| Accuracy | | + | S | + | + |

**Figure H.2** Pugh Matrix for determining force

| Steering Angle Mechanism | Concept | 1 Pin | 2 Pins | 3 Pins | Guide |
|---|---|---|---|---|---|
| **Criteria** | | | | | |
| Ruggedness | | Datum | + | + | + |
| Cost | | | S | S | - |
| Bulk | | | - | - | - |
| Life Span | | | + | + | + |
| Ease of Adjustment | | | S | S | S |
| Stability | | | + | + | + |

**Figure H.3** Pugh Matrix for steering angle mechanism

| Locking Angle | Concept | Pins in holes | Clamp Plates | Tighten Pivot | Bolt in Hole | Claw & Notch |
|---|---|---|---|---|---|---|
| **Criteria** | | | | | | |
| Ruggedness | | Datum | - | - | + | - |
| Cost | | | S | S | S | - |
| Resolution | | | + | + | S | S |
| Bulk | | | - | + | - | - |
| Life Span | | | + | S | S | - |
| Precision | | | + | + | + | + |
| Ease of Implementation | | | + | + | S | - |
| Ease of Adjustment | | | - | - | - | S |
| Accuracy | | | S | S | S | S |
| Efficacy | | | + | - | + | + |

**Figure H.4** Pugh Matrix locking angle

| Determining Axial Load | Concept | Load Cell on Motor | Strain Gauge on Shaft | Strain Gauge on Moun |
|---|---|---|---|---|
| Criteria | | | | |
| Ruggedness | | Datum | - | - |
| Cost | | | - | + |
| Resolution | | | S | S |
| Bulk | | | + | + |
| Life Span | | | S | S |
| Accuracy | | | S | S |
| Ease of Implementation | | | - | - |

**Figure H.5** Pugh Matrix for determining axial load

| Determining Torque | Concept | Calculate w/ Torque Equations | Strain Gauge on Shaft | Force Sensors On Motor |
|---|---|---|---|---|
| Criteria | | | | |
| Ruggedness | | Datum | - | - |
| Cost | | | - | - |
| Resolution | | | + | + |
| Bulk | | | - | - |
| Life Span | | | - | - |
| Ease of Physical Implementation | | | - | - |
| Ease of Control Implementation | | | S | S |
| Accuracy | | | + | + |

**Figure H.6** Pugh Matrix for determining torque

| Determining Position | Concept | Encoder | Photoelectric sensor |
|---|---|---|---|
| **Criteria** | | | |
| Ruggedness | | Datum | - |
| Cost | | | + |
| Resolution | | | - |
| Bulk | | | - |
| Life Span | | | - |
| Ease of Physical Implementation | | | - |
| Ease of Control Implementation | | | S |
| Accuracy | | | - |
| Stability | | | - |

**Figure H.7** Pugh Matrix for determining position

| Determining Rotational Velocity | Concept | Encoder | Proximity Sensor | Photoelectric Sensor | Mechanical Centrifugal force |
|---|---|---|---|---|---|
| **Criteria** | | | | | |
| Ruggedness | | Datum | + | - | - |
| Cost | | | + | + | + |
| Resolution | | | - | - | - |
| Bulk | | | - | - | - |
| Life Span | | | S | - | - |
| Ease of Physical Implementation | | | - | - | - |
| Ease of Control Implementation | | | S | S | S |
| Accuracy | | | - | - | - |
| Ability to Sense Direction | | | - | - | - |

**Figure H.8** Pugh Matrix for determining rotational velocity

**Appendix I: Weighted Matrices**

| Setting Force | | | Manual + Spring | Manual + Elastic | Stacked Weights | Weight + Pulley/Tension | Manual Lever + Piston | Hydraulic | Manual + Pulley/Tension | Manual + Rack/Pinion | Manual + Lead Screw | Spring + Lead Screw |
|---|---|---|---|---|---|---|---|---|---|---|---|---|
| Criteria | Cost | 0.1 | 90% | 85% | 50% | 45% | 75% | 20% | 85% | 50% | 80% | 60% |
| | Resolution | 0.05 | 90% | 90% | 50% | 50% | 90% | 90% | 90% | 85% | 90% | 95% |
| | Stability | 0.1 | 50% | 50% | 80% | 70% | 90% | 90% | 90% | 85% | 80% | 70% |
| | Ease of Adjustment | 0.1 | 40% | 40% | 90% | 85% | 50% | 90% | 50% | 50% | 70% | 85% |
| | Bulk | 0.05 | 80% | 80% | 50% | 40% | 60% | 50% | 70% | 60% | 70% | 70% |
| | Design Simplicity | 0.1 | 70% | 70% | 95% | 80% | 70% | 20% | 70% | 40% | 85% | 75% |
| | Ease of Force Determining | 0.1 | 90% | 90% | 100% | 100% | 70% | 90% | 70% | 50% | 60% | 85% |
| | 2-5 lb Range | 0.15 | 90% | 90% | 90% | 90% | 60% | 30% | 60% | 40% | 70% | 90% |
| | Fun/Satisfaction | 0.05 | 60% | 60% | 70% | 75% | 70% | 95% | 60% | 75% | 75% | 85% |
| | Ruggedness | 0.1 | 80% | 80% | 95% | 90% | 75% | 75% | 85% | 70% | 90% | 85% |
| | Life Span | 0.1 | 80% | 80% | 100% | 100% | 95% | 75% | 95% | 75% | 90% | 80% |
| | | 1 | 75% | 75% | 83% | 79% | 73% | 62% | 75% | 59% | 78% | 80% |

**Figure I.1** Pugh Matrix for setting force

| Determining Force | | | Spring Constant | Weight | Hydraulic/Pnuematic | Strain Gauge on Shaft | Load Cell Under Moto |
|---|---|---|---|---|---|---|---|
| Criteria | Ruggedness | 0.15 | 90% | 95% | 75% | 30% | 60% |
| | Cost | 0.15 | 95% | 70% | 25% | 30% | 70% |
| | Resolution | 0.1 | 50% | 30% | 70% | 90% | 90% |
| | Additional Bulk | 0.05 | 100% | 100% | 100% | 90% | 90% |
| | Life Span | 0.1 | 70% | 100% | 85% | 80% | 90% |
| | Ease of Physical Implementation | 0.25 | 100% | 100% | 100% | 30% | 60% |
| | Accuracy | 0.2 | 70% | 100% | 85% | 90% | 90% |
| | | 1 | 84% | 88% | 78% | 56% | 75% |

**Figure I.2** Pugh Matrix for determining force

| Steering Angle Mech | | Concept | | | |
|---|---|---|---|---|---|
| | | 1 Pin | 2 Pins | 3 Pins | Guide |
| Criteria: Ruggedness | 0.25 | 50% | 70% | 90% | 90% |
| Bulk | 0.1 | 95% | 90% | 85% | 90% |
| Life Span | 0.2 | 60% | 70% | 90% | 90% |
| Ease of Adjustment | 0.3 | 90% | 90% | 90% | 80% |
| Stability | 0.15 | 50% | 70% | 90% | 95% |
| | 1 | 69% | 78% | 90% | 88% |

**Figure I.3** Pugh Matrix for steering angle mechanism

| Locking Angle | | Concept | | | | |
|---|---|---|---|---|---|---|
| | | Pins in holes | Clamp Plates | Tighten Pivot | Bolt in Hole | Claw & Notch |
| Criteria: Ruggedness | 0.1 | 80% | 90% | 60% | 90% | 50% |
| Cost | 0.05 | 70% | 80% | 90% | 65% | 30% |
| Resolution | 0.05 | 50% | 100% | 100% | 50% | 50% |
| Bulk | 0.05 | 80% | 70% | 90% | 70% | 60% |
| Life Span | 0.1 | 80% | 100% | 70% | 90% | 60% |
| Precision | 0.15 | 60% | 90% | 80% | 70% | 80% |
| Ease of Implementation | 0.05 | 70% | 90% | 90% | 70% | 40% |
| Ease of Adjustment | 0.05 | 90% | 70% | 70% | 90% | 80% |
| Accuracy | 0.2 | 90% | 80% | 70% | 100% | 90% |
| Efficacy | 0.2 | 90% | 80% | 60% | 100% | 80% |
| | 1 | 79% | 85% | 73% | 86% | 70% |

**Figure I.4** Pugh Matrix for locking angle

| Criteria | Determining Axial Load | | Concept: Load Cell on Motor | Concept: Strain Gauge on Shaft | Concept: Strain Gauge on Moun |
|---|---|---|---|---|---|
| | Ruggedness | 0.15 | 90% | 25% | 50% |
| | Cost | 0.15 | 70% | 50% | 80% |
| | Resolution | 0.1 | 90% | 90% | 90% |
| | Bulk | 0.05 | 70% | 50% | 90% |
| | Life Span | 0.15 | 90% | 80% | 90% |
| | Accuracy | 0.2 | 90% | 90% | 90% |
| | Ease of Implementation | 0.2 | 90% | 25% | 50% |
| | | 1 | 86% | 58% | 75% |

**Figure I.5** Pugh Matrix for determining axial load

| Criteria | DC Motor | | Brushed | Brushless |
|---|---|---|---|---|
| | Ruggedness | 0.15 | 80% | 95% |
| | Cost | 0.25 | 95% | 70% |
| | Speed Range | 0.1 | 100% | 100% |
| | Size | 0.05 | 85% | 95% |
| | Life Span | 0.2 | 80% | 95% |
| | Ease of Implementation | 0.2 | 95% | 75% |
| | Efficiency | 0.05 | 80% | 95% |
| | | 1 | 89% | 85% |

**Figure I.6** Pugh Matrix for DC Motor

| Determining Torque | | | Concept | | |
|---|---|---|---|---|---|
| | | | Calculate w/ Torque Equation | Strain Gauge on Shaft | Force Sensors On Motor |
| Criteria | Ruggedness | 0.1 | 100% | 70% | 80% |
| | Cost | 0.15 | 100% | 90% | 50% |
| | Resolution | 0.15 | 100% | 100% | 100% |
| | Bulk | 0.05 | 100% | 90% | 75% |
| | Life Span | 0.1 | 100% | 90% | 90% |
| | Ease of Physical Implementation | 0.2 | 100% | 70% | 80% |
| | Accuracy | 0.25 | 30% | 90% | 90% |
| | | 1 | 83% | 86% | 82% |

**Figure I.7** Pugh Matrix for determining torque

| Determining Position | | | Encoder | Photoelectric sensor |
|---|---|---|---|---|
| Criteria | Ruggedness | 0.15 | 80% | 50% |
| | Cost | 0.1 | 40% | 90% |
| | Resolution | 0.15 | 100% | 60% |
| | Bulk | 0.1 | 90% | 70% |
| | Life Span | 0.1 | 90% | 90% |
| | Ease of Physical Implementation | 0.2 | 95% | 70% |
| | Accuracy | 0.2 | 90% | 70% |
| | | 1 | 86% | 70% |

**Figure I.8** Pugh Matrix for determining position

| | Determining Velocity | | Encoder | Proximity Sensor | Photoelectric Sensor |
|---|---|---|---|---|---|
| Criteria | Ruggedness | 0.1 | 80% | 90% | 50% |
| | Cost | 0.1 | 40% | 90% | 90% |
| | Resolution | 0.15 | 100% | 40% | 60% |
| | Bulk | 0.1 | 90% | 70% | 70% |
| | Life Span | 0.1 | 90% | 90% | 90% |
| | Ease of Physical Implementation | 0.2 | 95% | 70% | 70% |
| | Accuracy | 0.2 | 90% | 40% | 70% |
| | Ability to Sense Direction | 0.05 | 100% | 0% | 0% |
| | | 1 | 87% | 62% | 67% |

**Figure I.9** Pugh Matrix for determining velocity

# Appendix J: Bill of Materials

| # | Type | Name | Vendor | Vendor Part Number | Description | Unit | Website | Qty needed/assembly | Qty/pack | # packs | Price/pack | Price/unit | Total | Price of parts in assembly | Notes |
|---|---|---|---|---|---|---|---|---|---|---|---|---|---|---|---|
| 1 | Hardware | 10-24 threaded rod | McMaster | 91565A865 | Low-Strength steel threaded rod; 10-24 thread size 3' long | ea | https://www.mcmaster.com/[illegible] | 3 | 50 | 1 | $12.18 | $0.24 | $12.18 | $0.73 | Shaft for the bearings surrounding the bottom motor |
| 2 | Nuts | 10-24 narrow hex nut | McMaster | 90760A120 | Zinc-plated steel narrow hex nut; 10-24 thread size | ea | https://www.mcmaster.com/[illegible] | 18 | 50 | 1 | $8.18 | $0.16 | $8.18 | $2.94 | Narrow nuts for the 10-24 threaded rod |
| 3 | Bearings | Ball bearing 1/2" OD | McMaster | 60355K42 | Ball bearing; Double Shielded, for 3/16" Shaft Diameter, 1/2" OD | ea | https://www.mcmaster.com/[illegible] | 2 | 1 | 2 | $6.56 | $6.56 | $13.12 | $13.12 | Both go on the upper 10-24 threaded rod |
| 4 | Bearings | Ball bearing 3/8" OD | McMaster | 57155K[illegible] | Stainless Steel Open Ball Bearing Precision, Trade No. R166; for 3/16" shaft diameter, 3/8" OD | ea | https://www.mcmaster.com/[illegible] | 4 | 1 | 4 | $4.06 | $4.06 | $16.24 | $16.24 | They go on the lower two 10-24 threaded rods (2 on each), used to support the bottom motor |
| 5 | T-slot | T-slot fastener compact | McMaster | 47065T139 | T-slotted framing compact end-feed fastener, for 1" high single rail | ea | https://www.mcmaster.com/[illegible] | 27 | 4 | 7 | $1.85 | $0.46 | $12.95 | $12.49 | Mainly used for the T-slot brackets, consists of two parts: the screw and the T-slot guide |
| 6 | T-slot | T-slot fastener standard | McMaster | 47065T142 | T-Slotted Framing standard End-Feed Fastener, for 1" High Single Rail | ea | https://www.mcmaster.com/[illegible] | 16 | 4 | 4 | $2.30 | $0.58 | $9.20 | $9.20 | Only used to secure the T-slot rails to the base |
| 7 | Fastener | 10-32, 7/16" screw | McMaster | 92196A268 | 18-8 Stainless Steel Socket Head Screw 10-32 Thread Size, 7/16" Long | ea | https://www.mcmaster.com/[illegible] | 9 | 100 | 1 | $8.72 | $0.09 | $8.72 | $0.78 | Attaches Linear rails and Axial load bracket to the Angle bar, top |
| 8 | Fastener | M6x12mm screw | McMaster | 91274A106 | Zinc-Aluminum-Coated Alloy Steel Socket Head Screw M6 x 1 mm Thread, 12 mm Long | ea | https://www.mcmaster.com/[illegible] | 8 | 50 | 1 | $9.03 | $0.18 | $9.03 | $0.81 | Attaches Bottom motor support brackets to the Linear bearings |
| 9 | Fastener | 10-24, 3/8" load cell mount screw | McMaster | 91251A240 | Black-Oxide Alloy Steel Socket Head Screw 10-24 Thread Size, 3/8" Long | ea | https://www.mcmaster.com/[illegible] | 4 | 100 | 1 | $11.48 | $0.11 | $11.48 | $0.46 | For mounting the load cells to their respective brackets |
| 10 | Fastener | 6-32, 3/8" motor/load cell screw | McMaster | 92196A146 | 18-8 Stainless Steel Socket Head Screw 6-32 Thread Size, 3/8" Long | ea | https://www.mcmaster.com/[illegible] | 10 | 100 | 1 | $4.71 | $0.05 | $4.71 | $0.47 | Attaching motor to mount and torque arm. Also used to transfer torque and axial force to load cells |
| 11 | Fastener | 1/4"-20, 7/8" screw | McMaster | 91251A540 | Black-Oxide Alloy Steel Socket Head Screw 1/4"-20 Thread Size, 7/8" Long | ea | https://www.mcmaster.com/[illegible] | 14 | 50 | 1 | $8.41 | $0.17 | $8.41 | $2.35 | Used in various places |
| 12 | Nuts | 1/4"-20 hex nut | McMaster | 90473A029 | Low-Strength Steel Hex Nut Grade 2, Zinc-Plated, 1/4"-20 Thread Size | ea | https://www.mcmaster.com/[illegible] | 17 | 100 | 1 | $2.77 | $0.03 | $2.77 | $0.47 | Quantity per assembly may vary |
| 13 | Nuts | 10-24 low-profile hex nut | McMaster | 90730A011 | 18-8 Stainless Steel Narrow Hex Nut 10-24 Thread Size | ea | https://www.mcmaster.com/[illegible] | 4 | 100 | 1 | $5.58 | $0.06 | $5.58 | $0.22 | Nuts for the screws securing load cells to their mounts, normal |
| 14 | Washers | 1/4" size washer | McMaster | 92141A029 | 18-8 Stainless Steel Washer for 1/4" Screw Size, 0.281" ID, 0.625" OD | ea | https://www.mcmaster.com/[illegible] | 31 | 100 | 1 | $3.37 | $0.03 | $3.37 | $1.04 | Not the type on the physical device currently. Quantity per assembly may vary |
| 15 | Washers | 10 size washer | McMaster | 92141A011 | 18-8 Stainless Steel Washer for Number 10 Screw Size, 0.203" ID, 0.438" OD | ea | https://www.mcmaster.com/[illegible] | 9 | 100 | 1 | $2.33 | $0.02 | $2.33 | $0.21 | Quantity per assembly may vary |
| 16 | Fastener | Wing screw 1/4"-20, 1.5" | McMaster | 91404A546 | Zinc-Plated Iron Wing-Head Thumb Screw 1/4"-20 Thread Size, 1-1/2" Long | ea | https://www.mcmaster.com/[illegible] | 1 | 1 | 1 | $4.07 | $4.07 | $4.07 | $4.07 | Used to tighten down the Angle Bars, once the angle is set and the pin is in place, before running motor |
| 17 | Fastener | Cap screw 1/4"-20, 1.5" | McMaster | 91236A546 | Low-Strength Zinc-Plated Steel Hex Head Screw 1/4"-20 Thread Size, 1-1/2" Long, Partially Threaded | ea | https://www.mcmaster.com/[illegible] | 1 | 100 | 1 | $6.94 | $0.07 | $6.94 | $0.07 | Acts as the pivot point for the Angle Bars |
| 18 | Fastener | Thumb screw 1/4"-20, 5/8" | McMaster | 91510A149 | Zinc-Plated Steel Wing-Head Thumb Screws 1/4"-20 Thread Size, 5/8" Long | ea | https://www.mcmaster.com/[illegible] | 2 | 10 | 1 | $13.10 | $1.31 | $13.10 | $2.62 | For locking the linear slider that mounts the upper motor |
| 19 | Hardware | Angle pin | McMaster | 98404A105 | 18-8 Stainless Steel Ring-Grip Quick-Release Pin 3/32" Diameter, 1-1/4" Usable Length | ea | https://www.mcmaster.com/[illegible] | 1 | 1 | 1 | $1.89 | $1.89 | $1.89 | $1.89 | Quick-release pull-pin for setting the angle of the angle change mechanism |
| 20 | T-slot | T-slot corner bracket 2x1 | McMaster | 47065T237 | T-Slotted Framing Corner Bracket for 2" High Double and Quad Rail, Silver | ea | https://www.mcmaster.com/[illegible] | 2 | 1 | 2 | $8.47 | $8.47 | $16.94 | $16.94 | Used to attach the T-slot vertical tower to the back 13" T-slot rail |
| 21 | T-slot | T-slot corner bracket 2x2 | McMaster | 47065T231 | T-Slotted Framing Extended Corner Bracket for 2" High Double and Quad Rail | ea | https://www.mcmaster.com/[illegible] | 2 | 1 | 2 | $8.79 | $8.79 | $17.58 | $17.58 | Used in the back corners of the apparatus. Attaches side 15" T-slot rails to the back 13" T-slot rail |
| 22 | Bearings | Thrust bearing | McMaster | 6655K130 | [illegible] Steel Washers, for 1/4" Shaft Diameter, 9/16" [illegible] | ea | https://www.mcmaster.com/[illegible] | 2 | 1 | 2 | $2.21 | $2.21 | $4.42 | $4.42 | Used for each motor shaft before the coupler, used to absorb thrust load, instead of internal motor [illegible] |
| 23 | Nuts | Press nut 1/4"-20 | McMaster | 94648A370 | [illegible] Metal & Plastic, 1/4"-20 Thread Size | ea | https://www.mcmaster.com/[illegible] | 1 | 10 | 1 | $14.68 | $1.47 | $14.68 | $1.47 | [illegible] Wing screw goes into it |
| 24 | Load cell | Load cell LSM300 | Futek | FSH00064 | LSM300 10lb. Fold back beam load cell standard; Material 2024-T6; #6-32 thread; Overload protection; 4 conductor flex cable, 1mm Pit | ea | http://www.futek.com/product.aspx?stock=FSH00064 | 2 | 1 | 2 | ###### | $298.00 | $596.00 | $596.00 | Received initial two for free. Others can potentially be heavily discounted |
| 25 | 3D Print | Pulley Mount | Custom | | stl file for printing; Material PLA; Printed at The Innovation Sandbox | ea | | 1 | 1 | 1 | $0.00 | $0.00 | $0.00 | $0.00 | Custom made mount to achieve pulley leverage right at the points desired. 3D printed |
| 26 | 3D Print | Pulley Wheel | Custom | | stl file for printing; Material PLA; Printed at The Innovation Sandbox | ea | | 2 | 1 | 2 | $0.00 | $0.00 | $0.00 | $0.00 | Custom made pulley wheels to go with the mount. 3D printed |
| 27 | 3D Print | Pulley Pin | Custom | | stl file for printing; Material PLA; Printed at The Innovation Sandbox | ea | | 2 | 1 | 2 | $0.00 | $0.00 | $0.00 | $0.00 | Custom made pins to allow wheels to spin freely but be statically secured in the mount. 3D printed |
| 28 | T-slot | Linear T-slot slider double-length | McMaster | 47065T941 | Bearing for 1" Width Rail, Side-Mount, 6" Length T-Slotted Framing | ea | https://www.mcmaster.com/[illegible] | 1 | 1 | 1 | $55.86 | $55.86 | $55.86 | $55.86 | Slider for top motor assembly |
| 29 | T-slot | Linear T-slot slider single-length | McMaster | 47065T939 | Bearing for 1" Width Rail, Base-Mount, 1-7/8" Length T-Slotted Framing | ea | https://www.mcmaster.com/[illegible] | 1 | 1 | 1 | $46.16 | $46.16 | $46.16 | $46.16 | Slider for the weight box |
| 30 | Hardware | Drum Drum | McMaster | 8582K25 | White Delrin® Acetal Resin Rod 3" Long, 4" Diameter | [illegible] | https://www.mcmaster.com/[illegible] | 1 | 1 | 1 | $34.86 | $34.86 | $34.86 | $34.86 | Cylinder of Delrin. Already to size, but can be cut down or turned if desired. Press fit coupler into it |
| 31 | Hardware | Flywheel | McMaster | 6943T1 | Highly Machinable MIC6 Aluminum Disc 6" Diameter | [illegible] | https://www.mcmaster.com/[illegible] | 1 | 1 | 1 | $39.93 | $39.93 | $39.93 | $39.93 | Disc already to size, but can be turned down if desired. Coupler was secured in |
| 32 | Raw Material | Upper motor mount; Motor bearing structure (2); Motor torque arm; Pulley plate | McMaster | 89015K18 | 6061 Aluminum Sheet 1/8" Thick, 12" x 12" | [illegible] | https://www.mcmaster.com/[illegible] | 1 | 1 | 1 | $29.99 | $29.99 | $29.99 | $29.99 | Used to make Upper motor mount, Motor bearing structure (x2), Motor torque arm, and Pulley plate. Refer to their respective drawings for manufacturing |
| 33 | Raw Material | Base; Angle bar top; Angle bar bottom | McMaster | 8975K242 | 6061 Aluminum 1/4" Thick x 12" Wide x 2ft long | [illegible] | https://www.mcmaster.com/[illegible] | 1 | 1 | 1 | $92.06 | $92.06 | $92.06 | $92.06 | Used to make Base, Angle bar top, and Angle bar bottom. Refer to their respective drawings for manufacturing |
| 34 | T-slot | T-slot rail double-wide | McMaster | 47065T107 | T-Slotted Framing, Double Rail, Silver 2" High x 1" Wide, Solid, 4ft long | ea | https://www.mcmaster.com/[illegible] | 1 | 1 | 1 | $33.93 | $33.93 | $33.93 | $33.93 | Cut into lengths of 18" and 13"; Used as legs for the base |
| 35 | T-slot | T-slot rail single-wide | McMaster | 47065T101 | T-Slotted Framing, Single Rail, Silver 1" High x 1" Wide, Solid, 3ft long | ea | https://www.mcmaster.com/[illegible] | 1 | 1 | 1 | $11.53 | $11.53 | $11.53 | $11.53 | Cut into lengths of 12", 12", 12" 15", and 18" |
| 36 | Hardware | Red box | Schaller Corporation | 8304-1 | 3" X 4" X 3" RED PLASTIC BOX (ACTUAL DIMENSIONS: W 2.875 X L 3.875 X H 2.75) | ea | https://www.schallercorporation.com/3-x-4-x-3-red-plastic-box-actual-dimensions-w-2-875-x-l-3-875-x-h-2-75/ | 1 | 1 | 1 | $1.44 | $1.44 | $1.44 | $1.44 | Many other sizes of boxes can be sourced from this website |
| 37 | Hardware | Hex coupler | Pololu | 2687 | 12mm Hex Wheel Adapter for 4mm Shaft, Extended (2-Pack) | ea | https://www.pololu.com/product/2687 | 2 | 2 | 1 | $4.95 | $2.48 | $4.95 | $4.95 | Recommended to source different and better couplers than these |
| 38 | Hardware | Tire | RC Planet | HPI4702 | HPI X-Pattern Tire 26mm Wheel Mounted; Scale: 1/10; Vehicle type: on-road car | ea | https://www.rcplanet.com/[illegible] | 1 | 4 | 1 | $47.99 | $12.00 | $47.99 | $12.00 | Prices may vary. Other tires available on website |
| 39 | Hardware | Linear Bearing | VXB Bearings | [illegible] | 20mm Open Block Unit Motion Linear Bearings; Type: Linear Ball Bushing | ea | http://www.vxb.com/[illegible] | 2 | 1 | 2 | $9.95 | $9.95 | $19.90 | $19.90 | Mounts to the 2 linear rails, the lower motor assembly sits on top of these bearings |
| 40 | Hardware | Linear rail | VXB Bearings | SBR20-300mm | 20mm Fully Supported Linear Rail Shaft 300mm Long | ea | http://www.vxb.com/[illegible] | 1 | 1 | 1 | $14.45 | $14.45 | $14.45 | $14.45 | Cut in half to make the two needed linear rails |
| 41 | Raw Material | Bottom motor support bracket (2); Torque load cell mount; Axial force load cell mount; Axial load bracket | McMaster | 8982K23 | 6061 Aluminum 90 Degree Angle 1/8" Wall Thickness, 1-1/2" High x 1-1/2" Wide, 2ft long | [illegible] | https://www.mcmaster.com/[illegible] | 1 | 1 | 1 | $8.54 | $8.54 | $8.54 | $8.54 | Used to make Bottom motor support bracket (x2), Torque load cell mount, Axial force load cell mount, and Axial load bracket. Refer to their respective drawings for manufacturing |
| 42 | Hardware | Motor | Ametek | 14204S006-SP | Pittman Series 14000 LO-COG Brush Commutated DC Motors | ea | https://www.servocomponents.com/Pittman-Brush-Motor-14000-series/14204s006-SP | 2 | 1 | 2 | ###### | $321.44 | $642.88 | $642.88 | Sourced this from Servo components $288.34. Prices may vary |
| 43 | Hardware | Lab Weights | Amazon | CKW-1000G | HFS (R) Scale Balance Calibration Weight Set - 10-1000g 8Pc Set With Case | ea | https://www.amazon.com/[illegible]Calibration-Weights/dp/B01[illegible] | 1 | 1 | 1 | $12.99 | $12.99 | $12.99 | $12.99 | Prices may vary. Many other options for weights available elsewhere as well |
| | | | | | Refer to Drawings Folder for the drawing files. | | | | | | | Totals: | $1,893.28 | $1,727.69 | [illegible] parts such as the load cells or motors get discounted then it will be below budget |

## Appendix K: EES Analysis Code

```
m_motor = W_motor/g
m_beam = W_unitlength*L_beam/g
 m_eff = 33/140*m_beam+m_motor

omega_n = ((3*E_conv*I)/(m_eff*L_beam^3))^(1/2) "rad/s"
omega_nrpm = omega_n*60[s/min]/(2*pi)  "rpm"

sigma_max = F_max/A_xsec "worst case scenario stress seen"
delta_max = F_max*L_beam^3/(3*E*I)

"Sliding Friction of Journal Bearing"

mu_PTFE = 0.04 "PTFE on PTFE contact"
F_friction = mu_PTFE*(W_motor+W_vehicle) "Faxial = Ffriction = mu*m*g"
T_friction = F_friction*r_motor
T_frictionconv = T_friction*16 [oz/lbf]
T_seen = T_motor*r_dyno/r_scaletire

"Finding Operational Torque"
a_desired = V_operational/acceltime
F_req = m_vehicle*a_desired
T_req = F_req*r_scaletire

T_motor = T_req*12[in/ft]*16[oz/lbf]

"Determining Required Flywheel Inertia"
tau = 1 [s]
r_flywheel = 3 [in]
K_t = 0.06122 [N-m/A]
K_e = 0.06122 [V-s/rad]
R = 1.01 [ohm]
J_arm = 0.0000261 [kg-m2]

J_tot = tau*K_t*K_e/R

J_flywheel = J_tot - J_arm

m_flywheel = 2*J_flywheel/r_flywheel^2*convert(m2,in2)

W_flywheel = m_flywheel*convert(kg,slug)*32.2 [ft/s2]

"80/20 Structural & Vibrational Analysis"

E = 10200000 [slug-ft/s2-in2]
E_conv = E*12 [in/ft] "original units lbf/in2, multiplied by 12 to convert lbf = slug*ft/s2 to slug*in/s2"
sigma_yield = 35000 [lbf/in2]
I = 0.0442 [in4]
A_xsec = 0.4379 [in2]
W_unitlength = 0.047 [lbf/in]
W_motor = 37*1/16 "weight given in oz, 1lbf = 16oz"
L_beam = 12 [in]
F_max = 10 [lbf]
```

## Appendix L: DVPR

| ME428 DVP&R Format | | | | | | | | | | | | | |
|---|---|---|---|---|---|---|---|---|---|---|---|---|---|
| | | | Sponsor | Dr. Birdsong | | | | Component/Assembly | | Dyno-Mite | | | |
| TEST PLAN | | | | | | | | | TEST REPORT | | | | |
| Item No | Specification or Clause Reference | Test Description | Acceptance Criteria | Test Responsibility | Test Stage | SAMPLES Quantity | TIMING Start date | TIMING Finish date | TEST RESULTS Quantity Result | Pass | Fail | Partial | NOTES |
| 1 | Maintenance Time | Estimate/calculate maintenance time using specs from parts and usage estimates | < 1 hour per device per quarter | Daniel | PV | 1 | After CDR | 12/3/2017 | - | Pass | | | Only quarterly maintenance required: cleaning, torque check |
| 2 | Decibel level | Run the device at loudest setting and record decibel level | < 50 dB | Trey | DV | 5 | After CDR | 12/3/2017 | - | Pass | | | Max volume at 50dB, light buzzing |
| 3 | Time to access parts | Assemble device and perform disassembly/re-assembly runs accessing common replaceable components and time the process | < 5 min | Brandon | PV | 10 | After CDR | 12/3/2017 | - | Pass | | | All parts are easily accessible |
| 4 | Labels for adjustable features | Visual inspection along with lifetime check of the labels/indicators | yes or no check | Daniel | DV | 1 | After CDR | 12/3/2017 | - | | Fail | | Adjustable features and measurements not labeled |
| 5 | Physical adjustment limits | visual and functional test to check if physical limits implemented work correctly | yes or no check | Trey | DV | 2 per function | After CDR | 12/3/2017 | - | | | Partial | Adjustment limits not necessary for some features |
| 6 | # of accessible pinch points | Visual inspection. Run the device and poke pinchable objects into device, attempting to snag. (use something that won't damage device) | 0 | Brandon | DV | 10 | After CDR | 12/3/2017 | - | | | Partial | Pinch points present, but magnitude of danger low |
| 7 | # of accessible tangle points | Visual inspection. Run the device and poke tangleable objects into device, attempting to get tangled. (use something that won't damage device) | 0 | Daniel | DV | 10 | After CDR | 12/3/2017 | - | | | Partial | Tangle points present, but magnitude of danger low |
| 8 | % error btw data and theory | Perform calculations for theoretical value, then run the test, obtain data and compare experimental value to theoretical | 10% | Trey | DV | 10 | After CDR | 12/3/2017 | Undetermined | | | | Theory may need to be reassessed for scaled version with unique RC tire characteristics |
| 9 | Ability of sensors to detect | Verify that the sensors implemented accurately and reliably sense the desired parameters | Can sense axial force, motor velocity, and motor position. | Brandon | DV | 5 | After CDR | 12/3/2017 | - | | | Partial | Sensors scaled for right magnitude of forces, tested and work. Voltage output still unscaled |
| 10 | Interchangeable loads | Make sure that the current load is easily detachable such that new modules can be added without modifying the motors and structure much | Yes | Daniel | DV | 10 | After CDR | 12/3/2017 | - | Pass | | | Selection of alternative bearing suggested due to binding |
| 11 | Cost per device | Add up cost of all components bought, and components manufactured, along with technician time | < $1500 | Trey | PV | 1 | After CDR | 12/3/2017 | - | | | Partial | Total assembly cost overbudget $1,727.69; with discounted load cells and motors, devices are under budget |
| 12 | Footprint area | Measure dimensions of device base | < 2'x2' | Brandon | DV | 1 | After CDR | 12/3/2017 | 12"x17" | Pass | | | |
| 13 | Emergency shut off | Turn on device, use emergency shut off to stop the device. Make sure it works. Must be within reach if something gets caught | yes or no check | Trey | DV | 5 | After CDR | 12/3/2017 | - | | | | Emergency stop is out of project scope |
| 14 | Tool clearance | Test to see if required tools fit where they are needed with none to minimal removal of other parts | yes or no check | Daniel | DV | 1 | After CDR | 12/3/2017 | - | Pass | | | |
| 15 | Total time for initial assembly | Time ourselves assembling the device from scratch | < 3 hours | Trey | PV | 3 | After CDR | 12/3/2017 | ~2hrs | Pass | | | |
| 16 | Weight | Weigh the assembled device (including potential lab weights) | < 50 lbs | Brandon | DV | 2 | After CDR | 12/3/2017 | ~30lbs | Pass | | | |
| 17 | % of parts contained in the frame | Make sure all parts are connected to each other. When lifted all components should lift as well (not including lab weights) | Zero loose parts. Or any that fall off | Daniel | DV | 1 | After CDR | 12/3/2017 | 100% | Pass | | | Not including weight set |
| 18 | Max operational voltage | Based off of motor specifications | < 45 V | Trey | DV | 2 | After CDR | 12/3/2017 | 6-12V | Pass | | | Good operational range |
| 19 | Motor time constant | Run our prototype and use a DAQ to obtain the time constant | > 1 seconds | Brandon | DV | 10 | After CDR | 12/3/2017 | ~3seconds | Pass | | | Using dyno drum as flywheel, depends on motor inputs |
| 20 | Settling time | Use a DAQ to obtain settling time | > 4 seconds | Daniel | DV | 10 | After CDR | 12/3/2017 | Not tested | | | | |
| 21 | % overshoot | Use a DAQ with our prototype to obtain % overshoot | < 80% | Trey | DV | 10 | After CDR | 12/3/2017 | Not tested | | | | |
| 22 | scaled torque value | Calculations coupled with sensor data | | Brandon | DV | 10 | After CDR | 12/3/2017 | Undetermined | | | | Torque values depend on resistance between poles of driven motor |

# Appendix M: Product Data Sheets

MODEL LBB200

## Cantilever Bending Beam Load Cell

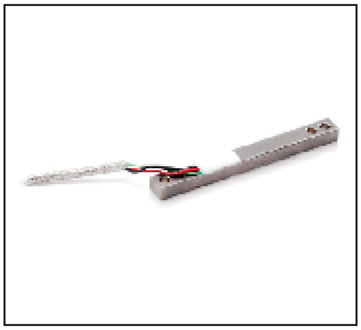

### FEATURES

- Ideal for OEM Applications
- Can be utilized to measure force, pressure, and displacement for OEM Applications
- Light Weight

| SPECIFICATIONS | |
|---|---|
| **ELECTRICAL** | |
| Rated Output (RO) | 1 mV/V nom |
| Excitation (VDC or VAC) | 18 max |
| Bridge Resistance | 1000 Ohm nom |
| Insulation Resistance | ≥500 MOhm @ 50 VDC |
| Connection | #28 AWG, 4 conductor, braided shielded PVC cable 1 ft [0.3 m] long |
| Wiring Code | WC3 |
| **MECHANICAL** | |
| Weight | 1 oz [28 g] |
| Safe Overload | 150% of RO |
| Material | 17-4 PH stainless-steel |
| IP Rating | IP64 |
| **TEMPERATURE** | |
| Operating Temperature | -45 to 200°F [-42 to 93°C] |
| Compensated Temperature | 60 to 160°F [15 to 72°C] |
| Temperature Shift Zero | ±0.02% of RO/°F [0.036% of RO/°C] |
| Temperature Shift Span | ±0.02% of Load/°F [0.036% of Load/°C] |

AMETEK®
ADVANCED MOTION SOLUTIONS

Haydon Kerk Motion Solutions, Inc. - www.HaydonKerk.com - Phone: 1-203-756-7441 | Pittman Motors - www.Pittman-Motors.com - Phone: 1-267-933-2105

Brush DC Motor
Product Number 14204S006-SP
$331.08

| | |
|---|---|
| Motor Series | Series 14000 LO-COG Brush Commutated DC Motors |
| Price (USD) | $331.08 |
| Frame Size (Mounting Face) (in) | 2.125 |
| Motor Frame Size (in) | 2.125 |
| Gear Frame Size (in) | n/a |
| Overall Body Length (in) | 4.668 |
| Supply Voltage (V) | 24 |
| Continuous Output Torque (oz-in) | 26 |
| Output Speed @ Cont. Torque (RPM) | 3200 |
| Current @ Cont. Torque (A) | 3.7 |
| Continuous Output Power (W) | 61 |
| No Load Current (A) | 0.26 |
| No Load Output Speed (RPM) | 3630 |
| Peak Current (A) | 24 |
| Peak Output Torque (oz-in) | 200 |
| Motor Constant (oz-in/√W) | 8.63 |
| Motor Torque Constant (oz-in/A) | 8.67 |
| Motor Voltage Constant (V/krpm) | 6.41 |
| Terminal Resistance (Ohms) | 1.01 |
| Inductance (mH) | 1.6 |
| Coulomb Friction Torque (oz-in) | 1.6 |
| Viscous Damping Factor (oz-in/krpm) | 0.18 |
| Electrical Time Constant (ms) | 1.6 |
| Mechanical Time Constant (ms) | 7 |
| Thermal Time Constant (min) | 29 |
| Thermal Resistance (°C/Watt) | 7.7 |
| Maximum Winding Temperature (°C) | 155 |
| Rotor Inertia (oz-in-s2) | 0.0037 |
| Output Bearing | Ball |
| Gear Series | n/a |
| Gear Ratio (xx.x:1) | n/a |
| Gear Type | n/a |
| Gear Efficiency | n/a |
| Gear Maximum Torque (oz-in) | n/a |
| Encoder Series | E30B |
| Encoder Resolution (CPR) | 500 |
| Encoder Output Channels | 3 |
| Weight (Mass) (oz) | 37 |
| Voltage Note | n/a |

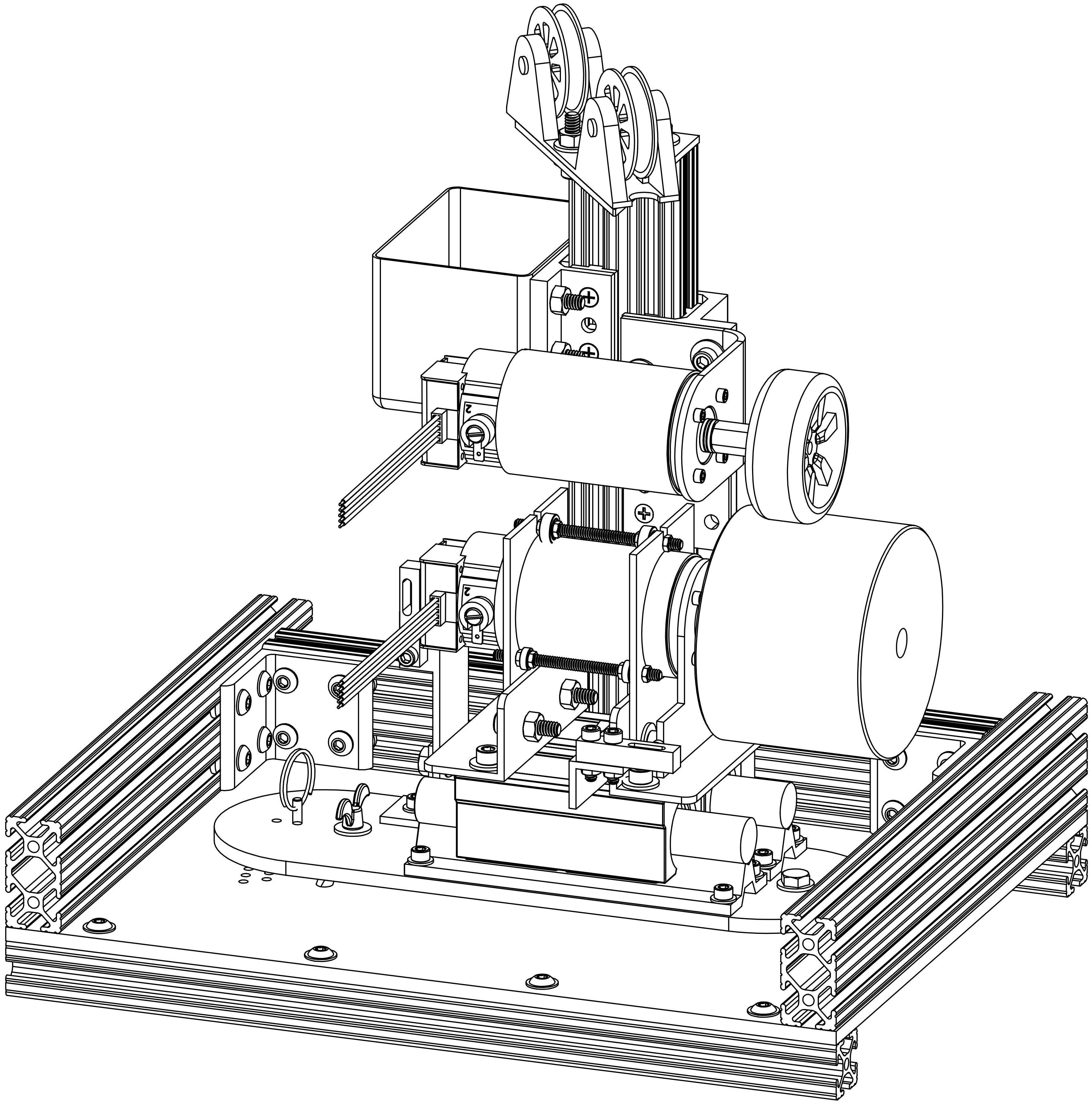

| Cal Poly Mechanical Engineering<br>DYNO-MITE APPARATUS | SENIOR PROJECT | Title: DYNO-MITE COMPLETE ASSEMBLY | | | Drwn. By: DANIEL HOFFMAN |
|---|---|---|---|---|---|
| | Dwg. #: | Nxt Asb: | Date: 12/3/17 | Scale: 1:2 | Chkd. By: BRANDON MILLER |

NOTES:
1. MATERIAL: 6061 ALUMINUM 1/4" THICK.
2. RECOMMENDED WATER-CUTTING THIS PART.

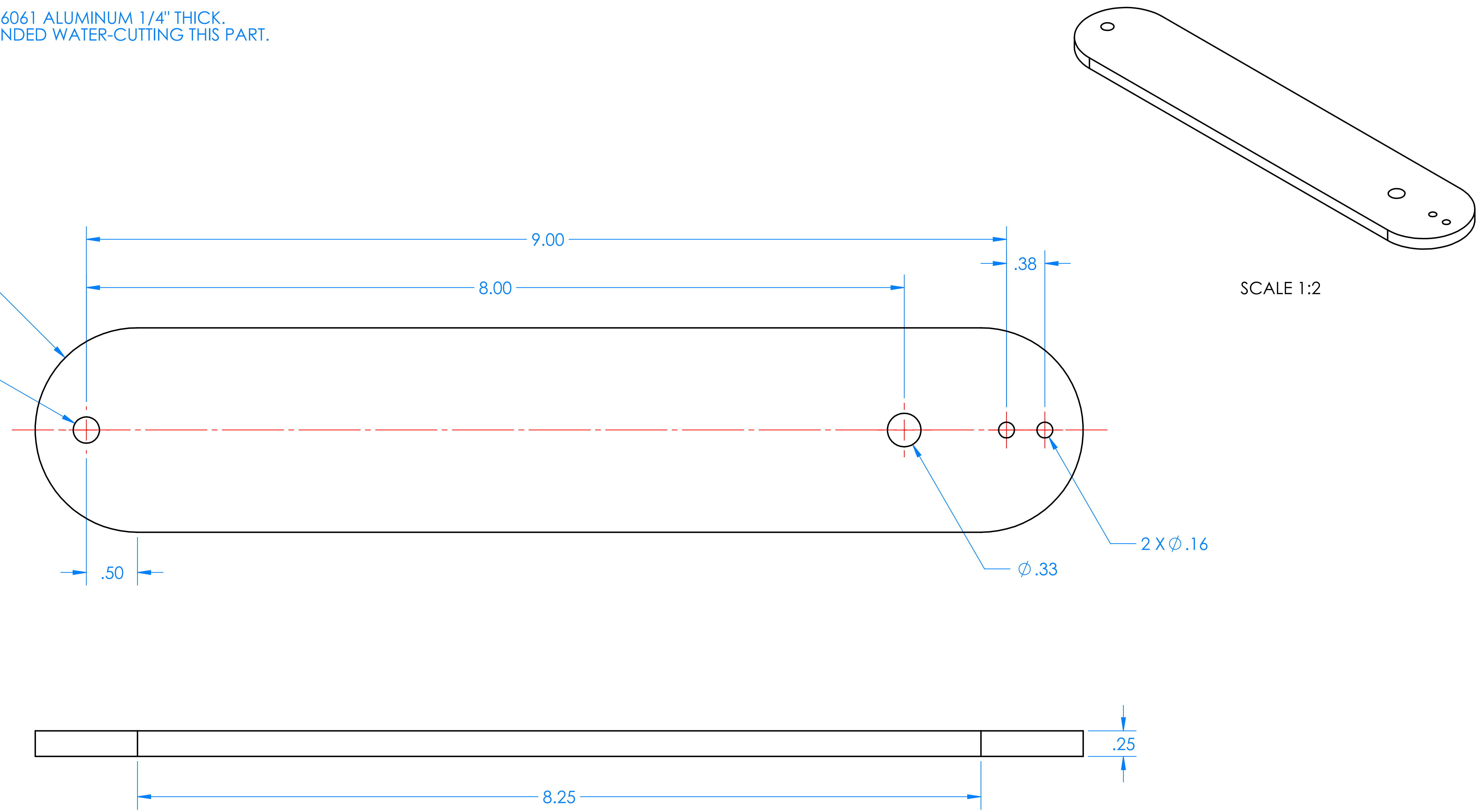


| Cal Poly Mechanical Engineering DYNO-MITE APPARATUS | SENIOR PROJECT | Assignment # | Title: ANGLE BAR BOTTOM | | Drwn. By: DANIEL HOFFMAN |
|---|---|---|---|---|---|
| | Dwg. #: 33.3 | Nxt Asb: | Date: 12/3/17 | Scale: 1:1 | Chkd. By: BRANDON MILLER |

NOTES:
1. MATERIAL: 6061 ALUMINUM 1/4" THICK.
2. HIGHLY RECOMMENDED WATER-CUTTING THIS PART.

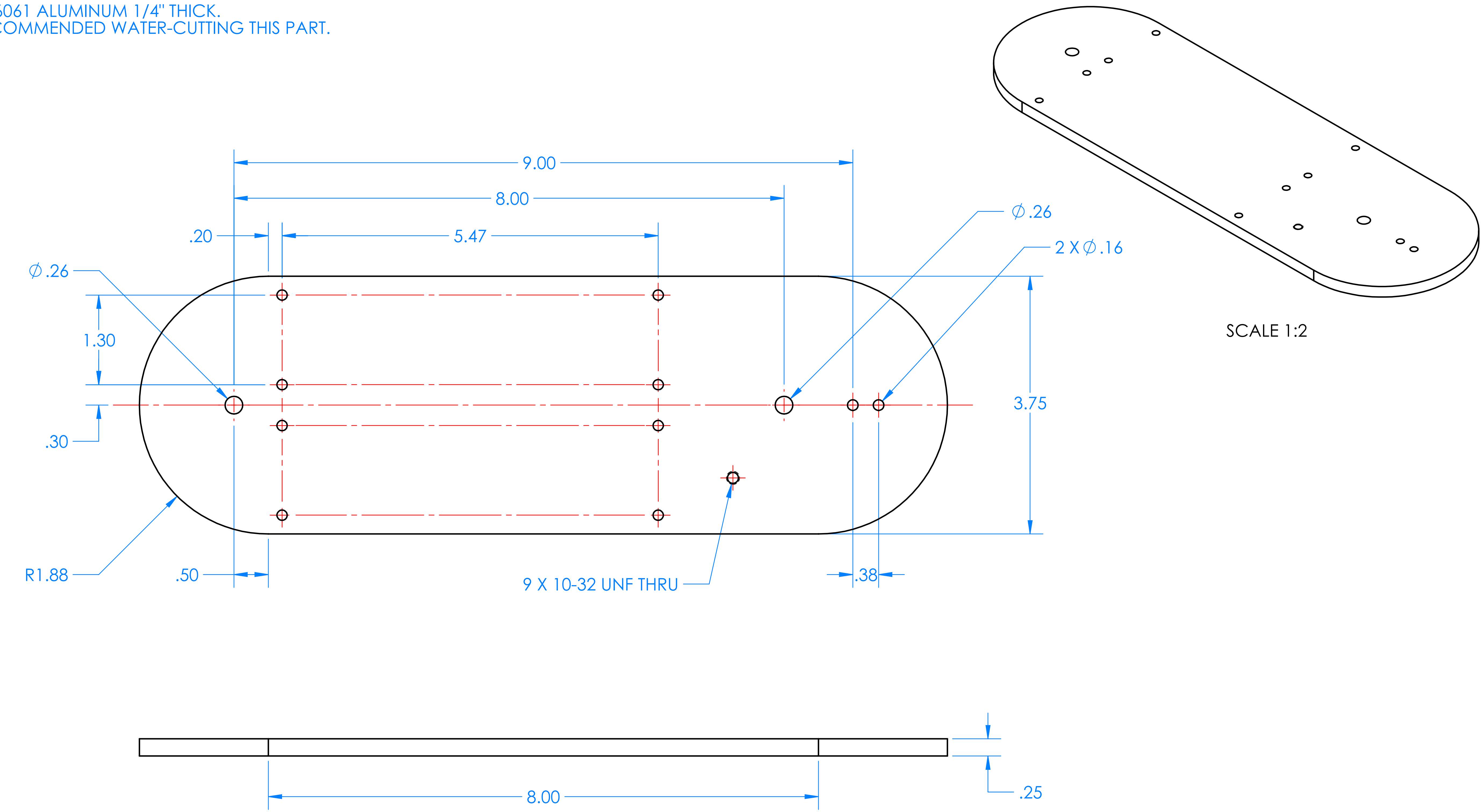


| | | | | |
|---|---|---|---|---|
| Cal Poly Mechanical Engineering | SENIOR PROJECT | Assignment # | Title: ANGLE BAR TOP | Drwn. By: DANIEL HOFFMAN |
| DYNO-MITE APPARATUS | Dwg. #: 33.2 | Nxt Asb: | Date: 12/3/17 / Scale: 2:3 | Chkd. By: BRANDON MILLER |

NOTES:

1. MATERIAL: 6061 ALUMINUM 90° ANGLE 1/8" THICK, 1.5"W X 1.5"H.
2. THE 0.73" DIM. IS NOT CRITICAL.
3. THE 1.38" DIM. IS NOT CRITICAL.
4. START WITH ANGLE STOCK THEN CUT OFF PORTIONS OF IT TO MAKE THIS PART.

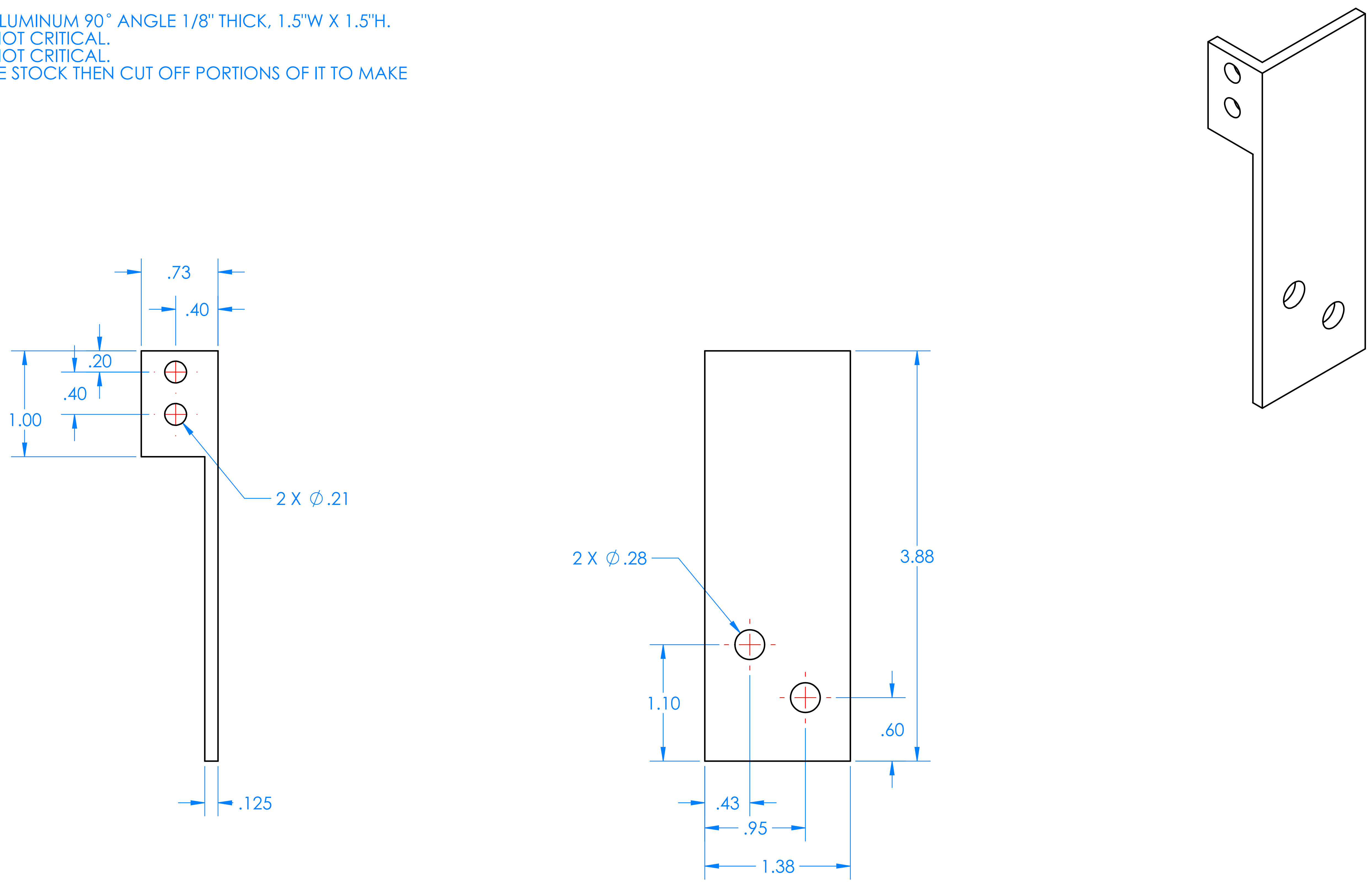


| | | | | |
|---|---|---|---|---|
| Cal Poly Mechanical Engineering | SENIOR PROJECT | Title: AXIAL FORCE LOAD CELL MOUNT | | Drwn. By: DANIEL HOFFMAN |
| DYNO-MITE APPARATUS | Dwg. #: 41.3 | Nxt Asb: | Date: 12/3/17 | Scale: 1:1 | Chkd. By: BRANDON MILLER |

NOTES:
1. MATERIAL: 6061 ALUMINUM 90° ANGLE 1/8" THICK, 1.5"W X 1.5"H.
2. THE 1.125" DIM. IS NOT CRITICAL.
3. THE 1.00" DIM. IS NOT CRITICAL.

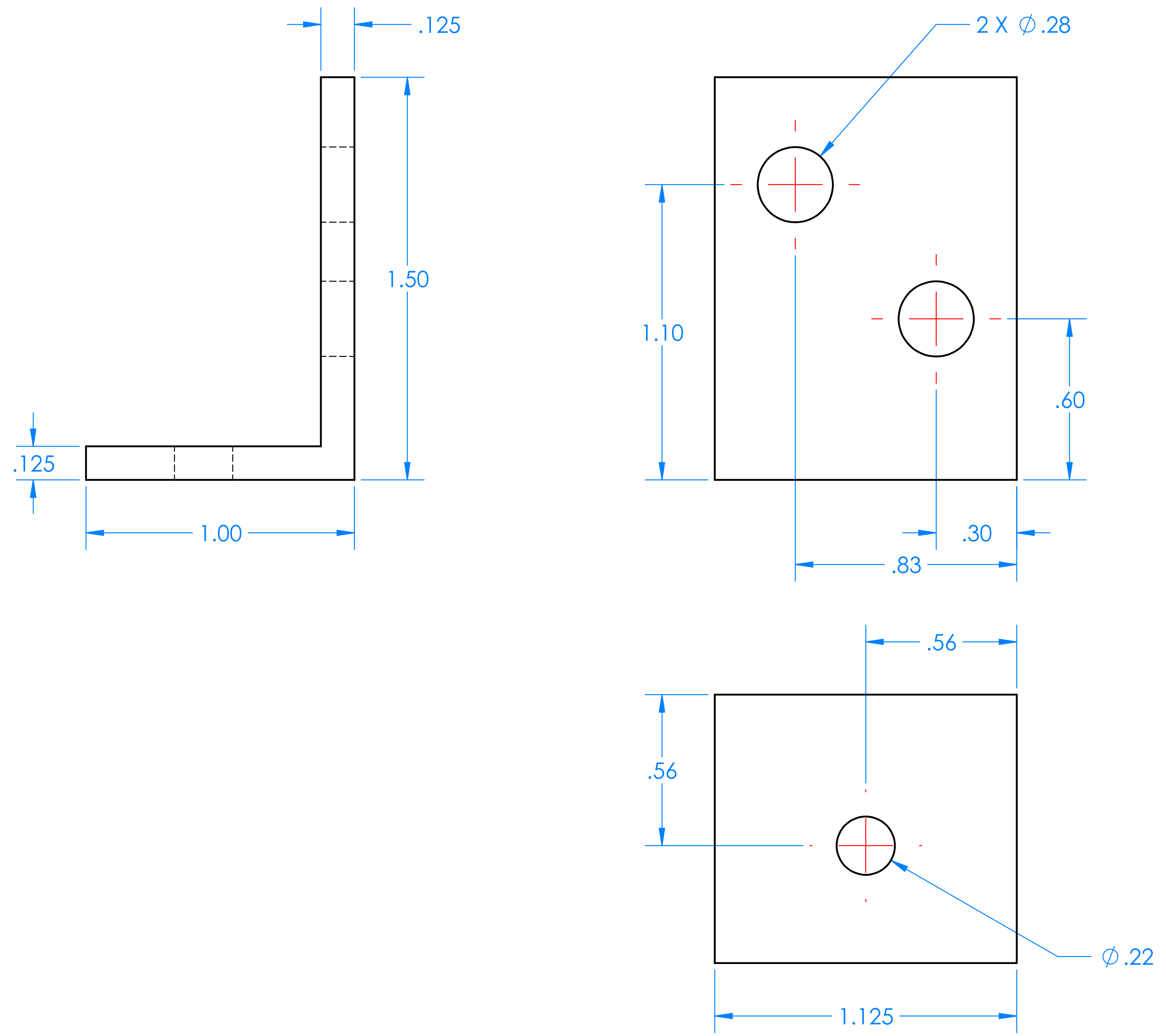


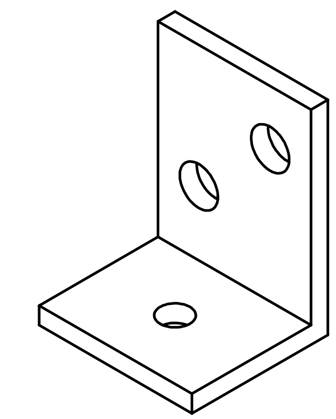

SCALE 1:1

| | | | | |
|---|---|---|---|---|
| Cal Poly Mechanical Engineering | SENIOR PROJECT | Assignment # | Title: AXIAL LOAD BRACKET | Drwn. By: DANIEL HOFFMAN |
| DYNO-MITE APPARATUS | Dwg. #: 41.4 | Nxt Asb: | Date: 12/3/17 / Scale: 2:1 | Chkd. By: BRANDON MILLER |

NOTES:
1. MATERIAL: 6061 ALUMINUM 1/4" THICK.
2. HIGHLY RECOMMENDED WATER-CUTTING THIS PART.
POSITIONS OF ANGLE HOLES ARE CRITICAL.

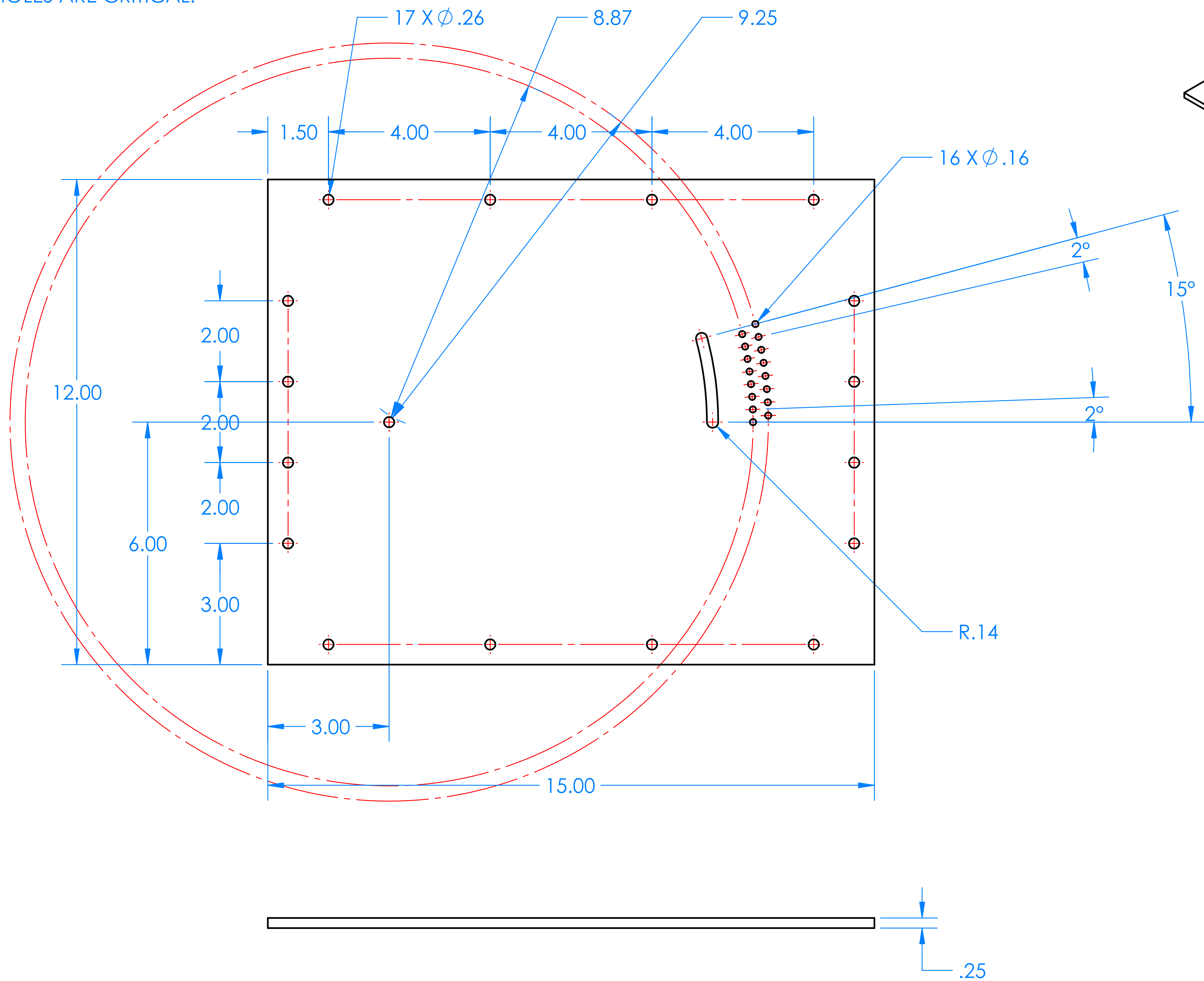


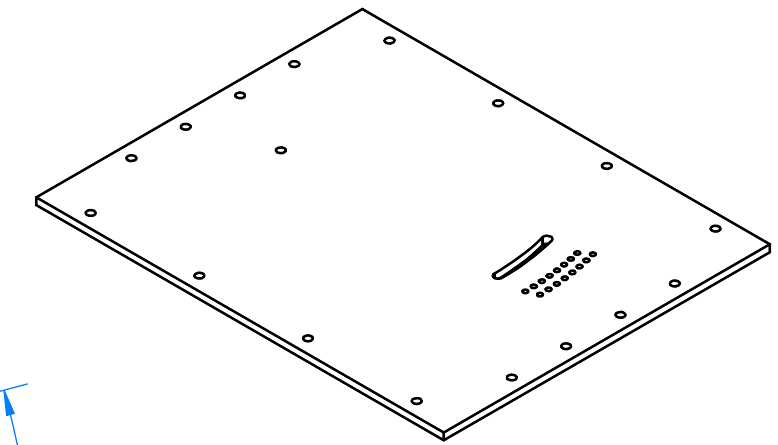

SCALE 1:5

| | | | | | |
|---|---|---|---|---|---|
| Cal Poly Mechanical Engineering | SENIOR PROJECT | Assignment # | Title: BASE | | Drwn. By: DANIEL HOFFMAN |
| DYNO-MITE APPARATUS | Dwg. #: 33.1 | Nxt Asb: | Date: 12/3/17 | Scale: 1:3 | Chkd. By: BRANDON MILLER |

NOTES:
1. MATERIAL: 6061 ALUMINUM 90° ANGLE 1/8" THICK, 1.5"W X 1.5"H.
2. MAKE SURE THE BOTTOM VIEW HOLES LINE UP WITH THE LINEAR BEARING HOLES.
3. MAKE SURE THE BACK VIEW HOLES LINE UP WITH THE HOLES ON THE MOTOR BEARING STRUCTURE.

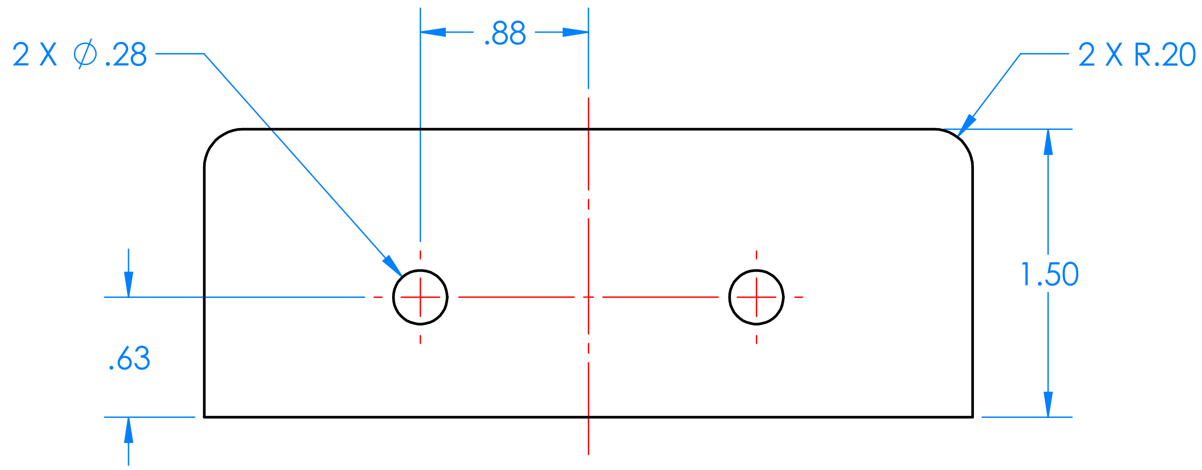


BACK VIEW

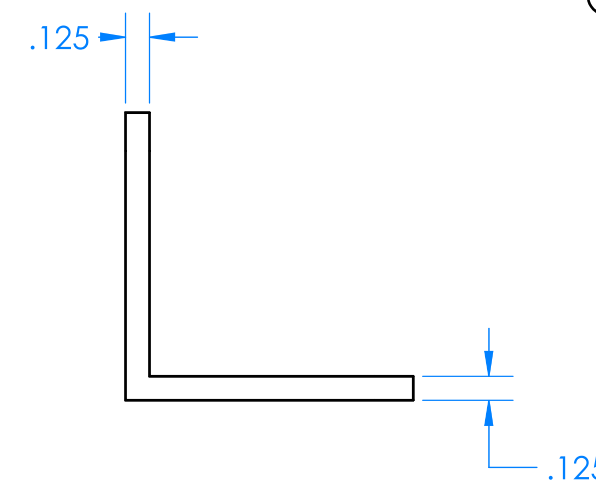


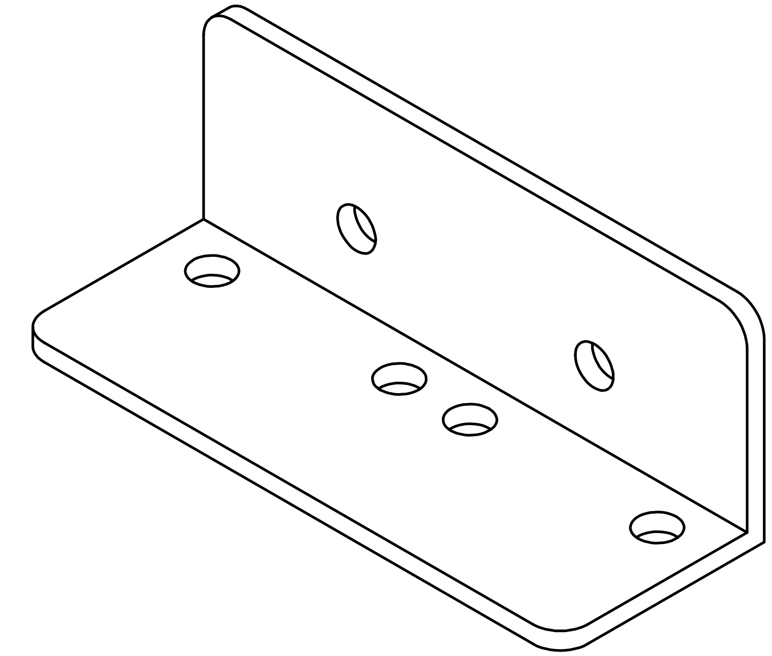

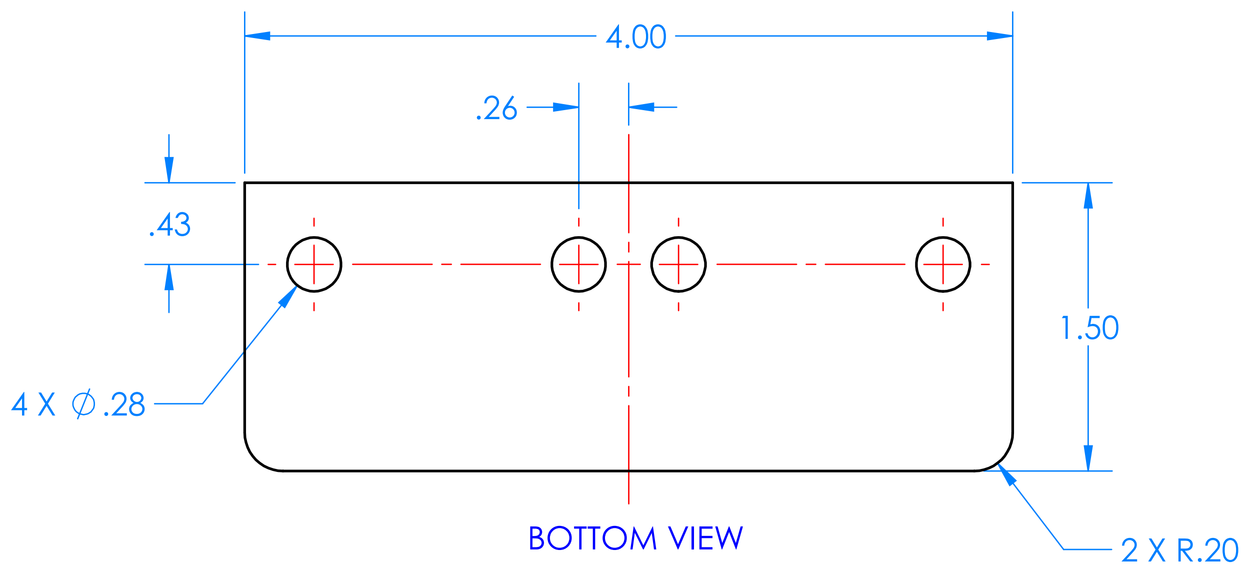


BOTTOM VIEW

| | | | | |
|---|---|---|---|---|
| Cal Poly Mechanical Engineering | SENIOR PROJECT | Title: BOTTOM MOTOR SUPPORT BRACKET | | Drwn. By: DANIEL HOFFMAN |
| DYNO-MITE APPARATUS | Dwg. #: 41.1 | Nxt Asb: | Date: 12/3/17 | Scale: 1:1 | Chkd. By: BRANDON MILLER |

NOTES:
1. USE FILE TO GET THE BEST HEX SHAPE YOU CAN.
2. PRESS-FIT HEX COUPLER INTO THE HEX, USE EPOXY.

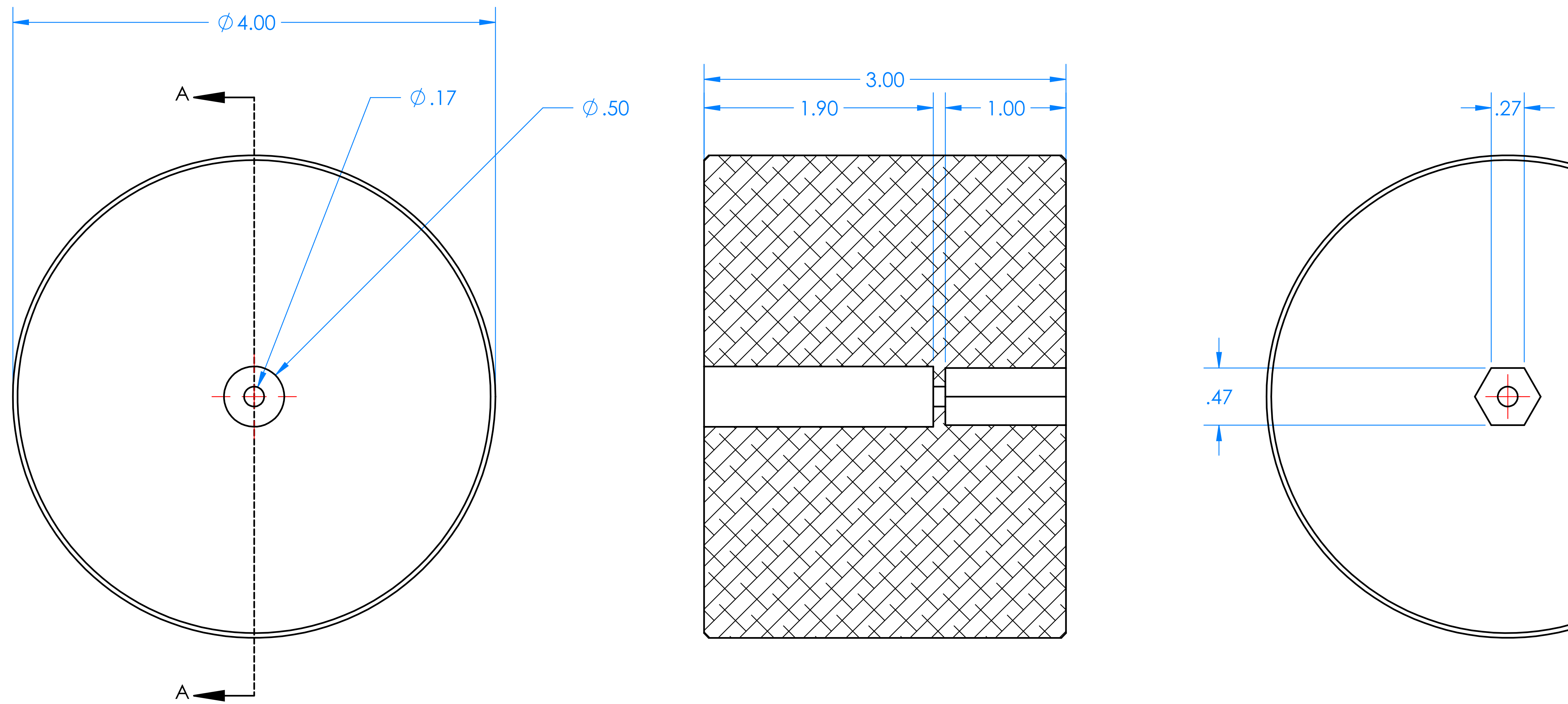


SECTION A-A
SCALE 1 : 1

| | | | | |
|---|---|---|---|---|
| Cal Poly Mechanical Engineering | SENIOR PROJECT | Assignment # | Title: DYNO DRUM | Drwn. By: DANIEL HOFFMAN |
| DYNO-MITE APPARATUS | Dwg. #: 30 | Nxt Asb: | Date: 12/3/17 | Scale: 1:1 | Chkd. By: ME STAFF |

NOTES:
1. MATERIAL 6061 ALUMINUM SHEET 1/8" THICK.
2. RECOMMEND WATER-CUTTING THIS PART.

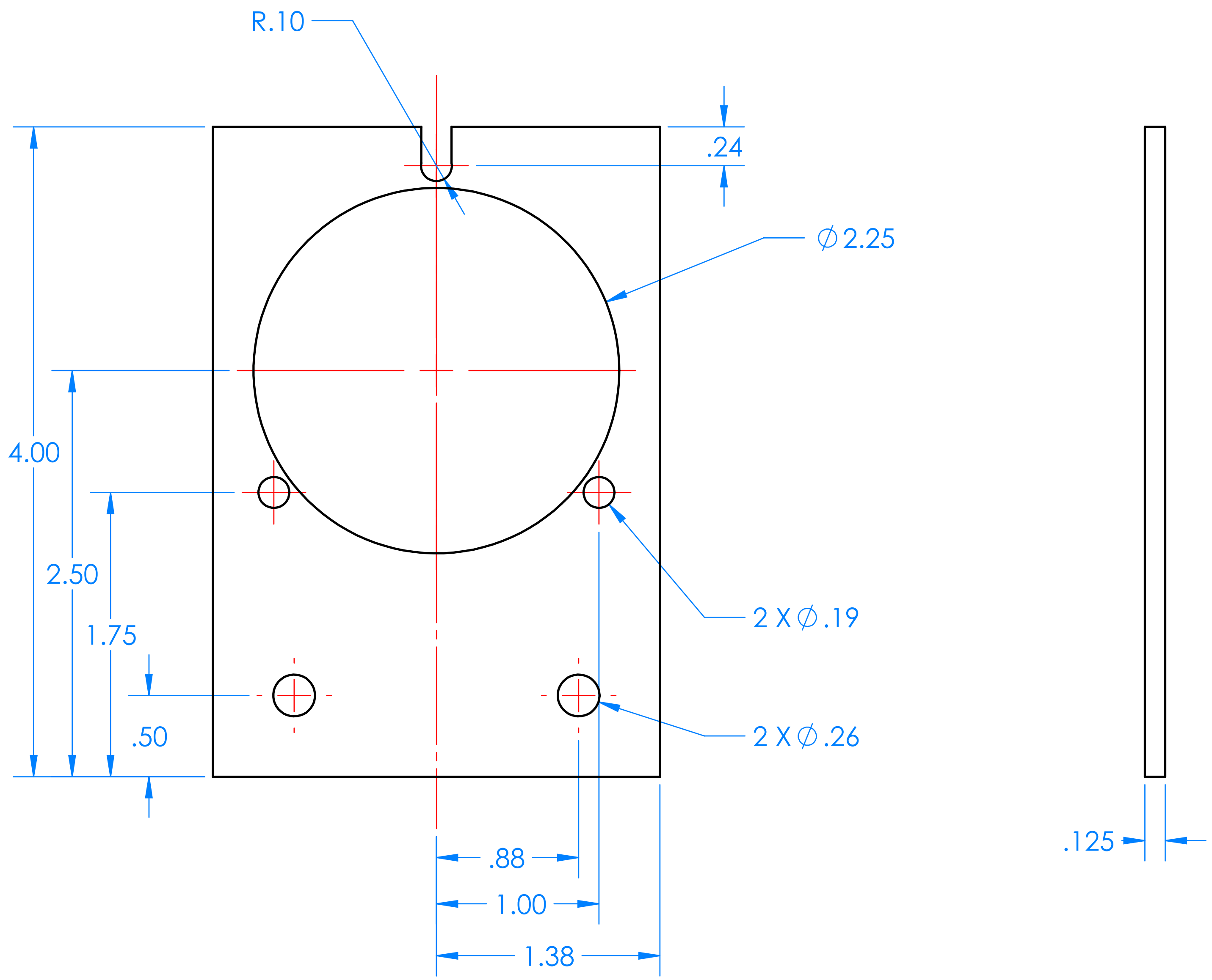


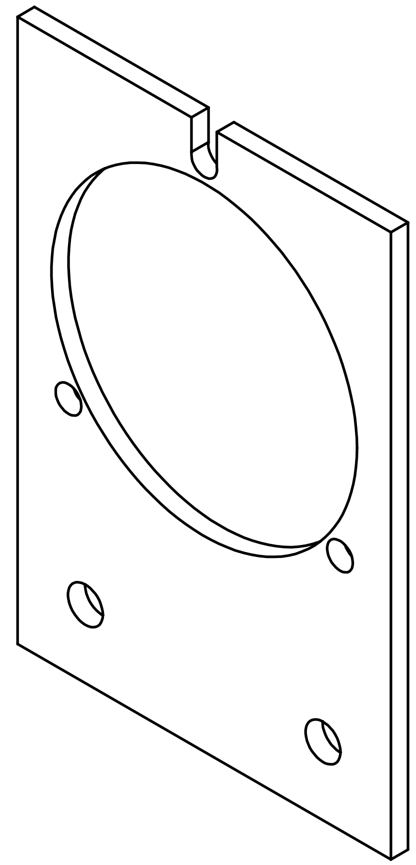

| | | | | |
|---|---|---|---|---|
| Cal Poly Mechanical Engineering<br>DYNO-MITE APPARATUS | SENIOR PROJECT | Assignment # | Title: MOTOR BEARING STRUCTURE | Drwn. By: DANIEL HOFFMAN |
| | Dwg. #: 32.2 | Nxt Asb: | Date: 12/3/17 | Scale: 1:1 | Chkd. By: BRANDON MILLER |

NOTES:
1. MATERIAL: 6061 ALUMINUM SHEET 1/8" THICK.
2. DO NOT UNDERSIZE LARGE CIRCLE CUTOUT.
3. RECOMMEND WATER-CUTTING THIS PART.

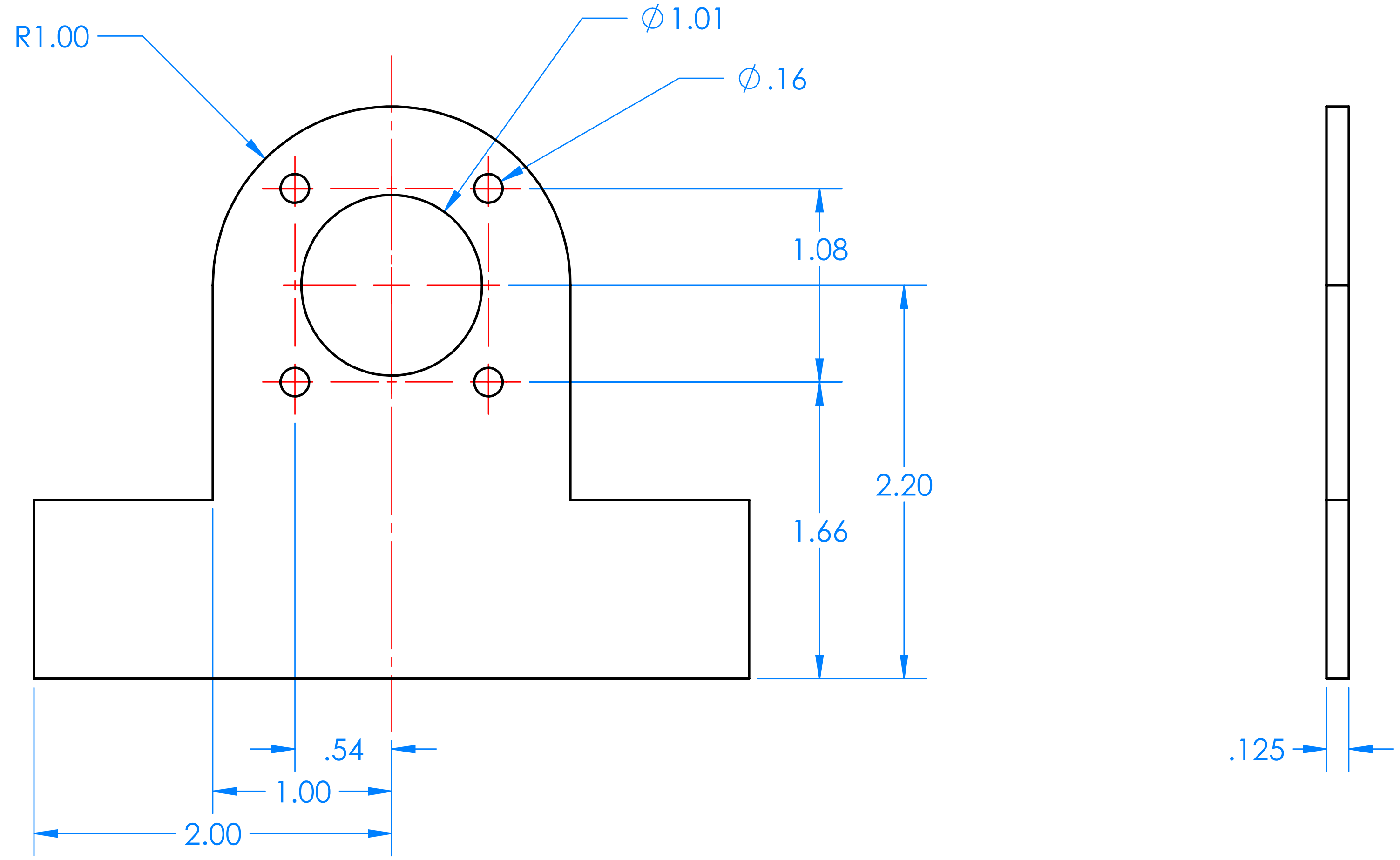


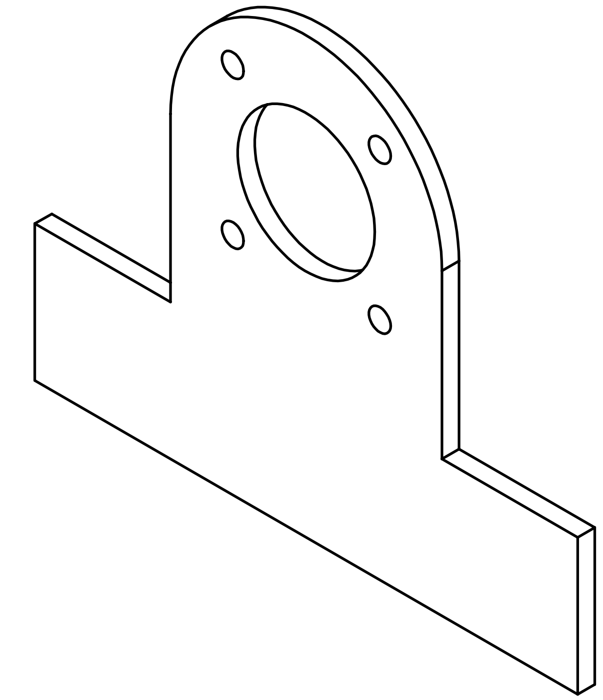

| | | | | |
|---|---|---|---|---|
| Cal Poly Mechanical Engineering | SENIOR PROJECT | Assignment # | Title: MOTOR TORQUE ARM | Drwn. By: DANIEL HOFFMAN |
| DYNO-MITE APPARATUS | Dwg. #: 32.3 | Nxt Asb: | Date: 12/3/17 / Scale: 1:1 | Chkd. By: BRANDON MILLER |

NOTES:
1. THE HOLE WITH THE DIAMETER CALLOUT MAY END UP GETTING COVERED UP BY THE PULLEY MOUNT.
2. THE LOWER TWO HOLES, MAKE SURE THEY LINE UP WITH THE PULLEY MOUNT HOLES.
3. PLACE PULLEY MOUNT PARALLEL AND COINCIDENT TO THE SLANTED EDGE.
4. MATERIAL: 6061 ALUMINUM SHEET 1/8" THICK.

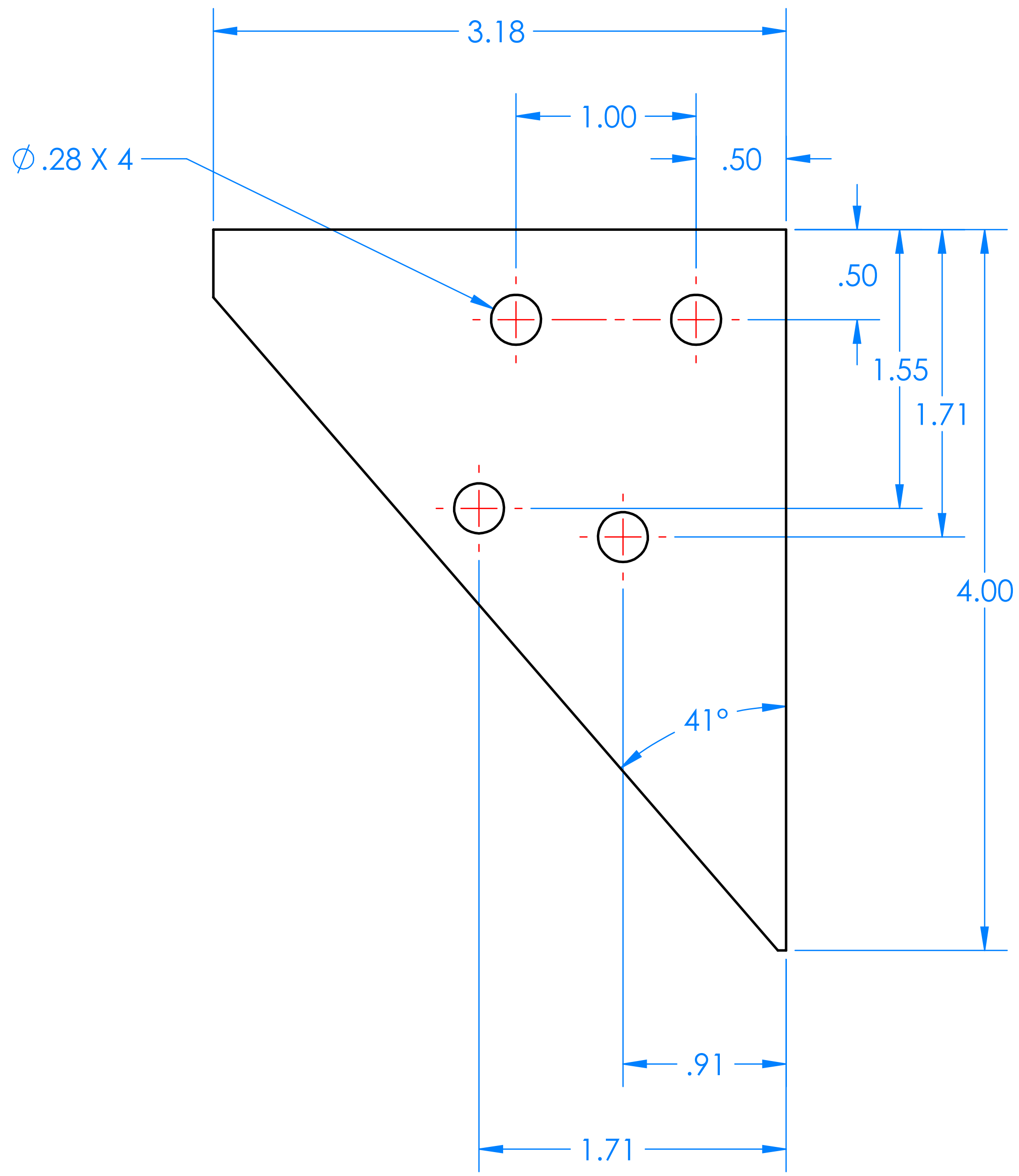


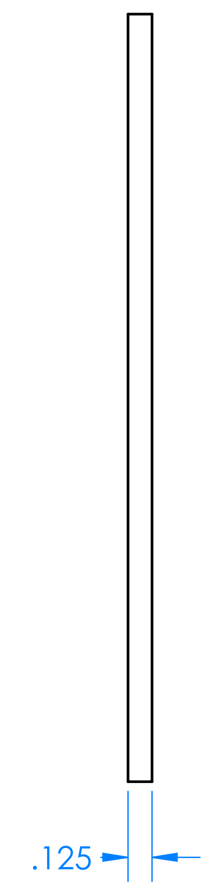


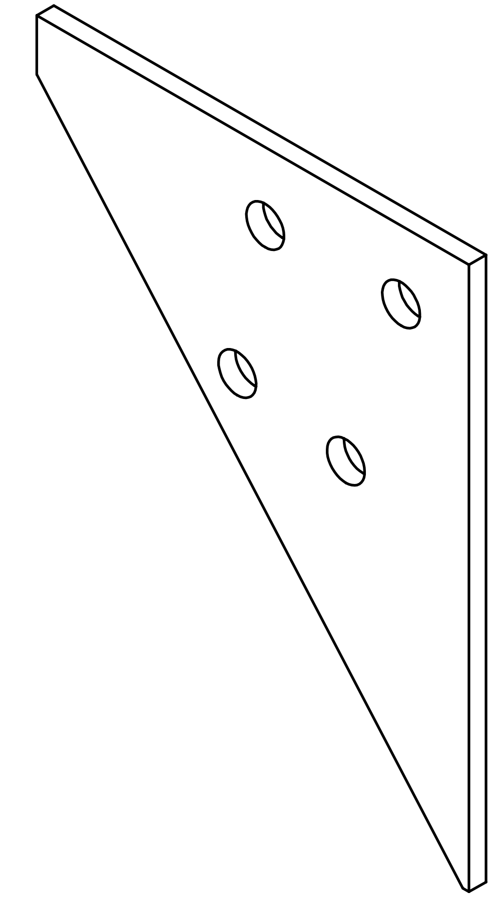

| | | | | |
|---|---|---|---|---|
| Cal Poly Mechanical Engineering | SENIOR PROJECT | Assignment # | Title: PULLEY PLATE | Drwn. By: DANIEL HOFFMAN |
| DYNO-MITE APPARATUS | Dwg. #: 32.4 | Nxt Asb: | Date: 12/3/17 · Scale: 1:1 | Chkd. By: BRANDON MILLER |

NOTES:
1. MATERIAL: 6061 ALUMINUM 90° ANGLE 1/8" THICK, 1.5"W X 1.5"H.
2. MAKE SURE THE HOLES ALIGN WITH THE BOTTOM MOTOR SUPPORT BRACKET.

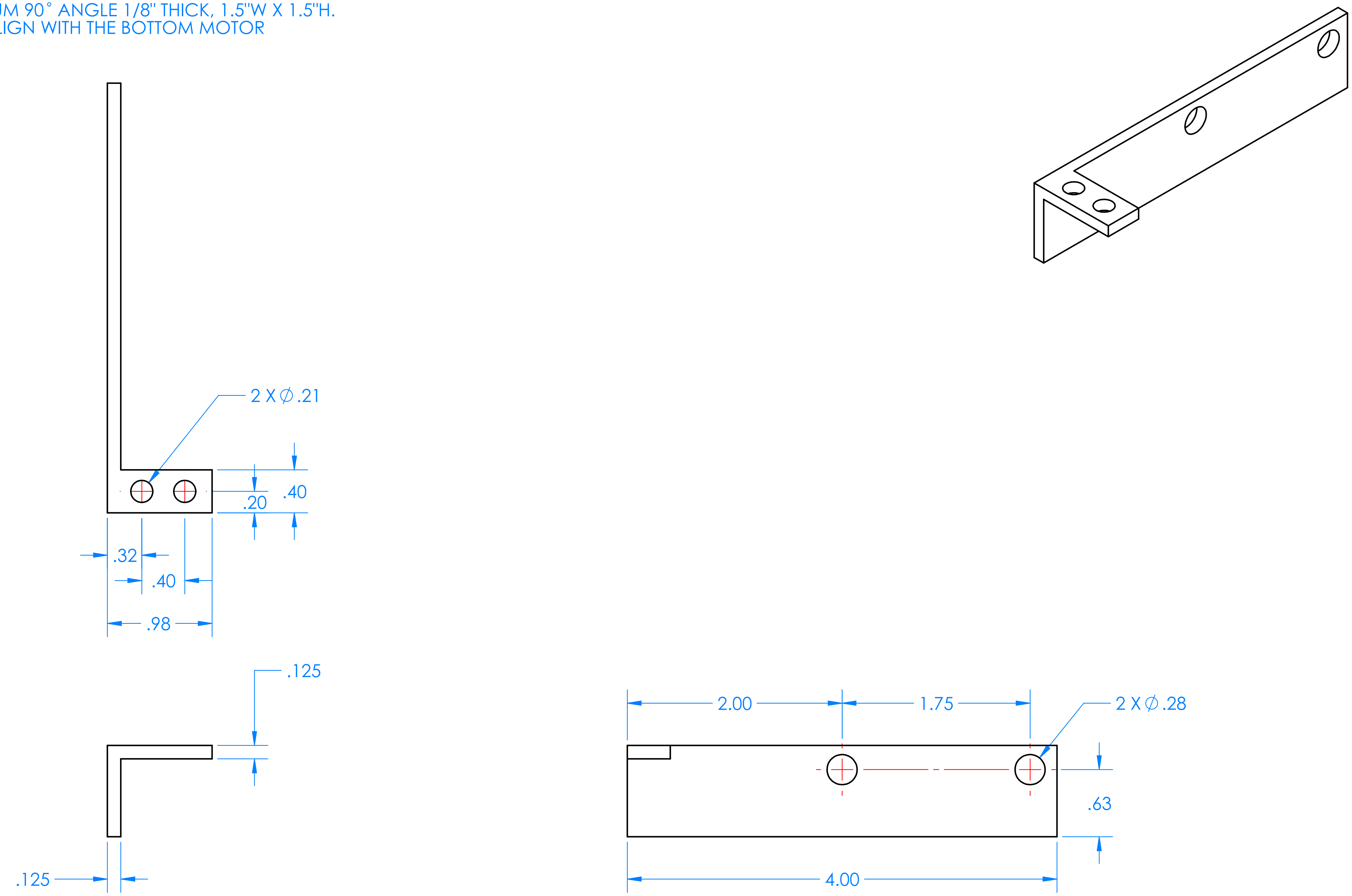


| Cal Poly Mechanical Engineering<br>DYNO-MITE APPARATUS | SENIOR PROJECT | Assignment # | Title: TORQUE LOAD CELL MOUNT | | Drwn. By: DANIEL HOFFMAN |
|---|---|---|---|---|---|
| | Dwg. #: 41.2 | Nxt Asb: | Date: 12/3/17 | Scale: 1:1 | Chkd. By: BRANDON MILLER |

NOTES:

1. MATERIAL: 6061 ALUMINUM SHEET 1/8" THICK.
2. RADUIS OF BEND IS NOT CRITICAL.
3. THE LARGE CIRCLE IS CENTERED WITH THE CENTERLINE OF THE PART.
4. RECOMMEND WATER-CUTTING THIS PART.

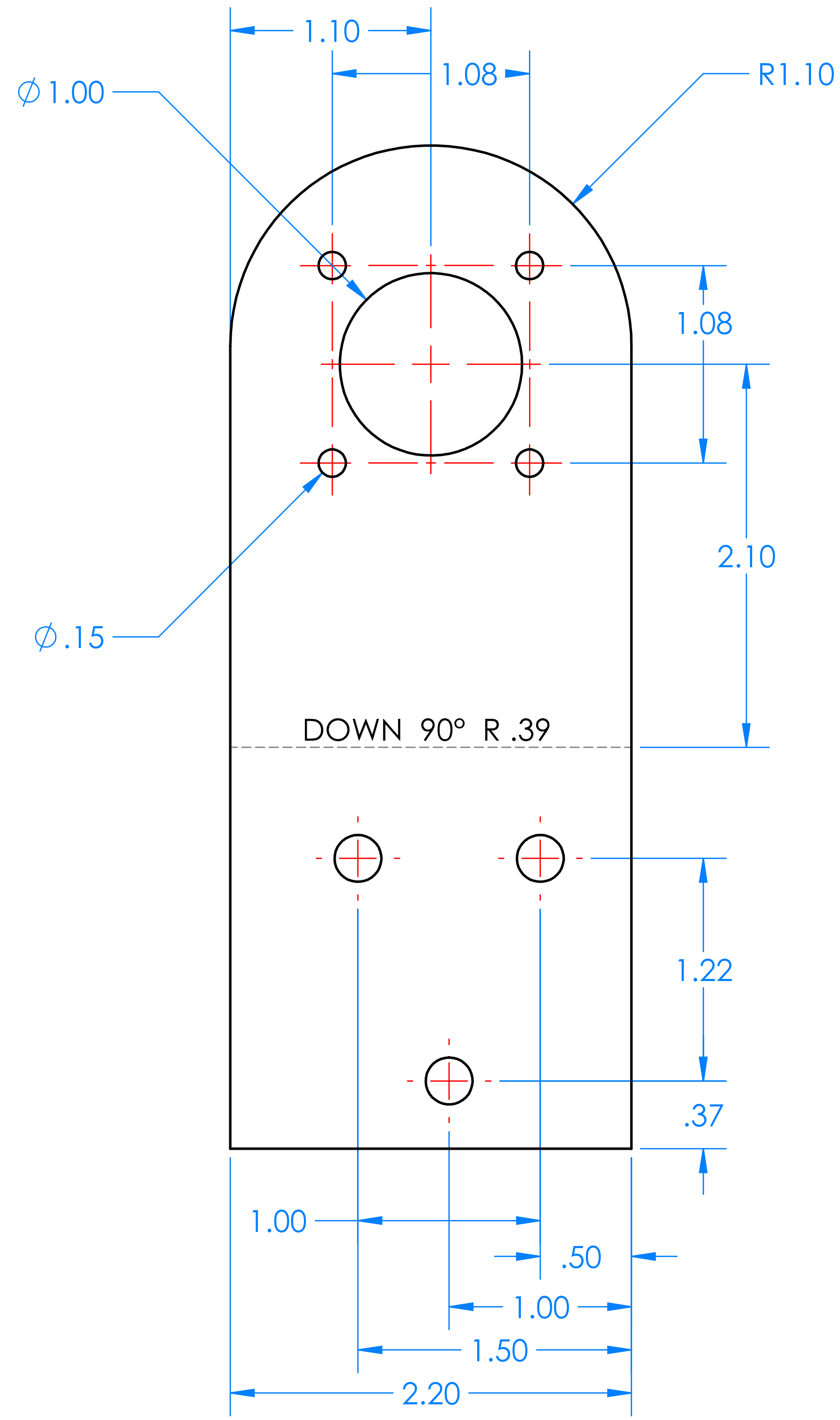


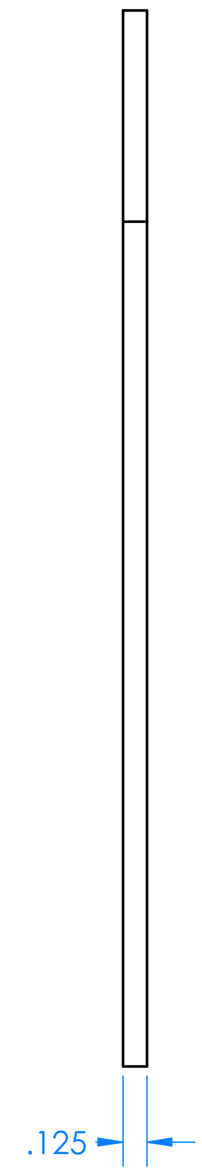


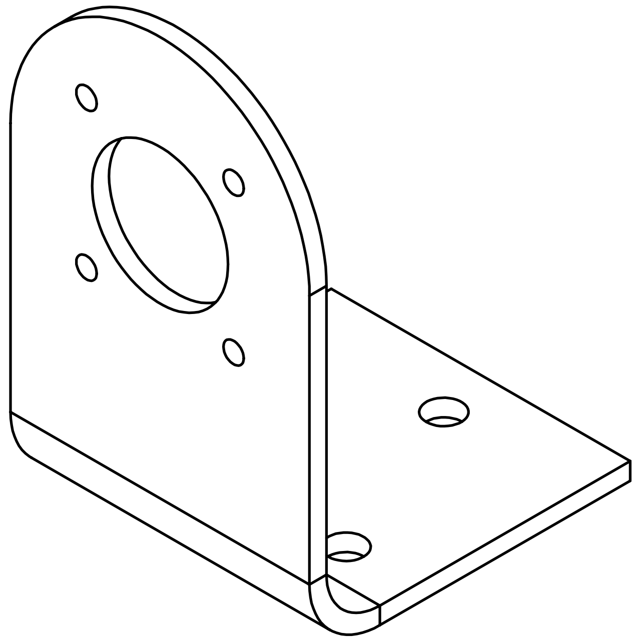

| | | | | |
|---|---|---|---|---|
| Cal Poly Mechanical Engineering | SENIOR PROJECT | Assignment # | Title: UPPER MOTOR MOUNT | Drwn. By: DANIEL HOFFMAN |
| DYNO-MITE APPARATUS | Dwg. #: 32.1 | Nxt Asb: | Date: 12/3/17 / Scale: 1:1 | Chkd. By: BRANDON MILLER |